MF-67
COO-3077-49

Courant Institute of

Mathematical Sciences

Magneto-Fluid Dynamics Division

AEC Computing and Applied Mathematics Center

Three Dimensional Computation of Magnetohydrodynamic Equilibrium of Toroidal Plasma without Axial Symmetry

Octavio L. Betancourt

AEC Research and Development Report

Plasma Physics
Mathematics and Computers

New York University

Magneto-Fluid Dynamics Division
AEC Computing and Applied Mathematics Center
Courant Institute of Mathematical Sciences
New York University

Plasma Physics MF-67
Mathematics and Computers COO-3077-49

THREE DIMENSIONAL COMPUTATION OF MAGNETOHYDRODYNAMIC EQUILIBRIUM OF TOROIDAL PLASMA WITHOUT AXIAL SYMMETRY

Octavio L. Betancourt

June 1974

U. S. Atomic Energy Commission
Contract No. AT(11-1)-3077

Table of Contents

Table of Contents

(Continued)

1. Introduction

One of the significant contributions to controlled thermonuclear research in recent years has been the experimental work of the Russians in developing their Tokamak machine. A useful mathematical model of the Tokamak can be obtained from magnetohydrodynamics in the form of a free boundary problem in potential theory. Different methods have been developed to compute equilibrium configurations for cases which possess some type of symmetry, for example, axial or helical symmetry [3,5,7].

More important than the computation of equilibrium configurations is the determination of their stability. At the present time, various devices have been built, or are in the process of being built. Some of them are axially symmetric devices with different kinds of cross-sections; others are nonaxially symmetric, as for example those with helical windings.

This raises the question of which is the best configuration from the point of view of magnetohydrodynamic stability. In order to answer this question, it is important that we formulate a model in which we allow for three independent space coordinates.

The subject of this paper is the formulation and implementation of a numerical method to compute configurations of magnetohydrodynamic equilibrium in three-dimensional space. Moreover, our method gives an indication

about stability and makes it possible to compare different configurations and decide which one is the most stable.

As a mathematical model of the Tokamak, we investigate the magnetohydrodynamic equilibrium of a plasma contained in a toroidal region D_1 of space that is separated by a sharp free boundary Γ from an outer vacuum region D_2 bounded by a conductor shell C. The plasma is assumed to be a perfectly conducting compressible fluid at constant pressure p and internal energy $e = p/(\gamma-1)$.

We express the magnetic field B_2 in the vacuum region as a linear combination

$$B_2 = c_1 \nabla\psi_1 + c_2 \nabla\psi_2$$

of the gradients of two harmonic functions which yield unit currents, and the magnetic field B_1 in the plasma as a multiple

$$B_3 = c_3 \nabla\psi_3$$

of the gradient of a single harmonic function with unit current. The scalars c_1, c_2, c_3 are determined in such a way that B_1 and B_2 yield prescribed fluxes.

The basic idea is that the total potential energy

$$E = \frac{1}{2} \int_{D_2} B_2^2 \, dV + \frac{1}{2} \int_{D_1} B_1^2 \, dV + \int_{D_1} e \, dV$$

is stationary for an equilibrium position. In the case of a stable equilibrium, the energy is a minimum with respect to perturbations of the free boundary Γ, but a maximum

with respect to variations of ψ_1 , ψ_2 , ψ_3 . Thus the problem can be characterized as a minimax problem.

To determine the shape of the free boundary Γ we apply the idea of paths of steepest descent to the variational principle, using the requirement that the first variation of the energy

$$\delta E = \int_{\Gamma} \left(\frac{1}{2} B_2^2 - \frac{1}{2} B_1^2 - p\right) \delta n \, dS$$

vanish at the equilibrium position. We thus introduce an artificial time parameter t , and the solution is obtained by solving a time dependent system of equations which converge to a steady state. This enables us to study questions of equilibrium and stability with far less computational effort than would be necessary if we examined dependence on physical time instead.

We have developed a finite difference scheme based entirely on a discrete version of the variational principle. We establish a parametric formulation by introducing a fixed cube in an auxiliary domain [5]. One section of the cube is mapped onto the vacuum, and the remainder is mapped onto the plasma, in such a way that an intermediate plane is mapped onto the free boundary Γ . We seek the potentials ψ_1 , ψ_2 , ψ_3 as solutions to Neumann problems in the cube. The difficulty of locating the free boundary is overcome because we solve all equations in the fixed cube.

The coordinate system becomes singular along a closed

curve inside the plasma analogous to the axis in cylindrical coordinates. Difficulties with approximating Laplace's equation at the axial curve, with Neumann boundary conditions and with avoiding incompatibility of the Neumann problem for ψ_1, ψ_2, ψ_3 are all solved by the discrete variational principle. Furthermore, the method converges exclusively to equilibria that are physically stable, so that the convergence of the process is a measure of the stability of the solution.

The fundamental conclusion is that the method can be applied successfully to fully three-dimensional configurations, and that it yields results concerning their stability.

The computer program has been used to find three-dimensional magnetohydrodynamic equilibria both with and without axial symmetry. We have found a great number of stable configurations, and we have discovered geometries without axial symmetry that are shown by the method to be more stable than neighboring axially symmetric cases.

Even though we have considered only a very simple physical model, the difficulties arising from the three space space dimensions are enough to nearly exhaust the capacity of the CDC 6600 computer.

2. Magnetohydrodynamics Model.

We are interested in the problem of containment of an ionized gas, or plasma, by a strong magnetic field. Therefore our aim is to investigate the equilibrium of a conducting fluid in the presence of a magnetic field.

Magnetohydrodynamics is one of the models describing this behavior. The model is appropriate because it combines reasonable physical accuracy with mathematical simplicity.

In this approach, the plasma is considered to be a classical perfectly conducting fluid, characterized by its density ρ, its entropy S and its flow velocity u. The pressure is then a function of ρ and S. The magnetic field B and the current J interact with the plasma and exert a Lorentz force $J \times B$ on the plasma. In order to obtain a simple mathematical model, we neglect displacement currents, electrostatic forces and charge density. Similarly, the effects of viscosity and heat conduction will be omitted [1]. The basic principles which describe magnetohydrodynamic flow are Maxwell's equations and Newton's second law of motion, together with the laws of conservation of mass and energy.

2.1. The Lundquist Equations

According to Ohm's Law for a perfect conductor we have

$$E = B \times u \tag{1}$$

where E is the electric field vector. Since the displacement current is neglected, from Maxwell's equations we can express J in terms of the magnetic field by

$$J = \nabla \times B \tag{2}$$

and the Lorentz force per unit volume of fluid becomes

$$J \times B = - B\times(\nabla\times B) \ .$$

It is now possible to eliminate all of the electromagnetic variables except B. From Maxwell's equations we have

$$\nabla\cdot B = 0 \tag{3}$$

and Faraday's law of induction gives

$$\frac{\partial B}{\partial \tau} + \nabla\times E = 0$$

Using (1), (2) and putting $d/d\tau = \partial/\partial\tau + u\cdot\nabla$, Faraday's law reduces to

$$\frac{dB}{d\tau} + (\nabla\cdot u)B - (B\cdot\nabla)u = 0 \tag{4}$$

Newton's second law of motion yields

$$\rho \frac{du}{d\tau} + \nabla p + B\times(\nabla\times B) = 0 \tag{5}$$

where the last term represents the Lorentz force exerted on

the fluid by the magnetic field. The continuity equation for the fluid is

$$\frac{1}{\rho}\frac{d\rho}{d\tau} + \nabla\cdot u = 0 \tag{6}$$

We assume that the pressure and density of the fluid are connected with the entropy by an equation of state of the form

$$p = A(S)\rho^{\gamma} \tag{7}$$

where γ is the ratio of specific heats. The law of conservation of energy then states

$$\frac{dS}{d\tau} = 0 \tag{8}$$

The system of equations (4)-(8) together with the initial condition (3) are known as the Lundquist equations.

2.2 Equilibrium Equations

In this paper we shall be concerned with determining configurations of static equilibrium in magnetohydrodynamics for a perfectly conducting fluid which is contained by a magnetic field. In this case there is no flow and, therefore, $u \equiv 0$.

As a result of Ohm's law, the electric field E must also be zero. Next equation (6) states that

$$\frac{d\rho}{d\tau} = 0$$

and ρ must be a constant. Thus, for equilibrium, the Lundquist equations reduce to the system

(9) $$\nabla \cdot B = 0$$

(10) $$\nabla p + B \times (\nabla \times B) = 0$$

In order to derive boundary conditions to be imposed at the interface between two distinct media, we first have to convert (9) and (10) into integral relations which will determine the jumps of B and p across such a surface of discontinuity.

Let D be an arbitrary region. Applying the divergence theorem to (9) we have

(11) $$\iint_{\partial D} B \cdot n \, dS = 0$$

where ∂D is the boundary of D, n its normal and dS the area element on ∂D.

A combination of (9) and (10), and another application of the divergence theorem yields

(12) $$\iint_{\partial D} [(p + \frac{1}{2} B^2)n - (B \cdot n)B] \, dS = 0$$

Assume D lies across an interface Γ which separates two distinct media. Both of the integral relations (11) and (12) remain valid, even if the domain taken is arbitrarily small. Under the assumption that B is bounded, we obtain that $B \cdot n = 0$ on Γ and $B^2/2 + p$ must be continuous across Γ .

2.3 Description of the Physical Problem

We shall describe the equilibrium problem which will be considered. Let D_1 be the region occupied by the plasma, surrounded by a vacuum region D_2. The common boundary separating the plasma and vacuum regions will be denoted by Γ, and the outer boundary of D_2 will be denoted by C. We shall assume further that the location of C is fixed, and that it has a toroidal shape. The location of Γ is determined by the equilibrium position of the plasma (Figure 1).

We shall make the extra assumption that inside the plasma the current is zero; i.e., all the current is carried on the interface Γ (skin current). This assumption will be justified later in Chapter 3, by an application of the variational principle.

It follows from (2), (9) and (10) that B_1, the magnetic field inside the plasma satisfies

$$\nabla \cdot B_1 = 0 \tag{13}$$

$$\nabla \times B_1 = 0 \tag{14}$$

and that the pressure p reduces to a constant.

No current exists in the vacuum. Hence, it follows from (2) and (9) that B_2, the magnetic field in the vacuum, satisfies

$$\nabla \cdot B_2 = 0 \tag{15}$$

$$\nabla \times B_2 = 0 \ . \tag{16}$$

At the common boundary Γ between D_1 and D_2, the jump conditions which we derived in the last section yield the boundary conditions on Γ

$$\frac{1}{2} B_1^2 + p = \frac{1}{2} B_2^2 \tag{17}$$

$$B_1 \cdot n = B_2 \cdot n = 0 \tag{18}$$

where n is the normal to Γ, and $\cdot$ denotes the scalar product. Similarly, at the outer boundary C of the domain D_2 we have the boundary condition

$$B_2 \cdot n = 0 \tag{19}$$

where n is the normal to C.

In addition to the differential equations (13)-(16), and the boundary conditions (17)-(19), the free boundary problem requires the specification of an appropriate number of periods. The exact number is determined by the geometry of the problem, and in the case of a torus is three. These periods may be specified in two ways, either as fluxes or currents.

Let Ω_1, Ω_2, Ω_3 be the surfaces shown in Figure 1. Then the corresponding fluxes are defined by

$$F_i = \int_{\Omega_i} B \cdot dS , \qquad i = 1,2,3 \tag{20}$$

where dS is the vector area element on Ω_i. Let C_1, C_2, C_3 be the closed loops shown in Figure 1. Then the corresponding currents are defined by

(21) $$I_i = \oint_{C_i} B \cdot d\ell \ , \qquad i = 1,2,3$$

where $d\ell$ is the vector length element on C_i .

Since B_1 and B_2 are curl free, we can find scalar potentials α and β such that

(22) $$B_1 = \nabla\alpha$$
$$B_2 = \nabla\beta$$

It follows that equations (13)-(16) reduce to

(23) $$\Delta\alpha = 0 \quad \text{in} \quad D_1 \ ,$$
$$\Delta\beta = 0 \quad \text{in} \quad D_2$$

and the boundary conditions (17)-(19) reduce to

(24) $$\frac{\partial\alpha}{\partial n} = 0$$
$$\frac{\partial\beta}{\partial n} = 0$$

on Γ,

(25) $$\frac{\partial\beta}{\partial n} = 0$$

on C, and

(26) $$\frac{1}{2}\,(\nabla\alpha)^2 + p = \frac{1}{2}\,(\nabla\beta)^2$$

on Γ. Given the position of the boundary, the differential equations (23) and the boundary conditions (24), (25) together with the specification of the three periods (either (20) or (21)) determine the solutions α and β uniquely up to a constant.

The equilibrium condition (26) represents a balance of forces on the boundary Γ, and it determines the equilibrium position of the free boundary Γ.

3. Variational Principle for the Boundary

Of even greater importance than the computation of configurations of magnetohydrodynamic equilibrium is the determination of their stability. We choose a method which gives some indication of stability, for the numerical scheme we use is based on the idea of making the energy a minimum by the method of steepest descent.

As described in the previous chapter, to determine the solution of the differential equations we must prescribe three periods, which may be specified as fluxes or currents. However, Maxwell's equations with boundary conditions

$$B\cdot n = 0 \ , \quad (E+u\times B)\cdot \ell = 0$$

at the interface moving with fluid velocity u (where n and ℓ are unit vectors in the normal and tangential directions respectively) imply that the fluxes are constants of the motion [8]. To prove this statement let $\Omega_i(t)$ be the position of Ω_i at time t, and let $F_i(t)$ be the flux across Ω_i at time t. Then

$$\frac{dF_i}{dt} = \frac{d}{dt} \int_{\Omega_i(t)} B\cdot dS$$

$$= \int_{\Omega_i(t)} \left[\frac{\partial B}{\partial t} + (\nabla\cdot B)u\right]\cdot dS + \int_{L_i(t)} B\times u\cdot d\ell$$

where u is the velocity of the surface Ω_i, dS is the vector area element on Ω_i, L_i is the closed loop which bounds Ω_i, and $d\ell$ is the directed length element on L_i.

From Maxwell's equations, and from the initial condition $\nabla \cdot B = 0$, we have that $\nabla \cdot B = 0$ for all t. Using Faraday's law of induction, the last equation reduces to

$$\frac{dF_i}{dt} = - \int_{\Omega_i(t)} \nabla \times E \cdot dS + \int_{L_i(t)} B \times u \cdot d\ell$$

$$= - \int_{L_i(t)} (E + u \times B) \cdot d\ell = 0$$

Thus in order to obtain a physically meaningful equilibrium, we must choose a formulation in which the fluxes are kept fixed for different positions of the free boundary Γ.

If we assume that the problem has a certain type of symmetry, for example, axial or helical symmetry, we can introduce a flux function which satisfies Laplace's equation with given boundary values (the prescribed fluxes). In the general case of a fully three dimensional problem, no such single flux function exists and we are forced to work with the scalar potentials α and β .

In this chapter, a variational principle is formulated to find the equilibrium position of the plasma boundary which corresponds to a minimum of energy of the system.

3.1. The First Variation of the Energy.

We will determine the position of the free boundary by applying the method of steepest descent to the following variational principle associated with the free boundary

problem. Among all admissible boundaries Γ^*, each of which defines domains D_1 and D_2 in which we can find potentials α and β satisfying the equations (23) and the boundary conditions (24), (25) subject to the constraints (20), the appropriate free boundary Γ is characterized by the property that the energy E of the system is a minimum for a fixed mass M of plasma.

The appropriate expression for the energy of the system is [2]

$$E = \frac{1}{2}\int_{D_1} B_1^2 \, dV + \frac{1}{2}\int_{D_2} B_2^2 \, dV + \int_{D_1} e \, dV \tag{27}$$

where $e = p/(\gamma-1)$ is the internal energy per unit volume of the fluid. The first term represents the magnetic energy E_1 in the plasma, the second term represents the magnetic energy E_2 in the vacuum, and the last term E_3 represents the internal energy of the fluid.

To each position of the free boundary Γ we have associated a unique value of the energy $E(\Gamma)$ by requiring that the magnetic fields satisfy

$$\begin{aligned} \nabla\times B_i &= 0 \\ \nabla\cdot B_i &= 0 \end{aligned} \qquad i = 1,2$$

subject to the constraints (20), boundary conditions (18), and that the pressure p = constant. For this procedure to be physically meaningful, $E(\Gamma)$ must correspond to the minimum energy for all admissible states. To prove this

let $E(B_i,p)$ be the energy corresponding to a state characterized by magnetic fields B_i and pressure p, subject to $\nabla\cdot B_i = 0$, $\int_V \rho\, dV = M$, constraints (20) and boundary conditions (18).

If we minimize $E(B_i,p)$ within this class of states, the Euler equations for the variational problem yield

$$\nabla\times B_i = 0 \qquad i = 1,2$$

$$p = \text{constant}$$

so that

$$E(\Gamma) = \min_{B_i,p} E(B_i,p) \ .$$

For computational purposes, this variational principle is not practical in the case of a fully three dimensional problem. Instead, we use the reciprocal variational principle in which we maximize the magnetic energy subject to the constraint $\nabla\times B_i = 0$. That is, we use the same boundary conditions, constant fluxes but we replace the constraint $\nabla\cdot B_i = 0$ by the constraint $\nabla\times B_i = 0$. In this case, the Euler equations yield

$$\nabla\cdot B_i = 0 \ , \qquad i = 1,2$$

so that the maximum is attained by an admissible state, and because $\nabla\times B_i = 0$ the corresponding energy is minimum among all admissible states. In other words, both procedures yield the same magnetic fields corresponding to the minimum of energy $E(\Gamma)$ among all admissible states.

This is why we are justified in assuming that the current inside the plasma is zero, and we can express B as the gradient of a scalar function.

Going back to the variational principle for the energy $E(\Gamma)$ as a functional of the boundary position we have

Theorem. Let $\delta\nu$ be an arbitrary perturbation of the free boundary Γ along its outer normal (cf. Figure 2). Then

$$\delta E = \int_{\Gamma} \left(\frac{1}{2} B_2^2 - \frac{1}{2} B_1^2 - p\right) \delta\nu \, dS \tag{28}$$

where dS is the area element on Γ.

Proof: Let ψ_1 be the potential for the vacuum region corresponding to the currents $I_1 = 1$, $I_2 = 0$, i.e., ψ_1 satisfies Laplace's equation, Neumann boundary conditions, and its periods are

$$I_1 = \oint_{C_1} \nabla\psi_1 \cdot d\ell = 1 \; ; \qquad I_2 = \int_{C_2} \nabla\psi_1 \cdot d\ell = 0 \; .$$

Similarly, let ψ_2 be the potential for the vacuum region corresponding to $I_1 = 0$, $I_2 = 1$.

It is possible to express the potential β for the vacuum region in terms of ψ_1 and ψ_2 as follows:

$$\beta = c_1\psi_1 + c_2\psi_2 \tag{29}$$

where c_1 and c_2 are scale factors (physically they correspond to the currents for the potential β) which

will be determined so that β satisfies (20) for i = 1,2.

We define the inductance matrix A by

$$A = a_{ij} = \int_{\Omega_i} \nabla\psi_j \cdot dS , \qquad i = 1,2 \tag{30}$$

where dS is the vector area element on Ω_i. From (29) and (30) we have

$$f = Ac \tag{31}$$

where f is a vector whose components are the prescribed fluxes F_1, F_2 and c is a vector whose components are the scale factors c_1, c_2.

An application of Green's theorem shows that

$$a_{ij} = \int_{D_2} \nabla\psi_i \cdot \nabla\psi_j \, dV , \qquad i = 1,2;\ j = 1,2 \tag{32}$$

and furthermore from (29) and (32) we have

$$\int_{D_2} (\nabla\beta)^2 dV = c'Ac > 0 \tag{33}$$

where c' is the transpose of c.

These last two equations prove the well known result that the inductance matrix A is symmetric and positive definite.

We can compute the first variation of the magnetic energy

$$E_2 = \frac{1}{2} \int_{D_2} (\nabla\beta)^2 dV = \frac{1}{2} c'Ac = \frac{1}{2} c'f = \frac{1}{2} f'c .$$

Since f is constant, (31) yields

$$\delta E_2 = \frac{1}{2} f'\delta c = \frac{1}{2} c'A'\delta c = \frac{1}{2} c'A\delta c$$

and

$$\delta c = - A^{-1}\delta A\, c$$

so that

$$\delta E_2 = - \frac{1}{2} c'\delta A\, c \quad . \tag{34}$$

The expression for δA is given by the following

Lemma. We have

$$\delta a_{ij} = - \int_{\Gamma} (\nabla\psi_i \cdot \nabla\psi_j)\, \delta\nu \, dS$$

where dS is the surface area element on Γ .

Proof of the lemma: We will define a variation of D_2 onto D_2^* by introducing the notion of an interior variation of D_2 [1]. Let

$$S_j = S_j(x,y,z) \ , \qquad j = 1,2,3$$

be functions possessing continuous partial derivatives of a sufficiently high order in some neighborhood of D_2 . For small enough choices of ε , the transformation

$$\begin{aligned} x^* &= x + \varepsilon\, S_1(x,y,z) \\ y^* &= y + \varepsilon\, S_2(x,y,z) \\ z^* &= z + \varepsilon\, S_3(x,y,z) \end{aligned} \tag{35}$$

maps D onto D^* in a one-to-one fashion. The location of the fixed boundary C of the domain D_2 must be identical to that of the fixed boundary C^* of D_2^* . Hence,

$$S_1(x,y,z) = S_2(x,y,z) = S_3(x,y,z) = 0$$

for all points (x,y,z) lying on the boundary C . Let $\delta\nu$ be the displacement of the free boundary Γ under such a transformation. Then from (35) we have

$$\delta\nu = \varepsilon\left(S_1 \frac{\partial x}{\partial \nu} + S_2 \frac{\partial y}{\partial \nu} + S_3 \frac{\partial z}{\partial \nu}\right) . \tag{36}$$

We introduce on D_2^* potentials ψ_i^* which satisfy Laplace's equation with Neumann boundary conditions and with periods identical to those of ψ_i , i.e.

$$\Delta\psi_i^* = 0 \quad \text{in} \quad D_2^* , \qquad i = 1,2$$

$$\frac{\partial \psi_i^*}{\partial n} = 0 \quad \text{on} \quad C^*, \Gamma^* , \qquad i = 1,2$$

$$\int_{C_j^*} \nabla\psi_i^* \cdot d\ell = \int_{C_j} \nabla\psi_i \cdot d\ell , \qquad i = 1,2;\ j=1,2$$

and we define

$$a_{ij}^* = \int_{D_2^*} \nabla\psi_i^* \cdot \nabla\psi_j^* \, dV , \qquad i = 1,2;\ j=1,2$$

the inductance matrix in D_2^* , so that

$$\delta a_{ij} = \varepsilon \lim_{\varepsilon\to 0} \frac{a_{ij}^* - a_{ij}}{\varepsilon}$$

We introduce comparison functions ψ_i^{**} defined on D_2^* by

$$\psi_i^{**}(x^*,y^*,z^*) = \psi_i(x,y,z) , \qquad i = 1,2$$

and let

$$a_{ij}^{**} = \int_{D_2^*} \nabla\psi_i^{**} \cdot \nabla\psi_j^{**} , \qquad i = 1,2\ j=1,2.$$

Direct calculation shows that

$$\int_{C_j^*} \nabla\psi_i^{**}\cdot d\ell = \int_{C_j} \nabla\psi_i\cdot d\ell + O(\varepsilon^2)$$

so that ψ_i^{**} and ψ_i, and consequently ψ_i^{**} and ψ_i^*, have the same periods.

The function ψ_i^{**} is not harmonic in D_2^*, but we can appeal to Dirichlet's principle, which states that a_{ij}^* is stationary for solutions of Laplace's equation with Neumann boundary conditions. It follows that

$$a_{ij}^{**} = a_{ij}^* + O(\varepsilon^2)$$

so suffices to prove that

$$a_{ij}^{**} = a_{ij} - \int_\Gamma (\nabla\psi_i\cdot\nabla\psi_j)\ \delta\nu\ dS\ .$$

This last result follows from a direct but lengthy calculation which uses the fact that ψ_i, ψ_j are harmonic functions and satisfy Neumann boundary conditions [1]. This completes the proof of the lemma.

Continuing the proof of the main theorem, we have from (34) and the lemma

$$\delta E_2 = \frac{1}{2}\int_\Gamma (c_1^2\nabla\psi_1^2 + 2c_1c_2\nabla\psi_1\cdot\nabla\psi_2 + c_2^2\nabla\psi_2^2)\ \delta\nu\ dS$$

which by (29) reduces to

$$\delta E_2 = \frac{1}{2}\int_\Gamma (\nabla\beta)^2\ \delta\nu\ dS = \frac{1}{2}\int_\Gamma B_2^2\ \delta\nu\ dS\ . \tag{37}$$

We follow the same procedure to compute the first variation of E_1, the magnetic energy in the plasma. In this case only one period is needed to determine the

potential α , and the inductance matrix reduces to a scalar. Let ψ_3 be the potential for the plasma region corresponding to $I_3 = 1$. Then, instead of (29)-(32) we have

$$\alpha = c_3\psi_3 \tag{38}$$

$$a_{33} = \int_{\Omega_3} \nabla\psi_3 \cdot dS \tag{39}$$

$$F_3 = a_{33}c_3 \tag{40}$$

$$a_{33} = \int_{D_1} (\nabla\psi_3)^2 \, dV \ . \tag{41}$$

We compute the first variation of

$$E_1 = \frac{1}{2} \int_{D_1} (\nabla\alpha)^2 \, dV = \frac{1}{2} \, c_3F_3$$

From (39), and the fact that F_3 is constant, we have

$$\delta E_1 = - \frac{1}{2} \, c_3^2 \, \delta a_{33} \ .$$

Applying the lemma to D_1 we have

$$\delta a_{33} = \int_{\Gamma} (\nabla\psi_3)^2 \, \delta\nu \, dS$$

where the positive sign is due to the fact that $\delta\nu$ is positive along the outer normal to the domain D_1 , but $\delta\nu$ is positive along the inner normal to the domain D_2 .

And finally

$$\delta E_1 = - \frac{1}{2} \int_{\Gamma} (\nabla\alpha)^2 \, \delta\nu \, dS = - \frac{1}{2} \int_{\Gamma} B_1^2 \, \delta\nu \, dS \ . \tag{42}$$

Next we compute the first variation of the internal energy E_3, for a fixed mass M of plasma, with equation of state (7). We have

$$E_3 = \frac{1}{\gamma-1} \int_{D_1} p \, dV$$

$$p = k \rho^{\gamma} \tag{43}$$

$$\int_{D_1} \rho \, dV = M$$

where p and ρ are constant throughout the plasma. From (43) we find

$$\delta E_3 = \frac{1}{\gamma-1} \int_{\Gamma} p \, \delta\nu \, dS + \frac{1}{\gamma-1} \int_{D_1} \delta p \, dV$$

$$\delta p = \frac{\gamma p \, \delta\rho}{\rho}$$

$$\delta M = \int_{D_1} \delta\rho \, dV + \int_{\Gamma} \rho \, \delta\nu \, dS = 0 \, .$$

Since p and ρ are constant in D_1, the last equation implies

$$\int_{\Gamma} p \, \delta\nu \, dS + \int_{D_1} \frac{p \, \delta\rho}{\rho} \, dV = 0$$

which can be written as

$$\int_{D_1} \delta p \, dV = - \gamma \int_{\Gamma} p \, \delta\nu \, dS$$

so that

$$\delta E_3 = \frac{1}{\gamma-1} \int_{\Gamma} p \, \delta\nu \, dS - \frac{\gamma}{\gamma-1} \int_{\Gamma} p \, \delta\nu \, dS$$

(44) $$\delta E_3 = - \int_\Gamma p \, \delta\nu \, dS$$

finally combining (37), (42) and (44) we have

$$\delta E = \delta E_1 + \delta E_2 + \delta E_3 = \int_\Gamma \left(\frac{1}{2} B_2^2 - \frac{1}{2} B_1^2 - p\right) \delta\nu \, dS \ .$$

3.2. The Method of Steepest Descent.

To have equilibrium, it is a necessary and sufficient condition that the first variation δE must be equal to zero. Since $\delta\nu$ is arbitrary, the integrand in (28) must be identically zero. This is, of course, equivalent to the free boundary condition given by (26). The expression for the first variation provides us with a method of updating the position of the free boundary Γ so as to satisfy (26) and find a minimum for E.

We choose a path of steepest descent by setting

(45) $$\delta\nu = - \lambda \left(\frac{1}{2} B_2^2 - \frac{1}{2} B_1^2 - p\right)$$

where $\lambda > 0$ represents a convergence factor. Then δE will be negative, each new position of the boundary Γ will correspond to a lower energy, and by interation we will reach a minimum for which $\delta E = 0$. If such a minimum does not exist, for example if the equilibrium is unstable, the process will not converge.

3.3. Characterization of the Equilibrium Position as a Saddle Point for the Energy.

We have discussed the behavior of the energy as we vary the position of the free boundary. We shall now describe the behavior of the energy when we hold the free boundary fixed but vary the values of the potentials.

We define on D_2

$$\tilde{\mathcal{F}}_1 = \{\psi_1^* \mid I_1 = 0,\ I_2 = 1\}$$

$$\tilde{\mathcal{F}}_2 = \{\psi_2^* \mid I_1 = 1,\ I_2 = 0\}$$

and on D_1

$$\tilde{\mathcal{F}}_3 = \{\psi_3^* \mid I_3 = 1\}$$

Let

$$A^* = \int_{D_2} \nabla\psi_i^* \cdot \nabla\psi_j^* \, dV , \qquad i = 1,2;\ j = 1,2$$

and

$$a_{33}^* = \int_{D_1} \nabla\psi_3^* \cdot \nabla\psi_3^*$$

Then the corresponding expression for the energy E^* as a functional of ψ_i^* is

$$E^*(\psi_i^*) = \frac{1}{2}\,[f'(A^*)^{-1}f + F_3(a_{33}^*)^{-1}F_3] + \frac{p}{\gamma-1}\,V ,$$

where V is the volume of D_1. As we vary ψ_i^* in $\tilde{\mathcal{F}}_i$, E^* is maximum when ψ_i^* is a solution of Laplace's equation with Neumann boundary conditions. We can illustrate this

result by examining the axially symmetric case, for which the matrix A is diagonal. In that case, the expression for the energy reduces to

$$E^*(\psi_i^*) = \frac{1}{2} \sum_{i=1}^{3} F_i (a_{ii})^{-1} F_i + \frac{p}{\gamma-1} V$$

and by Dirichlet's principle we have that a_{ii} is minimum for ψ_i^* solving Laplace's equation with Neumann boundary conditions. Therefore, the last equation shows that E^* is maximum.

Let $E(\Gamma)$ denote the value of this maximum for a given position of the boundary Γ. As we vary Γ, a stationary point of $E(\Gamma)$ corresponds to an equilibrium position and a minimum of $E(\Gamma)$ corrresponds to a stable equilibrium. If such a minimum exists, the energy at the equilibrium position is given by

$$E = \min_{\Gamma} E(\Gamma) = \min_{\Gamma} \max_{\psi_i^*} E^*(\psi_i^*)$$

It follows that the problem viewed as a whole is a minimax problem. In other words, the equilibrium position corresponds to a saddle point of the energy. This characteristic of the solution is due to the fact that we have used a formulation in terms of a potential instead of a flux function.

3.4. Remarks on the Method.

The advantages of this method are the following: We have reduced the problem to the solution of three scalar

equations. This formulation allows us to express the first variation of the energy in terms of the first variation of Dirichlet's integral, so that we can use Dirichlet's principle. Furthermore, from the computational point of view, we have to solve Laplace's equation with fixed current , which are the natural periods for the potentials.

The disadvantage is that we have a minimax problem, and this requires that for each position of the boundary Laplace's equation must be solved very accurately.

The solution is obtained by the following steps:

1. We guess a position of the free boundary, and solve for the potentials ψ_1, ψ_2, ψ_3.
2. We compute the inductance matrix and use it to compute the scale factors c_1, c_2, c_3 so that (31) and (40) are satisfied.
3. We use the method of steepest descent to find a new position of the boundary Γ . The process is terminated when the free boundary condition (17) is satisfied within a given accuracy.

The next chapter deals with a numerical method for computing the solutions for the potentials ψ_1, ψ_2, ψ_3 for any given boundary Γ and a numerical method for updating the boundary position.

4. Discrete Variational Principle for Laplace's Equation

The basic difficulty in developing a numerical scheme for a free boundary problem is to be able to handle the changing shape and location of the free boundary. If the problem involves two independent variables, conformal mapping techniques can be used [3,4] to solve the problem in a fixed auxiliary domain R, and then the region of solution is given as the conformal image of R. Thus, the problem of computing the location of the free boundary is transferred to that of finding such a conformal mapping.

In the general case of three independent variables, no such conformal mapping exists, but the basic idea of mapping the flow region into a fixed auxiliary domain R can be used. In this case, since the mapping is not conformal, the equation in R will be more complicated, which in turn means that finding the solution will require a greater amount of computation. Nevertheless, our experience shows that solving the problem directly in the flow region is practically impossible due to the changing location of the free boundary.

The first step is to choose an appropriate coordinate system, so that the mapping and the resulting numerical scheme in the auxiliary domain are as simple as possible. Thus we keep the amount of computation to a minimum.

The second step is to write a numerical scheme for the partial differential equation and boundary conditions in

the auxiliary domain. There are three problems to be considered here. The first one is how to write the equation on the boundary using Neumann boundary conditions. The second is how to get a compatible system of difference equations. If we write the difference equations as a system of the form $Ax = b$, the coefficient matrix A has zero determinant because a constant is a solution of the homogeneous problem. Therefore, in order for a solution x to exist, the system $Ax = b$ must be compatible. The third problem is how to write the difference equations for singular points of the coordinate system like those in the case of cylindrical coordinates where $r = 0$.

These problems can be solved by using a discrete variational principle for Laplace's equation. Since Neumann boundary conditions are the natural boundary conditions for Laplace's equation, we can get the equations for boundary points by varying the values of the solution on the boundary, and they will automatically satisfy the boundary conditions. Since the difference equations are derived from a variational principle, the resulting system will be compatible. The variation of the solution at the singular points yields the appropriate mean value theorem for the solution at the singular points.

The third step is to write a numerical scheme for the updating of the position of the free boundary. Again, the appropriate approximation is suggested by the variational principle.

4.1. Coordinate System.

We choose an orthogonal system of coordinates r,ϕ,θ as follows (cf. Figure 3): First, we draw a circle of radius a corresponding to the major radius of a torus, which we center at the origin on the plane $z = 0$. Let the angle θ be the same as in cylindrical coordinates. In the plane θ = constant, with origin at the intersection with the circle of radius a, we use a polar coordinate system r, ϕ.

We assume that the circle of radius a on the plane $z = 0$ is always inside the plasma region D_1. This restriction can later be lifted if we replace the circle of radius a by any given closed curve in space, and we define a polar coordinate system on the plane θ = constant with origin at the intersection with the given curve. In this case, the restriction would be that the given curve has to be inside the plasma region.

The transformation of coordinates we have described is given by

$$x = (a + r \cos \phi) \cos \theta$$

$$y = (a + r \sin \phi) \sin \theta$$

$$z = r \sin \theta$$

and its Jacobian J is

$$J = \frac{\partial(x,y,z)}{\partial(r,\phi,\theta)} = r(a + r \cos \phi) \ .$$

The transformation is one-to-one for $0 < r < a$. We have singular points for $r = 0$ (in our case r is always less than a).

The expression for the gradient is given by

$$\nabla\psi(r,\phi,\theta) = \psi_r \hat{e}_r + \frac{\psi_\phi}{r}\hat{e}_\phi + \frac{\psi_\theta}{a+r\cos\phi}\hat{e}_\theta$$

where $\hat{e}_r$, $\hat{e}_\phi$, $\hat{e}_\theta$ are unit vectors in the r,ϕ,θ directions.

A general surface such as the free boundary will be given by $r = f(\phi,\theta)$, and f = constant corresponds to an axially symmetric torus with circular cross section.

4.2. Variational Principle for Laplace's Equation in the Vacuum Region.

Let the equations for the outer boundary C and the free boundary Γ be given by:

$$C: \quad r = x(\phi,\theta)$$

$$\Gamma: \quad r = f(\phi,\theta)$$

We define a mapping from the vacuum region D_2 onto D_2^* by

$$(46) \qquad \begin{aligned} s &= \frac{r-f(\phi,\theta)}{x(\phi,\theta) - f(\phi,\theta)} \\ \phi &= \phi \\ \theta &= \theta \end{aligned}$$

for $f \le r \le x$; $0 \le \phi \le 2\pi$; $0 \le \theta \le 2\pi$; so that

$$D_2^* = \{(s,\phi,\theta) \mid 0 \le s \le 1,\ 0 \le \phi \le 2\pi,\ 0 \le \theta \le 2\pi\}$$

and the corresponding images of C and Γ are

$$C^* = \{(s,\phi,\theta) \mid s = 1;\ 0 \le \phi \le 2\pi;\ 0 \le \theta \le 2\pi\}$$

$$\Gamma^* = \{(s,\phi,\theta) \mid s = 0;\ 0 \le \phi \le 2\pi;\ 0 \le \theta \le 2\pi\} .$$

In other words, D_2 is mapped onto a rectangle D_2^*, and the surfaces C and Γ are mapped onto planes s = 1 and s = 0 (cf. Figure 4).

Let $\psi(r(s,\phi,\theta),\phi,\theta) = g(s,\phi,\theta)$; we want to solve Laplace's equation in D_2^*, with Neumann boundary conditions on C^*, Γ^* and periodicity conditions

$$\int_{C_1} \nabla\psi \cdot d\ell = g(s,\phi+2\pi,\theta) - g(s,\phi,\theta) = I_1$$

(47)

$$\int_{C_2} \nabla\psi \cdot d\ell = g(s,\phi,\theta+2\pi) - g(s,\phi,\theta) = I_2$$

We now state the following variational principle for Laplace's equation. Let $\tilde{\mathcal{F}}$ be the class of all functions ψ with continuous second derivatives in D_2, continuous first derivatives on the boundary, and periodicity conditions

$$\int_{C_1} \nabla\psi \cdot d\ell = I_1 \; ; \qquad \int_{C_2} \nabla\psi \cdot d\ell = I_2 \; .$$

Let $\psi_0 \in \tilde{\mathcal{F}}$ be the function that renders the Dirichlet integral,

$$F(\psi) = \int_{D_2} (\nabla\psi)^2 \, dV$$

stationary. Then ψ_0 satisfies Laplace's equation in D_2, and $\partial\psi_0/\partial n = 0$ on the boundary, for

$$\delta F(\psi_0) = -\int_{D_2} \Delta\psi_0 \, \delta\psi \, dV + \int_{\partial D_2} \frac{\partial\psi_0}{\partial n} \, \delta\psi \, dS = 0$$

and since $\delta\psi$ is arbitrary, we have $\Delta\psi_0 = 0$ in D_2, and

$\partial\psi_0/\partial n = 0$ on ∂D_2.

We now use this variational principle to derive the equation for g in D_2^*. Using (46) we write Dirichlet's integral in D_2^* in the form

$$F(g) = \int_{D_2} (\nabla\psi)^2 \, dV$$

(48)

$$= \int_{D_2^*} (ag_s^2+bg_\phi^2+cg_\theta^2+2dg_dg_\phi+2eg_sg_\theta) \, ds \, d\phi \, d\theta$$

where

$$r(s,\phi,\theta) = s(x-f) + f$$

$$a(s,\phi,\theta) = \frac{r(a+r\cos\phi)}{x-f}\left[1+\frac{(f_\phi(s-1)-sx_\phi)^2}{r^2}+\frac{(f_\theta(s-1)-sx_\theta)^2}{(a+r\cos\phi)^2}\right]$$

$$b(s,\phi,\theta) = \frac{(a+r\cos\phi)(x-f)}{r}$$

$$c(s,\phi,\theta) = \frac{r(x-f)}{a+r\cos\phi}$$

$$d(s,\phi,\theta) = \frac{[f_\phi(s-1)-sx_\phi][a+r\cos\phi]}{r}$$

$$e(s,\phi,\theta) = \frac{[f_\theta(s-1)-sx_\theta]r}{a+r\cos\phi}$$

The Euler equation for (48) yields the following equation for g in D_2^*

$$\frac{\partial}{\partial s}(ag_s+dg_\phi+eg_\theta) + \frac{\partial}{\partial\phi}(bg_\phi+dg_s) + \frac{\partial}{\partial\theta}(cg_\theta+eg_s) = 0 \tag{49}$$

with boundary conditions on C^*, Γ^*

$$\frac{\partial}{\partial s}(a\,g_s + d\,g_\phi + eg_\theta) = 0 \, . \tag{50}$$

4.3. Difference Equations for the Vacuum Region.

The usual approach for deriving difference equations for g would be to write a discrete approximation to equations (49) and (50). Instead, we take as our basic idea the variational principle for Laplace's equation, and we define a second order accurate finite difference approximation to Dirichlet's integral F(g) given by (48). Then F is a function of the values of g at the lattice points, and we apply the variational principle requiring F to be stationary. This last step yields the difference equations for g.

We define on D_2^* a lattice with uniform mesh sizes h_s , h_ϕ , h_θ and approximate the continuous function $g(s,\phi,\theta)$ by

$$g_{ijk} = g(i\,h_s,\ j\,h_\phi,\ k\,h_\theta)\ ,\quad i=0,\ldots,n;$$
$$j=0,\ldots,m;\ k=0,\ldots,m$$

The first step is to write a finite difference approximation to Dirichlet's integral. For each rectangle in the lattice with sides h_s, h_ϕ, h_θ we make a second order accurate difference approximation to the integrand of (48), and write the integral as a sum over all rectangles in the lattice. There are many possible approximations, so we choose one with the minimum number of terms.

Figure 5 shows a rectangle whose vertices numbered from 1 to 8 are points in the lattice. We make the following

second order approximation to the integrand of (48) evaluated at the center 0 of the rectangle. For any function t, let t_{ij} , i,j = 1,...,8 denote the value of t evaluated at the middle point between points i and j. Then

$$a\ g_s^2 = \frac{1}{4}\left[(ag_s^2)_{14} + (ag_s^2)_{23} + (ag_s^2)_{67} + (ag_s^2)_{58}\right]$$

$$b\ g_\phi^2 = \frac{1}{4}\left[(bg_\phi^2)_{21} + (bg_\phi^2)_{78} + (bg_\phi^2)_{65} + (bg_\phi^2)_{34}\right]$$

$$c\ g_\theta^2 = \frac{1}{4}\left[(cg_\theta^2)_{18} + (cg_\theta^2)_{27} + (cg_\theta^2)_{36} + (cg_\theta^2)_{45}\right]$$

$$2dg_s g_\phi = \frac{1}{4}\ d_{10}\left[(g_s)_{67} + (g_s)_{58}\right]\left[(g_\phi)_{78} + (g_\phi)_{56}\right]$$

$$+ \frac{1}{4}\, d_9\left[(g_s)_{41} + (g_s)_{32}\right]\left[(g_\phi)_{43} + (g_\phi)_{12}\right]$$

$$2eg_s g_\phi = \frac{1}{4}\, e_{11}\left[(g_s)_{32} + (g_s)_{67}\right]\left[(g_\theta)_{27} + (g_\theta)_{36}\right]$$

$$+ \frac{1}{4}\, e_{12}\left[(g_s)_{41} + (g_s)_{58}\right]\left[(g_\theta)_{45} + (g_\theta)_{18}\right]$$

where the derivatives are approximated by centered differences. We have then

$$(51)\quad F(g) = h_s h_\phi h_\theta \sum (ag_s^2 + bg_\phi^2 + cg_\theta^2 + 2dg_s g_\phi + 2eg_s g_\theta)_O$$

Using the previous approximation we have $F = F(g_{ijk})$ and the variational principle implies

$$(52)\quad \frac{\partial F}{\partial g_{ijk}} = 0,\ i=0,\ldots,n;\ j=0,\ldots,m;\ k=0,\ldots,m$$

which yields the difference equation for each point ijk in the lattice.

If ijk is an interior point, (52) can be written as

(53) $L_1 + L_2 + L_3 + L_4 + L_5 = 0, \quad i=1,\ldots,n-1;\ j=0,\ldots,m;\ k=0,\ldots,m$

where

$$L_1 = \frac{1}{h_s}\left[(ag_s)_{i+1/2,j,k} - (ag_s)_{i-1/2,j,k}\right]$$

is a centered difference approximation to $\frac{\partial}{\partial s}(ag_s)$

$$L_2 = \frac{1}{h_\phi}\left[(bg_\phi)_{i,j+1/2,k} - (bg_\phi)_{i,j-1/2,k}\right]$$

is a centered difference approximation to $\frac{\partial}{\partial \phi}(bg_\phi)$

$$L_3 = \frac{1}{h_\theta}\left[(cg_\theta)_{i,j,k+1/2} - (cg_\theta)_{i,j,k-1/2}\right]$$

is a centered difference approximation to $\frac{\partial}{\partial \theta}(cg_\theta)$. The derivatives are also approximated by centered differences, so for example

$$(cg_\theta)_{i,j,k+1/2} = \frac{1}{h_\theta} c_{i,j,k+1/2}(g_{i,j,k+1} - g_{i,j,k}) .$$

L_1, L_2, L_3 correspond to the usual difference approximation to the corresponding terms in equation (49). The mixed derivative terms $\frac{\partial}{\partial s}(dg_\phi) + \frac{\partial}{\partial \phi}(dg_s)$ are approximated by

$$\begin{aligned} L_4 = \frac{1}{2h_s h_\phi}\Big[& d_{i+1/2,j+1/2,k}(g_{i+1,j+1,k} - g_{i,j,k}) \\ & - d_{i-1/2,j-1/2,k}(g_{i,j,k} - g_{i-1,j-1,k}) \\ & - \{d_{i+1/2,j-1/2,k}(g_{i+1,j-1,k} - g_{ijk}) \\ & - d_{i-1/2,j+1/2,k}(g_{i,j,k} - g_{i-1,j+1,k})\}\Big] \end{aligned}$$

To interpret this approximation we make the change of variables

$$u = \frac{1}{2} h_u \left(\frac{\phi}{h_\phi} + \frac{s}{h_s}\right)$$

$$v = \frac{1}{2} h_v \left(\frac{\phi}{h_\phi} - \frac{s}{h_s}\right)$$

so that

$$\frac{\partial}{\partial s}(dg_\phi) + \frac{\partial}{\partial \phi}(dg_s) = \frac{1}{2h_\phi h_s}\left[h_u^2 \frac{\partial}{\partial u}(dg_u) - h_v^2 \frac{\partial}{\partial v}(dg_v)\right]$$

and we can see that L_4 is a centered difference approximation to the right-hand side. The mixed derivative terms $\frac{\partial}{\partial s}(eg_\theta) + \frac{\partial}{\partial \theta}(eg_s)$ are approximated by

$$\begin{aligned} L_5 = \frac{1}{2h_s h_\theta} \Big[& e_{i+1/2,j,k+1/2}\left(g_{i+1,j,k+1} - g_{i,j,k}\right) \\ & - e_{i-1/2,j,k-1/2}\left(g_{i,j,k} - g_{i-1,j,k-1}\right) \\ & - \{e_{i+1/2,j,k-1/2}\left(g_{i+1,j,k-1} - g_{i,j,k}\right) \\ & - e_{i-1/2,j,k+1/2}\left(g_{i,j,k} - g_{i-1,j,k+1}\right)\}\Big] \end{aligned}$$

which can be interpreted in a similar way. Equation (53) is a 15 point formula for Laplace's equation in D_2^* instead of a 7 point formula we would get for Laplace's equation in the original domain. This is a consequence of the fact that the mapping is not conformal and therefore the equation in D_2^* contains mixed derivatives.

For boundary points (52) can be written as

$$(54) \quad L_1 + \frac{1}{2}(L_2 + L_3) + L_4 + L_5 = 0, \quad i=0,\ldots,n; \; j,k=0,\ldots,m$$

where by definition the coefficients a,d,e are zero outside the domain, that is

$$a_{-1/2,j,k} = d_{-1/2,j+1/2,k} = e_{-1/2,j,k+1/2} = 0$$

and

$$a_{n+1/2,j,k} = d_{n+1/2,j+1/2,k} = e_{n+1/2,j,k+1/2} = 0$$

The periodicity conditions (47) are given by

$$\begin{aligned} g_{i,m+1,k} &= g_{i,0,k} + I_1 \\ g_{i,-1,k} &= g_{i,m,k} - I_1 \\ g_{i,j,m+1} &= g_{i,j,0} + I_2 \\ g_{i,j,-1} &= g_{i,j,m} - I_2 \end{aligned} \qquad \begin{aligned} &i=0,\ldots,n; \\ &j,k=0,\ldots,m \end{aligned} \tag{55}$$

which together with (53), (54) determine the solution.

4.4. Variational Principle for Laplace's Equation in the Plasma Region.

We follow the same procedure as in the previous case. We define a mapping from D_1 (plasma region) onto D_1^* by

$$\begin{aligned} s &= \frac{r}{f(\phi,\theta)} \\ \phi &= \phi \\ \theta &= \theta \end{aligned}$$

for $0 \leq r \leq f$; $0 \leq \phi \leq 2\pi$; $0 \leq \theta \leq 2\pi$; so that

$$D_1^* = \{(s,\phi,\theta) \mid 0 \le s \le 1,\ 0 \le \phi \le 2\pi;\ 0 \le \theta \le 2\pi\}$$

$$\Gamma^* = \{(s,\phi,\theta) \mid s = 1,\ 0 \le \phi \le 2\pi,\ 0 \le \theta \le 2\pi\}$$

Let $\psi(r(s,\phi,\theta),\phi,\theta) = g(s,\phi,\theta)$. We want to solve Laplace's equation in D_1^*, with Neumann boundary conditions on Γ^*, and periodicity conditions

$$(56) \qquad \int_{C_3} \nabla\psi \cdot d\ell = g(s,\phi,\theta+2\pi) - g(s,\phi,\theta) = I_3$$

Furthermore, since g must be harmonic for s = 0, we require that

$$(57) \qquad g(s,\phi+2\pi,\theta) - g(s,\phi,\theta) = 0 .$$

The expression for Dirichlet's integral has the same form as before (48), where the integral is taken over D_1^* and the coefficients are given by

$$a(s,\phi,\theta) = s(a+sf\cos\phi)\left(1 + \frac{f_\phi^2}{f^2} + \frac{s^2 f_\theta^2}{(a+sf\cos\phi)^2}\right)$$

$$b(s,\phi,\theta) = \frac{a+sf\cos\phi}{s}$$

$$c(s,\phi,\theta) = \frac{sf^2}{a+sf\cos\phi}$$

$$d(s,\phi,\theta) = -\frac{f_\phi(a+sf\cos\phi)}{f}$$

$$e(s,\phi,\theta) = -\frac{s^2 f\, f_\theta}{a+sf\cos\phi}$$

We define on D_1^* the same type of lattice as before. The equations for interior points are the same as before, given by (53). The free surface Γ^* corresponds to s = 1 and the corresponding equations are given by (54) with i=n.

The periodicity conditions (56) and (57) are given by

$$g_{i,m+1,k} = g_{i,0,k}$$

$$g_{i,-1,k} = g_{i,m,k} \qquad i=0,\ldots,n;$$

$$g_{i,j,m+1} = g_{i,j,0} + I_3 \qquad j,k=0,\ldots,m.$$

$$g_{i,j,-1} = g_{i,j,m} - I_3$$

4.5. Laplace's Equation at the Singular Curve

The points in D_1^* with $s = 0$ correspond to points in D_1 with $r = 0$, so they are singular points for the coordinate system. The general solution in the neighborhood of $r = 0$ is of the form $k_1(\theta) + k_2(\theta) \log r + O(r)$ and since we want the solution to be harmonic at $r = 0$, we need $k_2(\theta) = 0$. To achieve this, we must formulate a mean value theorem for $k_1(\theta)$ in terms of the values of the solution at adjacent points.

If g is harmonic at $s = 0$, Laplace's equation implies that $\frac{\partial}{\partial\phi}(bg_\phi) = 0$ at $s = 0$. Consequently, we eliminate the logarithmic solution at $s = 0$ by taking $L_2 = 0$ (since L_2 is the difference approximation to $\frac{\partial}{\partial\phi}(bg_\phi)$).

For any given k

$$g_{0,j,k} = g(0, jh_\phi, kh_\theta) , \qquad j = 0,\ldots,m$$

is the value of the solution for $r = 0$, $\theta = kh_\theta$ (i.e. for all values of j these represent the values of the solution at the same point). It then follows that when we vary the value of the solution at $r = 0$, $\theta = kh_\theta$, we must sum over j

the variations due to the variation of $g_{0,j,k}$, with the condition that $g_{0,j,k}$ is independent of j.

Therefore, the difference equation at a singular point is given by

$$\sum_j \left(L_1 + \frac{1}{2} L_3 + L_4 + L_5\right)_{ijk} = 0 \ , \quad i=0,\ k=0,\ldots,m$$

which corresponds to (54) summed over j, with the additional condition $L_2 = 0$.

4.6. Successive Overrelaxation Method

We solve the difference equations using the successive overrelaxation method [6]. We write the difference equations in the form

$$g_i = \sum_{k=0}^{i-1} \alpha_k g_k + \sum_{k=i+1}^{R} \alpha_k g_k + b_i \ , \quad i=0,\ldots,R$$

and we define a sequence $g_i^{(n)}$ of approximations to the solution as follows

$$g_i^{(n+1)} = (1-\omega) g_i^{(n)} + \sum_{k=0}^{i-1} \alpha_k g_k^{(n+1)} + \sum_{k=i+1}^{R} \alpha_k g_k^{(n)} + b_i$$

where $1 < \omega < 2$ is the relaxation factor. Then $g_i = \lim_{n\to\infty} g_i^{(n)}$ is the desired solution.

4.7. Numerical Method for Updating the Free Boundary Position.

The equation for the free boundary Γ is given by $r = f(\phi,\theta)$, which we approximate in the lattice by

$$f_{jk} = f(j\, h_\phi \ , \ k\, h_\theta) \ , \quad j=0,\ldots,m;\ k=0,\ldots,m$$

and let

$$\Delta_{jk} = \left(\frac{1}{2} B_2^2 - \frac{1}{2} B_1^2 - p\right)_{jk}$$

We denote by $f_{jk}^{(n)}$ the position of the free boundary at the nth step, and by $\Delta_{jk}^{(n)}$ the value of Δ_{jk} evaluated for the free boundary position at the nth step. Making the approximation $\delta\nu = \delta f$, the path of steepest descent is given by

$$f_{jk}^{(n+1)} = f_{jk}^{(n)} - \lambda\Delta_{jk}^{(n)}$$

This formula requires a difference approximation to Δ_{jk}, which will be discussed in the next section.

4.8. Numerical Approximation to the Square of the Gradient on the Free Boundary.

Our experience shows that in order to have a stable numerical scheme, it is crucial that we choose an approximation to the square of the gradient on the boundary which is consistent with the discrete variational principle in the interior. In principle, we could perform a discrete interior variation of the domain, and compute directly the discrete expression for the first variation of the energy. We would get a sum over the boundary which is an $O(h^2)$ approximation to the integral (28). This is the proper expression we should use for our method of steepest descent.

This point is made clear if we compare the solutions for a case of an elliptical cross section, axially symmetric, in only two independent variables. In this case, we know the

solution to be stable, so the scheme should yield solutions for which the residual on the boundary (i.e. the maximum over the boundary for the error in the free boundary condition (17)) is as small as we want. Nevertheless, if we use an approximation to the gradient such that the ϕ and θ derivatives are approximated by centered differences, and the s derivative by a three point formula, we find that the residuals on the boundary will decrease to 10^{-3}, and from that point on the scheme diverges. We also observe that if we split the mesh size in half, the residuals on the boundary will decrease to 10^{-5}, and then diverge.

On the other hand, if we use an approximation to the square of the gradient suggested by the discrete variational principle, the residuals on the boundary decrease to 10^{-12} which is within the round-off error for the CDC 6600 computer, since in this case the residual for Laplace's equation must be less than 10^{-14}.

These facts suggest that it is the terms of $O(h^2)$ in the approximation to the square of the gradient on the boundary which make the numerical scheme unstable in the first case.

We have chosen the expression below for the square of the gradient, as suggested by the variational principle. We have not carried out the exact calculation of the discrete expression for the first variation of the energy, so that the only proof we have that this approximation is

a good one is that it works in practice. From (48) we have that

$$(\nabla\psi)^2 J = a g_s^2 + b g_\phi^2 + c g_\theta^2 + 2d g_s g_\phi + 2e g_s g_\theta = \alpha$$

where $J = \partial(x,y,z)/\partial(s,\phi,\theta)$. To be consistent with the variational principle, we approximate α in the same manner in which we approximated Dirichlet's integral, that is

$$\alpha_{jk} = \frac{1}{4}(\alpha_{j+1/2,k+1/2} + \alpha_{j+1/2,k-1/2} + \alpha_{j-1/2,k+1/2} + \alpha_{j-1/2,k-1/2})$$

and each of the four terms are approximated on the boundary by the same differences which were used for the discrete variational principle. It is important to note that if we had evaluated α_{jk} directly instead of using the previous average, the resulting numerical scheme would be unstable.

Having α_{jk} we define

$$(\nabla\psi)^2_{jk} = \frac{\alpha_{jk}}{J_{jk}}$$

where J_{jk} is the Jacobian evaluated at the point j,k.

5. Results

We will first discuss some of the stability properties of the numerical scheme. It is important to point out that the main difficulties arise from the fact that we have used a formulation in terms of a potential function, which leads to Neumann boundary conditions. Since the mapping is not conformal, in the fixed auxiliary domain the boundary conditions correspond to a linear combination of normal and tangential derivatives (50). The same difficulties are present if we choose the same kind of formulation for a two dimensional problem. Therefore, we can use the two dimensional problem to check and study the properties of our numerical scheme. As it was described in the previous chapter, the main numerical problems were solved by appealing to a discrete variational principle.

We have found that the stability of the successive overrelaxation procedure for a given position of the free boundary is strongly dependent on the ratio of the mesh sizes h_s, h_ϕ, h_θ. The method is most stable and most efficient (i.e. requires fewer iterations) if the mesh sizes are nearly equal.

This point is very well illustrated by the following comparison. For an axially symmetric case (independent of θ), we computed the solution to Laplace's equation with Neumann boundary conditions and fixed boundaries. Keeping constant the total number of points in the mesh, we used mesh sizes

with $h_\phi = 2\pi h_s$ and $h_\phi = h_s$. In the first case the maximum value of the relaxation coefficient ω compatible with convergence was 1.5 and it took 10,000 iterations to solve the equation within an error of 10^{-7}. In the second case, we could use values of ω up to 1.9 and it took only 300 iterations to achieve the same accuracy.

Another practical problem is the computation of the inductance matrix. For a given position of the boundary, we have to allow for a given error in the solution of Laplace's equation in the interior, which in turn will produce an error in the inductance matrix. However, we can minimize this error if we use (32) to compute the matrix, instead of (30). The reason is that the volume integral given by (32) is stationary for solutions of Laplace's equation, so that the error in this case will be of second order. Of course this will require an extra amount of computation, but it is worthwhile since in practice we will perform several iterations in the interior (of the order of four to ten) for each iteration of the boundary.

5.1. Description of the Physical and Numerical Parameters.

The physical parameters to be prescribed for a given geometry are the three fluxes and the mass of the plasma.

Instead of prescribing the mass of the plasma, we prescribed the initial position of the free boundary (thus prescribing the initial volume of the plasma) and the initial

value of the pressure in the plasma. From these two values we computed the mass of the plasma, using an equation of state with $\gamma = 5/3$.

We also chose to prescribe the initial value of the currents I_1, I_2, I_3, and we computed the corresponding fluxes F_1, F_2, F_3 for the initial position of the free boundary. Once the fluxes and mass had been computed for the initial position of the free boundary, they were kept fixed throughout the rest of the computation.

As one of the results we have computed

$$\beta = \left(\frac{p}{\frac{1}{2} B_2^2} \right)_\Gamma$$

the average over the free boundary of the ratio of the plasma pressure to the magnetic pressure in the vacuum. A better parameter which we can compute would be the ratio of the internal energy E_3 to the total energy E of the system, but we will use β since it is widely used in the literature.

We will define two important numerical parameters. First,

$$\varepsilon_\Gamma = \max_\Gamma \frac{\left| \frac{1}{2} B_2^2 - \frac{1}{2} B_1^2 - p \right|}{\frac{1}{2} B_2^2}$$

the absolute value of the maximum error in the equilibrium condition, and second,

$$\varepsilon_D' = \max_{i=1,2,3} \max_{D_j} |\Delta \psi_i|$$

the maximum error for Laplace's equation in the interior,

where D_j is the corresponding domain for ψ_i. The minimax characteristic of the problem requires that we solve Laplace's equation very accurately in order to satisfy the free boundary condition. On the other hand, it is a waste of computation to make ε_D very small when we are still far away from the equilibrium position, In practice, we required ε_D to be small compared to ε_Γ, so that we prescribed

$$\varepsilon_D = \min\ (10^{-4},\ 0.1\ \varepsilon_\Gamma/c_1)$$

where $\min(a,b)$ denotes the minimum between a and b. The choice of the scale factor c_1 is due to the fact that the biggest error in Laplace's equation occurs in the potential ψ_1, which must be multiplied by the factor c_1.

The various convergence factors which occur in the formulation of the problem were determined by trial and error to produce a convergent scheme. For the relaxation factor ω in the successive overrelaxation method we used 1.9 for the vacuum region, and 1.8 for the plasma region. For the relaxation factor λ in the steepest descent method we used values ranging from 0.02 to 0.06.

5.2. Description of the Mesh Size and Computing Time.

For our production runs we have used a mesh with 30 points in the ϕ and θ directions and 12 points in the radial direction, six of which lie in the vacuum region and the other six in the plasma region. The program was

designed by trying to minimize the core space needed. For the mesh size just described, the amount of core needed is 110 K which is one-third of the total core available in the CDC 6600 computer. A program which takes less time per iteration can be written using a larger core space, but for practical purposes this is not convenient.

The computing time for a solution in this kind of a mesh varies with the geometry and stability of the solution. For a stable configuration it takes around 40 minutes to yield a solution with $\varepsilon_\Gamma = 10^{-7}$. In this case, 1800 iterations were needed to solve Laplace's equation for 300 iterations of the boundary position.

We also ran some cases in a bigger mesh to study the dependence of the solution in the mesh size. We started with a mesh with 25 points in the ϕ and θ directions, and 10 points in the radial directions. Then, we split the mesh size in half, getting a mesh with 50 points in the ϕ and θ directions, and 18 points in the radial directions. This gave us 2500 points in the free boundary, but it required 330 K of core space, which is the total capacity of the CDC 6600. In this case, three hours of computing time were required to yield a solution with $\varepsilon_\Gamma = 10^{-6}$ for a stable case.

5.3. Axially Symmetric Torus with Circular Cross-Section.

As a first test of our model, we have studied the equilibrium and stability properties of an axially symmetric torus with circular cross-section. Since we are

specifically interested in the Tokamak, we have used physical parameters comparable to those of the Tokamak. We are mainly interested in studying the stability properties as we vary the aspect ratio; i.e., the ratio of the major radius to the minor radius of the torus.

Our results are similar to those given by Richtmyer et al. in [9], that is, a torus with a small aspect ratio is more stable than one with a larger aspect ratio.

We have studied in particular the cases with ratios 10:4 and 10:3. In practice, for technical reasons the lowest aspect ratio that can be achieved in a Tokamak is around 3, so that the second case corresponds to a ratio which is found in practice.

For a fixed geometry, we studied the dependence of stability properties on the physical parameters. As expected, we found that an increase of the toroidal field (i.e., B_θ) will make the configuration more stable. On the other hand, if we keep the toroidal field fixed and increase the plasma current (i.e. the poloidal field), at some point the configuration will become unstable. Furthermore, if the plasma current tends to zero, no equilibrium exists and the plasma goes all the way to the outer wall.

We measure the stability of a configuration by looking at the convergence of the free boundary condition. We can catalog the results in three different groups, The first one is the case for which ε_Γ converges to zero which indi-

cates that the energy has a minimum at the equilibrium position, and therefore it corresponds to stable equilibrium. The second case for which ε_Γ diverges corresponds to unstable equilibrium or to the fact that equilibrium just doesn't exist. In this instance the energy decreases for each boundary position until the plasma touches the outer wall. In between we have a whole variety of cases for which ε_Γ stays bounded but it does not converge to zero; and the free boundary oscilates around the equilibrium position with amplitudes roughly proportional to ε_Γ.

We believe that the explanation for this behavior lies with the nonlinearity of the free boundary condition. Due to a bifurcation process more than one equilibrium position exists, and as the axially symmetric equilibrium becomes unstable the numerical method is not accurate enough to distinguish between neighboring solutions.

In Table I, results for an aspect ratio of 10:4 are shown. The initial position of the free boundary is a torus of minor radius equal to 3. The initial value of the currents are given by I_1, I_2, I_3 as defined in Chapter 2. Physically I_1 corresponds to the plasma current. The pressure is denoted by p, and β, ε_Γ were defined in Section 5.1. For stable cases, the error ε_Γ decreases rapidly to 10^{-7}, at which point we stopped the process. Therefore when reading the results $\varepsilon_\Gamma = 10^{-7}$ corresponds to a stable case.

In the first four cases denoted by N = 1,2,3,4, we have kept fixed the poloidal field, the plasma pressure and we varied the toroidal field. We see that the first two cases are stable as shown by $\varepsilon_\Gamma = 10^{-7}$. In cases 3 and 4, a very mild instability appears as shown by the value $\varepsilon_\Gamma = 10^{-6}$. This means that the process will not converge any further than 10^{-6}, but on the other hand it will not diverge and the free boundary oscillated around the equilibrium position with extremely small amplitudes.

In cases 5 to 8, we have fixed the values of the currents, but we have changed the values of the initial pressure (i.e. the mass of the plasma). Cases 5 to 7 are stable, and case 8 has a very mild instability.

In general we find that for this aspect ratio, configurations with β up to 0.05 are stable, and configurations with β up to 0.09 are very nearly stable.

In case number 9 the plasma current is extremely small, and in this case an equilibrium configuration does not exist and the plasma expands to the outer wall.

Figure 5.1 shows the equilibrium position for case 1 of Table I. In this case the equilibrium configuration is axially symmetric, and its cross-section is a circle with its center displaced away from the axis of the torus.

In Table II, results for an aspect ratio of 10:3 are shown. The initial position of the free boundary is a torus of minor radius equal to 2.

In cases 1 to 7 we kept fixed the plasma pressure and the plasma current, while we decrease the toroidal field. We can see that ε_Γ increases as the toroidal field decreases, so that the configuration becomes more unstable. In cases 5, 9 to 14 we have kept fixed the toroidal field and we have increased the plasma current and the plasma pressure in such a way that the initial pressure is the average of $\frac{1}{2} B_\phi^2$ (poloidal field) over the free boundary. These results indicate that the configuration becomes more unstable as we increase the plasma current. Cases 4, 15 to 17 show similar results for a different value of the toroidal field.

In general we find that even for values of β as small as 0.02 the configurations are not stable. If we compare the results in Table I and Table II, we conclude that for similar values of β a torus with aspect ratio 10:4 is more stable than a torus with aspect ratio 10:3.

5.4. Axially Symmetric Torus with Elliptical Cross-Section.

One important question which has been raised lately is that of the stability properties of an axially symmetric torus with a noncircular cross-section. In particular we want to compare the stability properties of an elliptical cross-section with those of a circular cross-section.

In Table III, results for an elliptical cross-section are shown. The ratio of the major axis to the minor axis a

of the ellipse is 1.5. Figure 5.2 shows the equilibrium position for case 2 in Table III. In this case the equilibrium configuration is axially symmetric, and the cross-section is an ellipse whose center has been displaced away from the axis of the torus.

From Table III we can draw the following conclusions. Case 1 is stable, as we would expect from its 10:4 aspect ratio. Cases 2 to 4 show that the configuration becomes more unstable as we decrease the toroidal field. A comparison of cases 2 and 3 with cases 6 and 7 shows that the stability becomes much worse as we increase the aspect ratio. Note that cases 2 and 6 correspond to the same value of β, but a small increase in the aspect ratio (from 10:3 to 10:2.45) makes a big difference in the value of ε_Γ .

The conclusion is that the dependence of stability properties on the physical parameters and the aspect ratio is similar for an elliptical cross section to that of a circular cross section.

Using Tables II and III we can compare the stability of an elliptical cross section with that of a circular cross section, for similar physical parameters and aspect ratio. We see that both yield similar results, and that the stability properties are comparable for equal values of β. We conclude then that our model shows that an elliptical cross section and a circular cross section have essentially the same stability properties.

5.5. Configurations without Axial Symmetry.

We have computed equilibrium configurations for several types of three dimensional geometries in order to compare their stability properties with those of axially symmetric cases.

The results shown in Table IV correspond to a torus with circular cross section whose center describes a helix as θ varies in 2π.

In cases 1 to 9 we have kept the physical parameters constant, while we varied the geometry. Case 1 corresponds to the axially symmetric torus and by comparison with the other cases we see that the effect of introducing a helical perturbation in the outer boundary is to make the configuration more stable. The same conclusion holds true if we compare cases 9 and 10. Case 11 is stable as we would expect from its 10:4 aspect ratio.

Figures 5.3 and 5.4 show the outer boundary and free boundary for case 11 in Table IV. We have plotted the surfaces $r = f(\phi,\theta)$ in the coordinate system defined in Chapter 4. It is useful to remember that a plane with r = constant corresponds to an axially symmetric torus with circular cross section. From these figures we observe that the solution for the free boundary is smooth and that it takes the same kind of shape as the outer boundary. By looking at the dependence on ϕ we can see that the plasma surface has been displaced away from the axis of the torus.

Figures 5.5 and 5.6 show the outer boundary and free boundary for case 4 in Table IV . We can clearly see the four helical turns of the outer surface and the free boundary.

The results shown in Table V correspond to a perturbation of the type A cos $(k_1\phi+k_2\theta)$. The results show that for $\beta = 0.09$, cases 3,4,5 are more stable than the axially symmetric case, and for $\beta = 0.28$ there is no improvement.

Figures 5.7 and 5.8 show the outer boundary and free boundary for case 4 in Table V, and figures 5.9 and 5.10 show the outer boundary and free boundary for case 5 in Table V.

The results shown in Table VI correspond to an outer surface which is obtained by rotating an elliptical cross section around its center as θ varies in 2π. They show that the three dimensional configurations obtained are more stable than the axially symmetric case.

5.6. Dependence of the Solutions on the Mesh Size.

To study the dependence of the solution as we vary the mesh size, we ran some of the previous cases for the biggest possible mesh within the capacity of the CDC 6600 computer (described in Section 5.2). We found that changing the mesh size did not change the kind of solutions obtained. That is, those cases which were stable for a smaller mesh were also stable for the bigger mesh and those cases which were unstable yielded the same values of ε_Γ as previously.

We expect the discrete solution to converge as $O(h^2)$ to a continuous solution, as h tends to zero, since all the approximations made were $O(h^2)$. To check this it would be necessary to split the mesh size by half at least two times, which we cannot do because of the limited capacity of the computer. The existence of a continuous solution to the equilibrium problem is another matter, and all we can say is that since the discrete solutions are quite smooth we would expect them to converge to a continuous solution as h tends to zero.

5.7. Conclusions.

The main conclusion is that we have developed a numerical scheme to compute configurations of fully three dimensional magnetohydrodynamic equilibrium, which also allows us to study their stability properties.

Our results show that a torus with small aspect ratio is more stable than one with a large aspect ratio. For the same aspect ratio, an axially symmetric torus with circular cross section and an axially symmetric torus with elliptical cross section have similar stability properties.

We also found several three dimensional configurations which are more stable than neighboring axially symmetric cases. However, the improvement in the stability properties by introducing a three dimensional perturbation of the outer boundary is not nearly as big as the improvement obtained by lowering the aspect ratio. This might not be the case

for three dimensional configurations which are very different from the axially symmetric case, a possibility which we can explore by extending our method to a more general coordinate system as previously discussed.

Bibliography

[1] Garabedian, P. R., Partial Differential Equations, John Wiley and Sons, Inc., New York, 1964.

[2] I. B. Bernstein, E. A. Frieman, M. D. Kruskal and R. M. Kulsrud, Proc. Roy. Soc., London, A244, 1958.

[3] Friedman, N., Computation of the Equilibrium of a Plasma with Helical Symmetry, AEC Computing and Applied Mathematics Center, New York University, Courant Institute Report NYO-1480-161, 1970

[4] Bloch, E., A Finite Difference Method for the Solution of Free Boundary Problems, AEC Computing and Applied Mathematics Center, New York University, Courant Institute Report NYO-1840-116, 1969.

[5] Bloch, E., Numerical Solution of Free Boundary Problems by the Method of Steepest Descent, Physics of Fluids, Vol. 12, part II, 1969.

[6] Young, D., Iterative Methods for Solving Partial Differential Equations of Elliptic Type, Trans. AMS 76, 1954.

[7] Stevens, D., Some Magnetohydrodynamic Free Boundary Equilibria, Physics of Fluids, Vol. 17, No. 7, January 1974.

[8] J. Berkowitz, H. Grad and H. Rubin, Magnetohydrodynamic Stability, Proceedings of the Second International Conference on the Peaceful Uses of Atomic Energy, U.N., Geneva, 1958, Vol. 31.

[9] R. Lüst, R. D. Richtmyer, A. Rotenberg, B. R. Suydam and D. Levy, The Hydromagnetic Stability of a Toroidal Gas Discharge, AEC Computing and Applied Mathematics Center, New York University, Courant Institute Report NYO-2882, 1960.

[10] Friedrichs, K. O., Pinch Buckling, Reviews of Modern Physics, Vol. 32 (1960).

[11] Yeh, T., Bifurcation and Stability of Long-Wavelength Helical Hydromagnetic Equilibria, Physics of Fluids, Vol. 16, No. 4, 1973.

TABLE I

Axially Symmetric - Circular Cross Section

Big Radius 10 Small Radius 4 Plasma Radius 3

No.	I_1	I_2	I_3	2p	β	ε_Γ
1	10	180	180	0.30	0.030	10^{-7}
2	10	150	150	0.30	0.041	10^{-7}
3	10	130	130	0.30	0.054	10^{-6}
4	10	110	110	0.30	0.073	10^{-6}
5	10	180	180	0.10	0.010	10^{-7}
6	10	180	180	0.25	0.024	10^{-7}
7	10	180	180	0.36	0.034	10^{-7}
8	10	180	180	1.00	0.086	10^{-6}
9	1	180	180	0.36	0.030	∞

TABLE II

Axially Symmetric - Circular Cross Section

Major Radius 10 Minor Radius 3 Plasma Radius 2

No.	I_1	I_2	I_3	2p	β	ε_Γ
1	10	270	270	0.65	0.03	10^{-6}
2	10	230	230	0.65	0.04	10^{-6}
3	10	200	200	0.65	0.05	10^{-5}
4	10	180	180	0.65	0.06	10^{-5}
5	10	150	150	0.65	0.09	10^{-2}
6	10	130	130	0.65	0.12	1
7	10	80	80	0.65	0.27	∞
8	10	149	151	0.65	0.09	10^{-2}
9	10	151	149	0.65	0.09	10^{-2}
10	15	150	150	1.47	0.18	10^{-1}
11	20	150	150	2.60	0.28	1
12	25	150	150	4.08	0.38	1
13	30	150	150	5.87	0.47	1
14	40	150	150	10.40	0.60	∞
15	6	180	180	0.23	0.02	10^{-6}
16	8	180	180	0.41	0.04	10^{-6}
17	15	180	180	1.46	0.13	1

TABLE III

Axially Symmetric - Elliptical Cross Section - $\frac{b}{a} = 1.5$

Major Radius 10

No.	Outer Shell a	Plasma a	I_1	I_2	I_3	2p	β	ε_Γ
1	4	3	10	180	180	0.114	0.01	10^{-7}
2	3	2	15	180	180	0.554	0.05	10^{-4}
3	3	2	15	150	150	0.554	0.08	10^{-4}
4	3	2	15	120	120	0.554	0.12	1
5	3	2	20	120	120	0.980	0.19	1
6	2.45	1.63	10	150	150	0.365	0.05	10^{-1}
7	2.45	1.63	10	130	130	0.365	0.07	1

TABLE IV

Major Radius 10 Minor Radius RO Plasma Radius RI

$r^2(\phi,\theta)=RO^2[(\cos\phi+A\cos k_1\theta\cos k_2\theta)^2+(\sin\phi+A\cos k_1\theta\sin k_2\theta)^2]$

No.	RO	RI	A	k_1	k_2	I_1	I_2	I_3	2p	β	ε_Γ
1	3	2	0.0	-	-	10	150	150	0.65	0.09	10^{-2}
2	3	2	0.10	0	2	10	150	150	0.65	0.09	10^{-3}
3	3	2	0.10	0	2	10	150	150	0.65	0.09	10^{-4}
4	3	2	0.15	0	4	10	150	150	0.65	0.09	10^{-4}
5	3	2	0.15	1	1	10	150	150	0.65	0.09	10^{-3}
6	3	2	0.15	2	2	10	150	150	0.65	0.09	10^{-4}
7	3	2	0.15	4	4	10	150	150	0.65	0.09	10^{-4}
8	3	2	0.15	6	6	10	150	150	0.65	0.09	10^{-4}
9	3	2	0.0	-	-	20	150	150	2.61	0.28	1
10	3	2	0.15	0	4	20	150	150	2.61	0.28	10^{-1}
11	4	3	0.10	1	1	10	180	180	0.30	0.03	10^{-7}
12	2	1.33	0.10	2	2	7	180	180	0.71	0.07	10^{-3}
13	3	2	0.15	2	2	10	180	180	0.65	0.06	10^{-5}

TABLE V

Major Radius 10 Minor Radius 3 Plasma Radius 2

$$r(\phi,\theta) = 3(1.0 + A \cos (k_1\phi + k_2\theta))$$

No.	A	k_1	k_2	I_1	I_2	I_3	2p	β	ε_Γ
1	0.0	-	-	10	150	150	0.65	0.09	10^{-2}
2	0.1	0	1	10	150	150	0.65	0.09	1
3	0.1	0	2	10	150	150	0.65	0.09	10^{-3}
4	0.1	1	2	10	150	150	0.65	0.09	10^{-4}
5	0.1	1	4	10	150	150	0.65	0.09	10^{-4}
6	0.0	-	-	20	150	150	2.61	0.28	1
7	0.1	0	8	20	150	150	2.61	0.28	1
8	0.1	1	4	20	150	150	2.61	0.28	1
9	0.1	2	4	20	150	150	2.61	0.28	1

TABLE VI

The outer surface is obtained by rotating the elliptical cross section as we go around the torus. The cross section is rotated k full turns as θ varies in 2π.

Major Radius 10 Elliptical Cross Section $\frac{b}{a} = 1.5$, $a = 3$

No.	k	I_1	I_2	I_3	2p	β	ε_Γ
1	0	15	120	120	0.55	0.12	1
2	1	15	120	120	0.55	0.12	10^{-1}
3	2	15	120	120	0.55	0.12	10^{-1}
4	4	15	120	120	0.55	0.12	10^{-2}

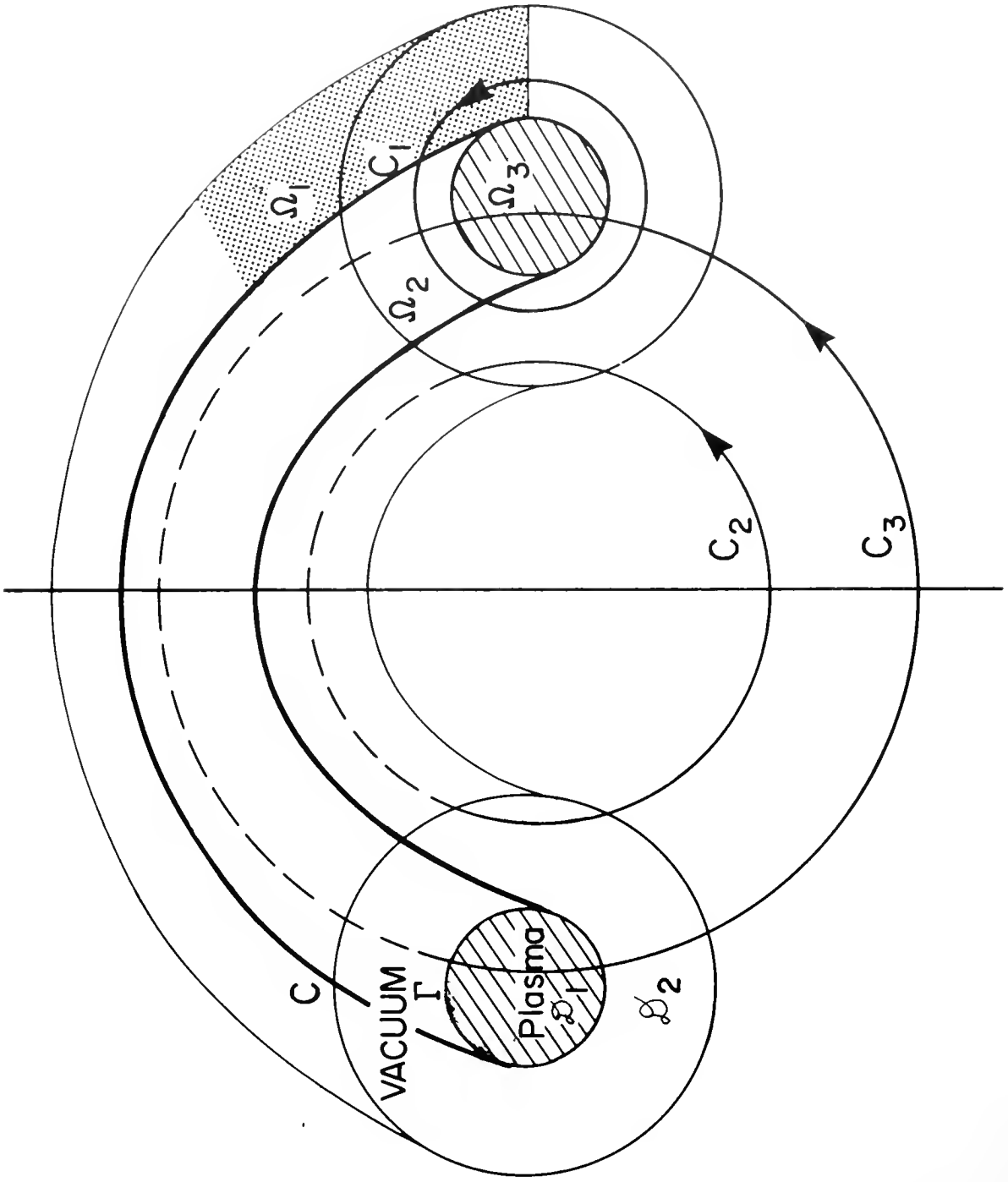
Ω_1
C_1
Ω_3
Ω_2
C_2
C_3
C
VACUUM
Γ
Plasma
Ω_1
Ω_2

fig. I

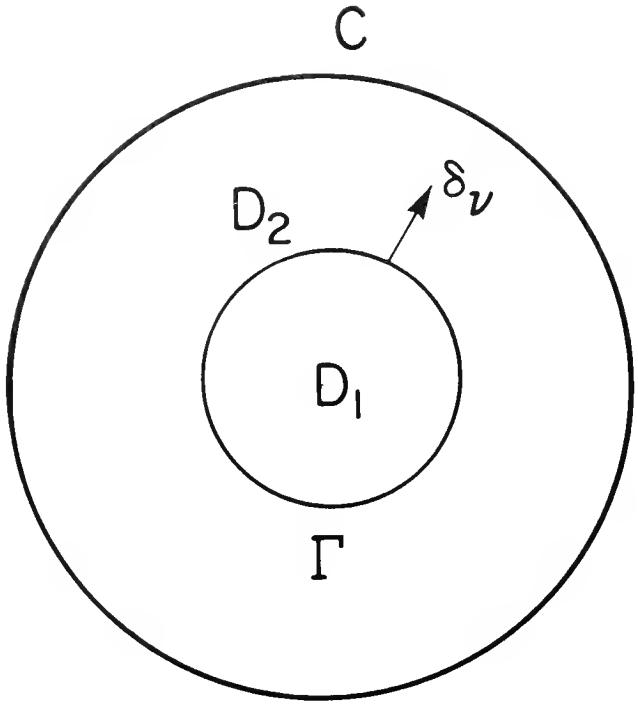

fig. 2

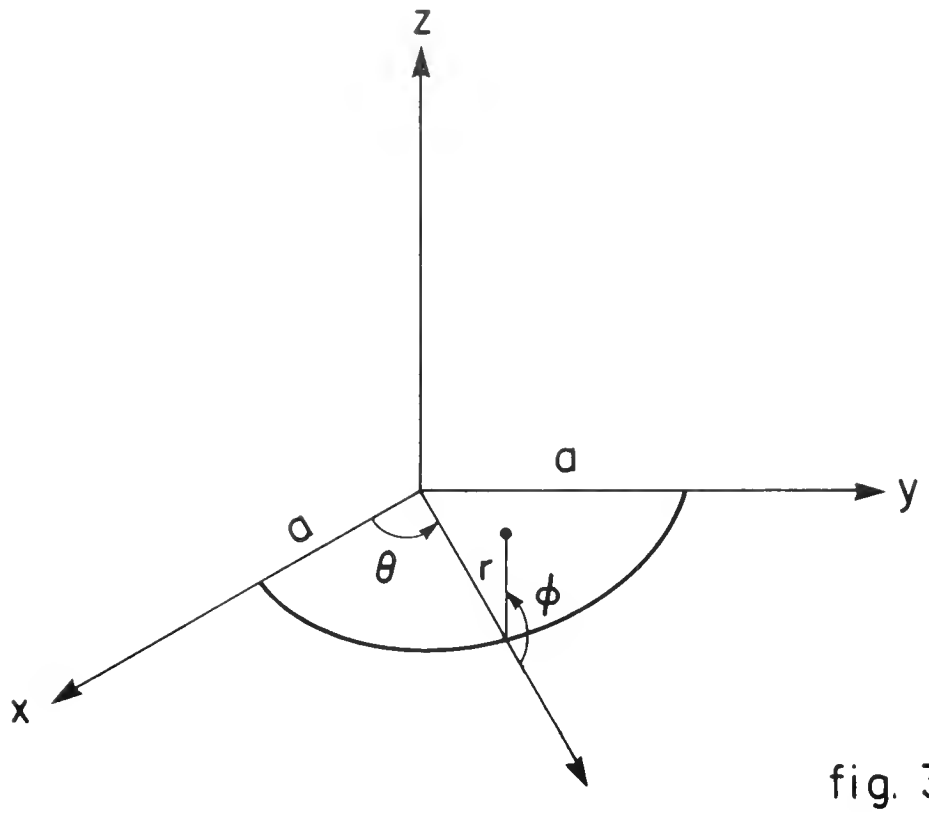

fig. 3

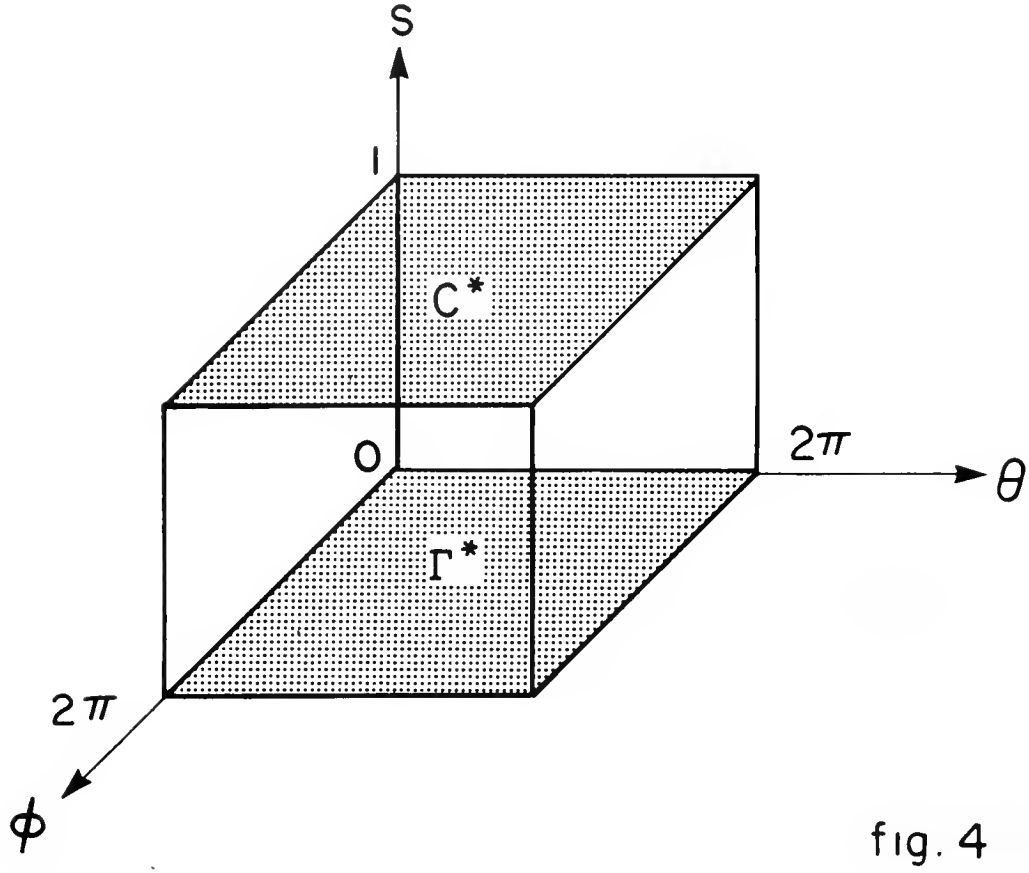

fig. 4

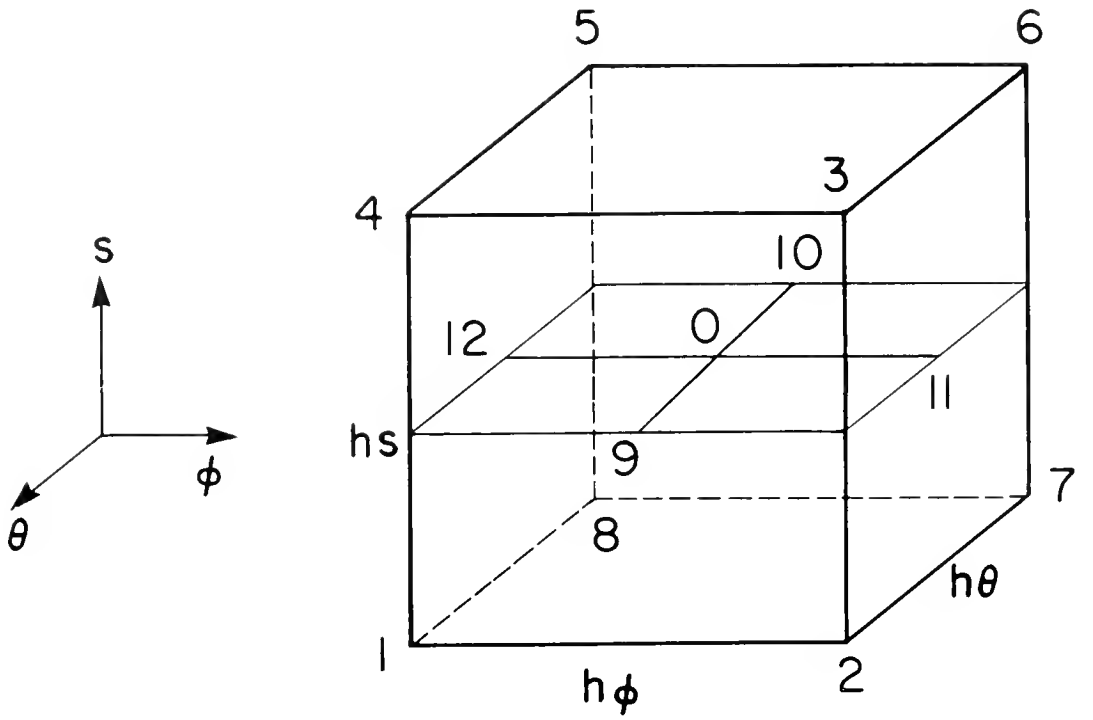

fig. 5

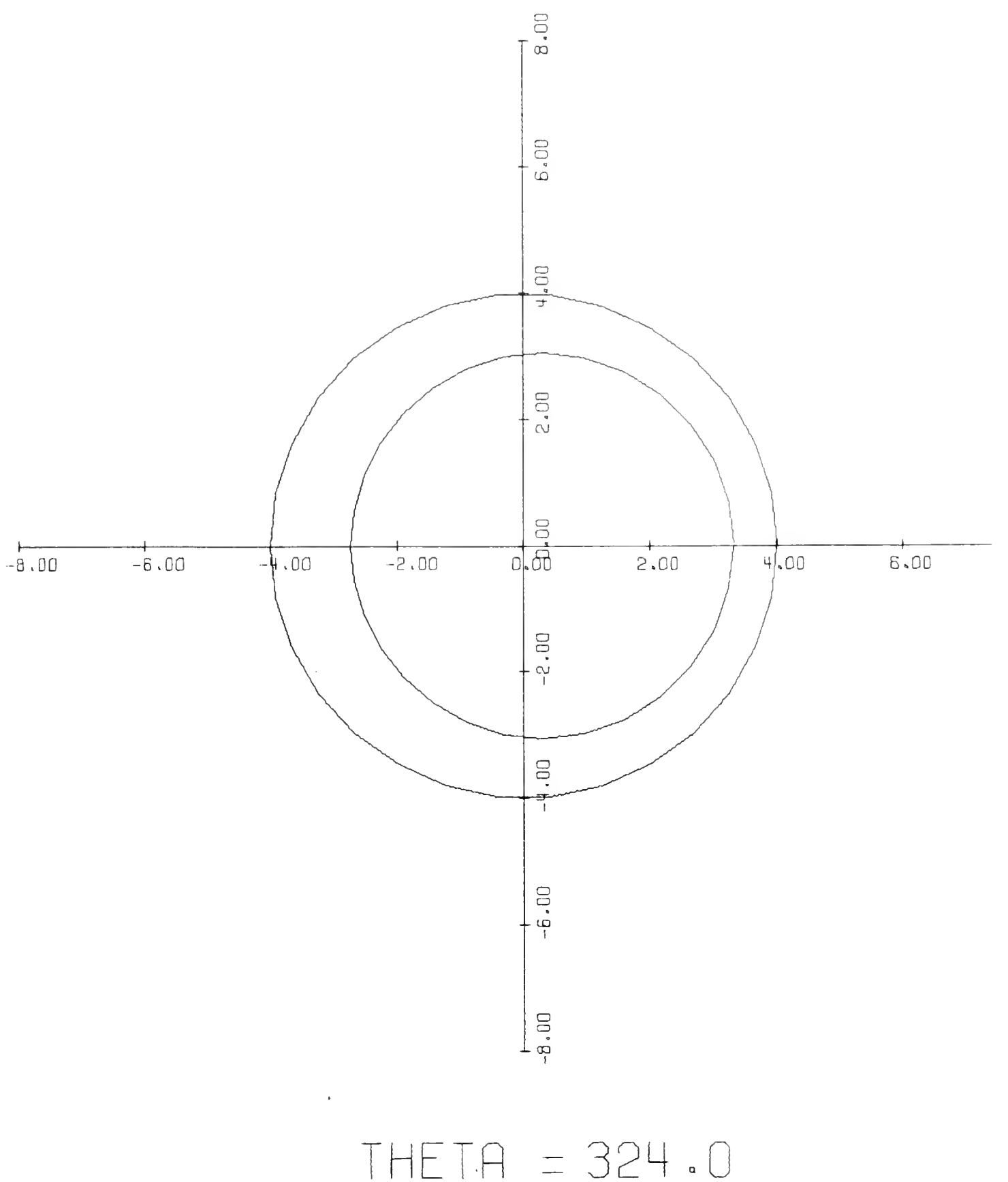

Fig. 5.1. Axially Symmetric Torus with Circular Cross Section.

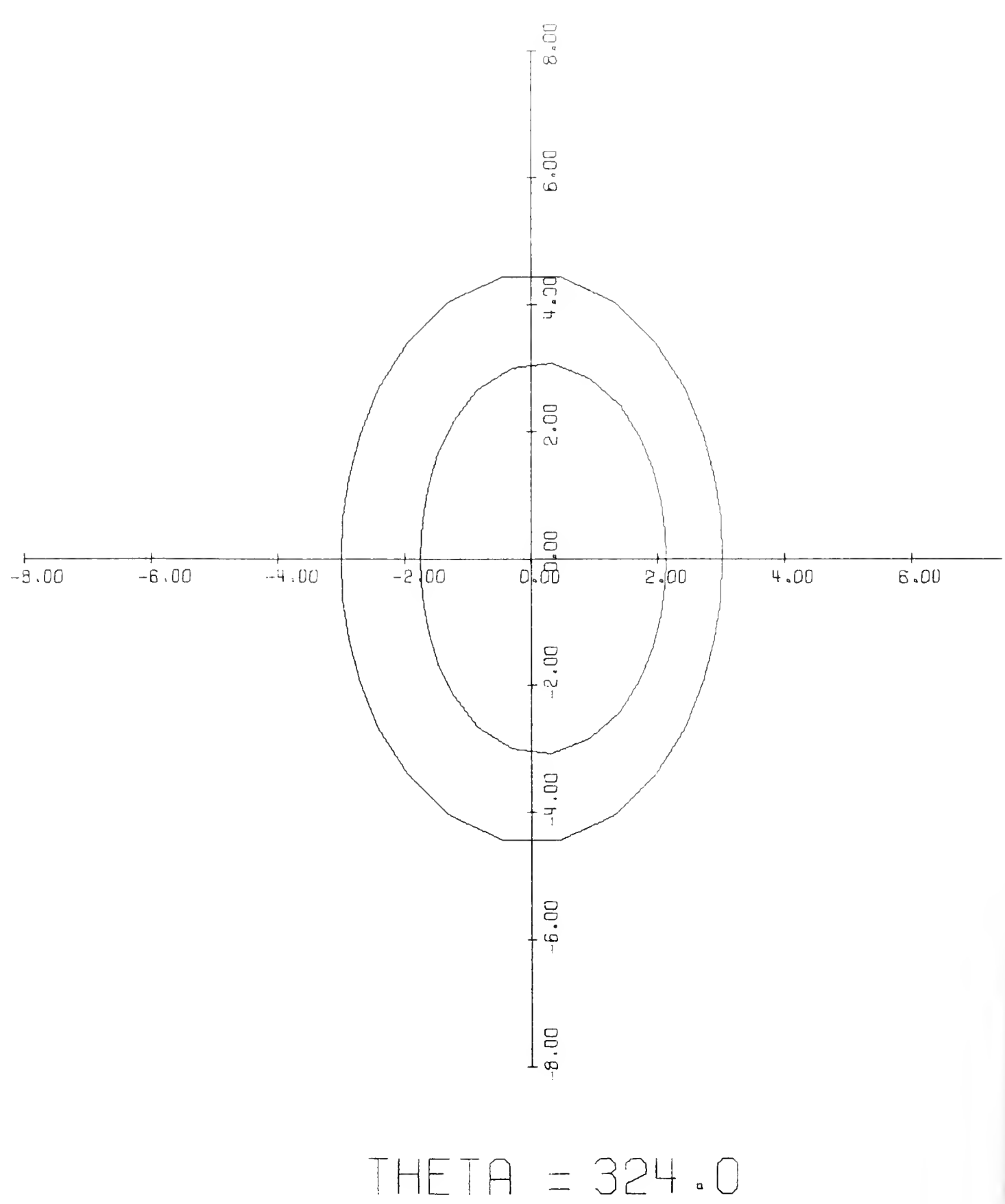

Fig. 5.2. Axially Symmetric Torus with Elliptical Cross Section.

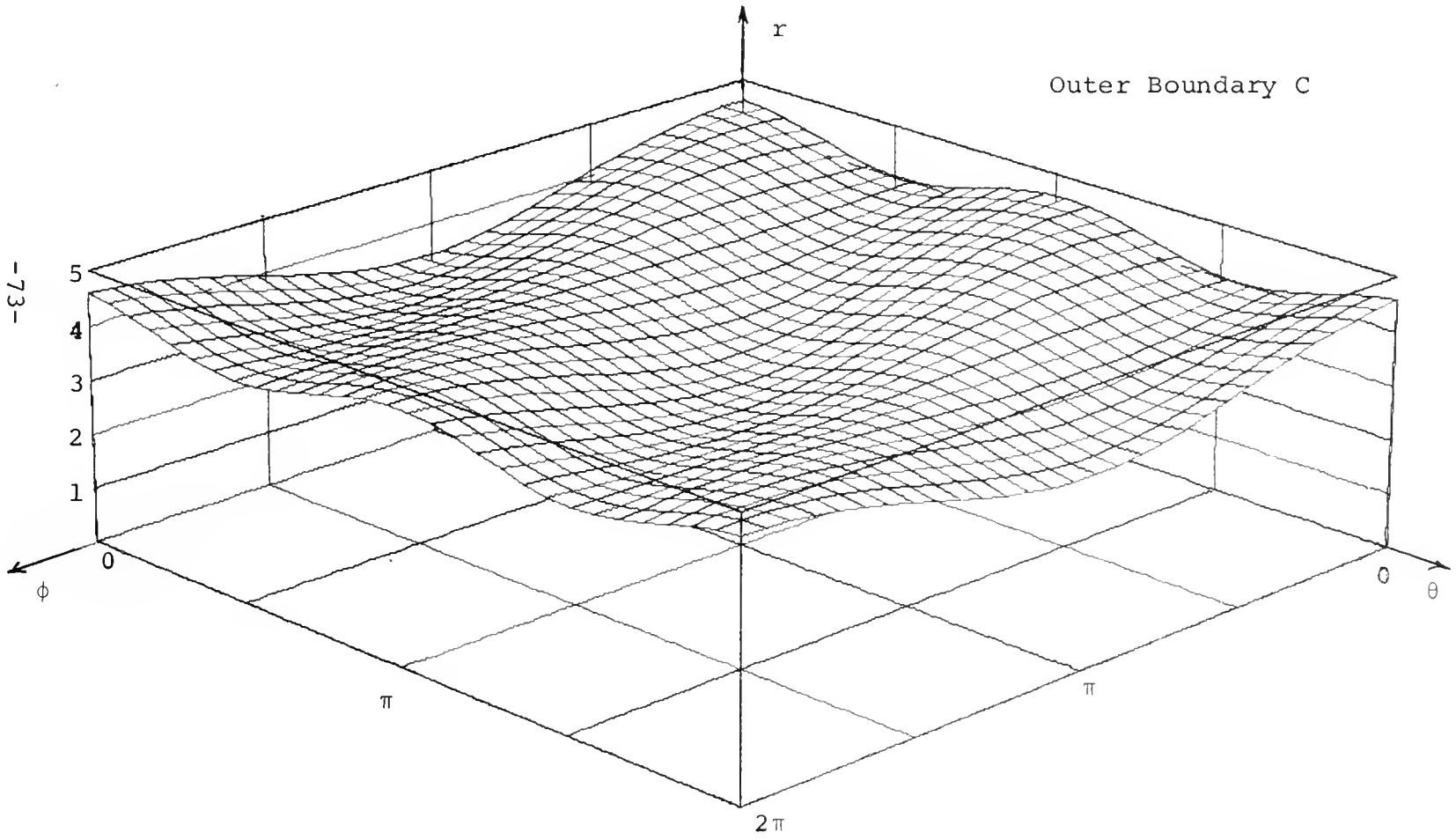

Fig. 5.3. C: $r^2(\phi,\theta) = 16[(\cos\phi + 0.1\cos^2\theta)^2 + (\sin\phi + 0.1\cos\theta\sin\theta)^2]$.

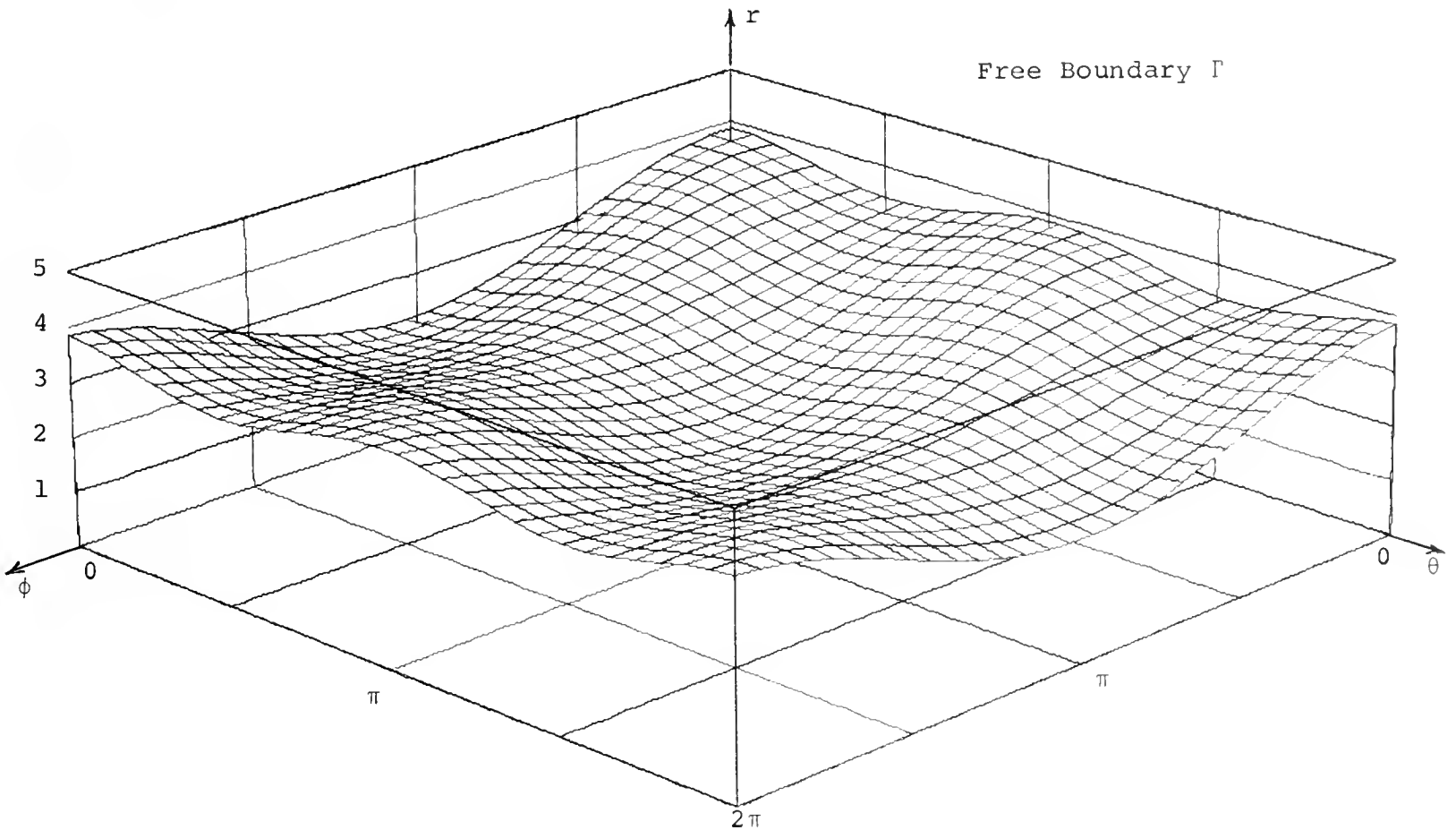

Fig. 5.4. C: $r^2(\phi,\theta) = 16[(\cos\phi + 0.1\cos^2\theta)^2 + (\sin\phi + 0.1\cos\theta\sin\theta)^2]$.

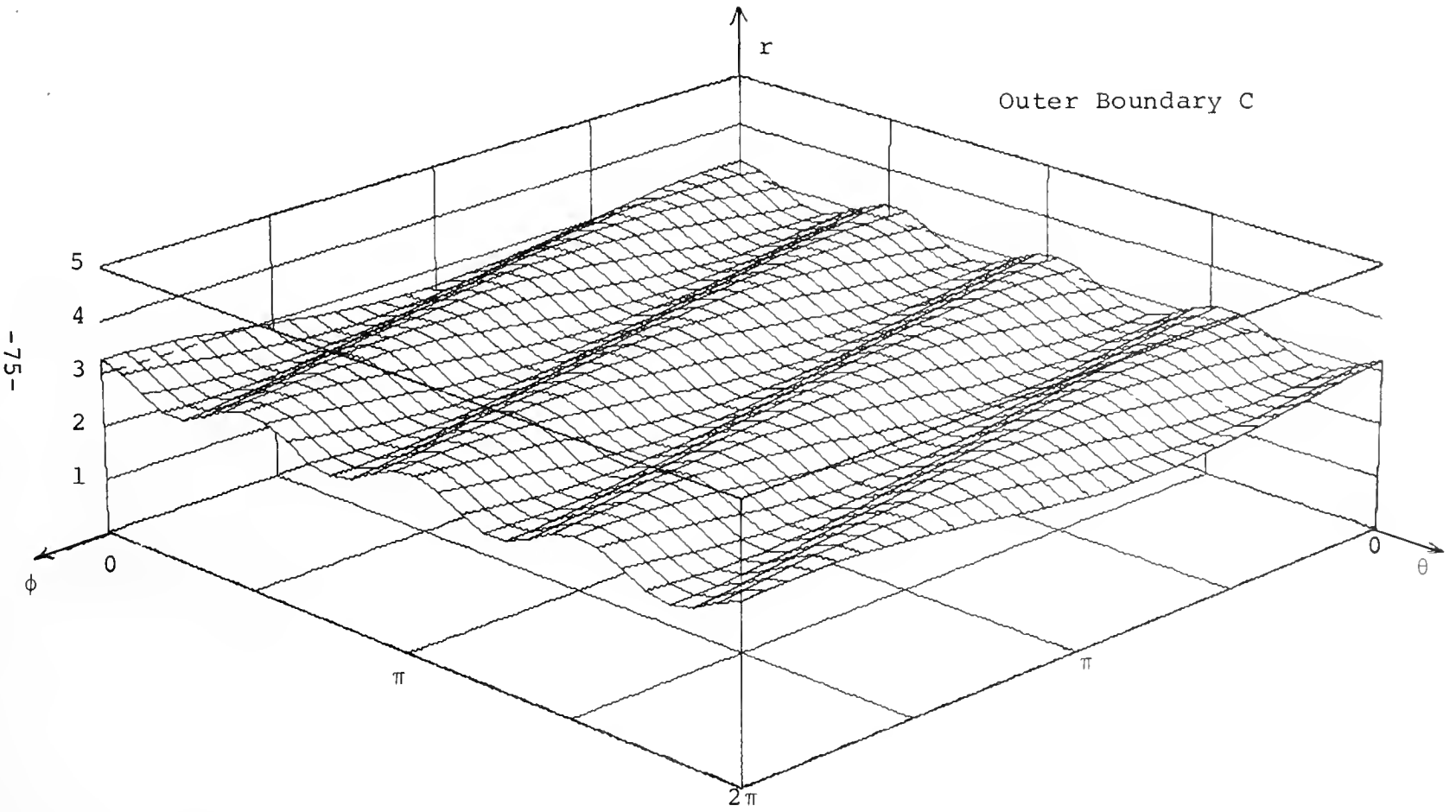

Fig. 5.5. C: $r^2(\phi,\theta) = 9[(\cos\phi + 0.15\cos 4\theta)^2 + (\sin\phi + 0.15\sin 4\theta)^2]$.

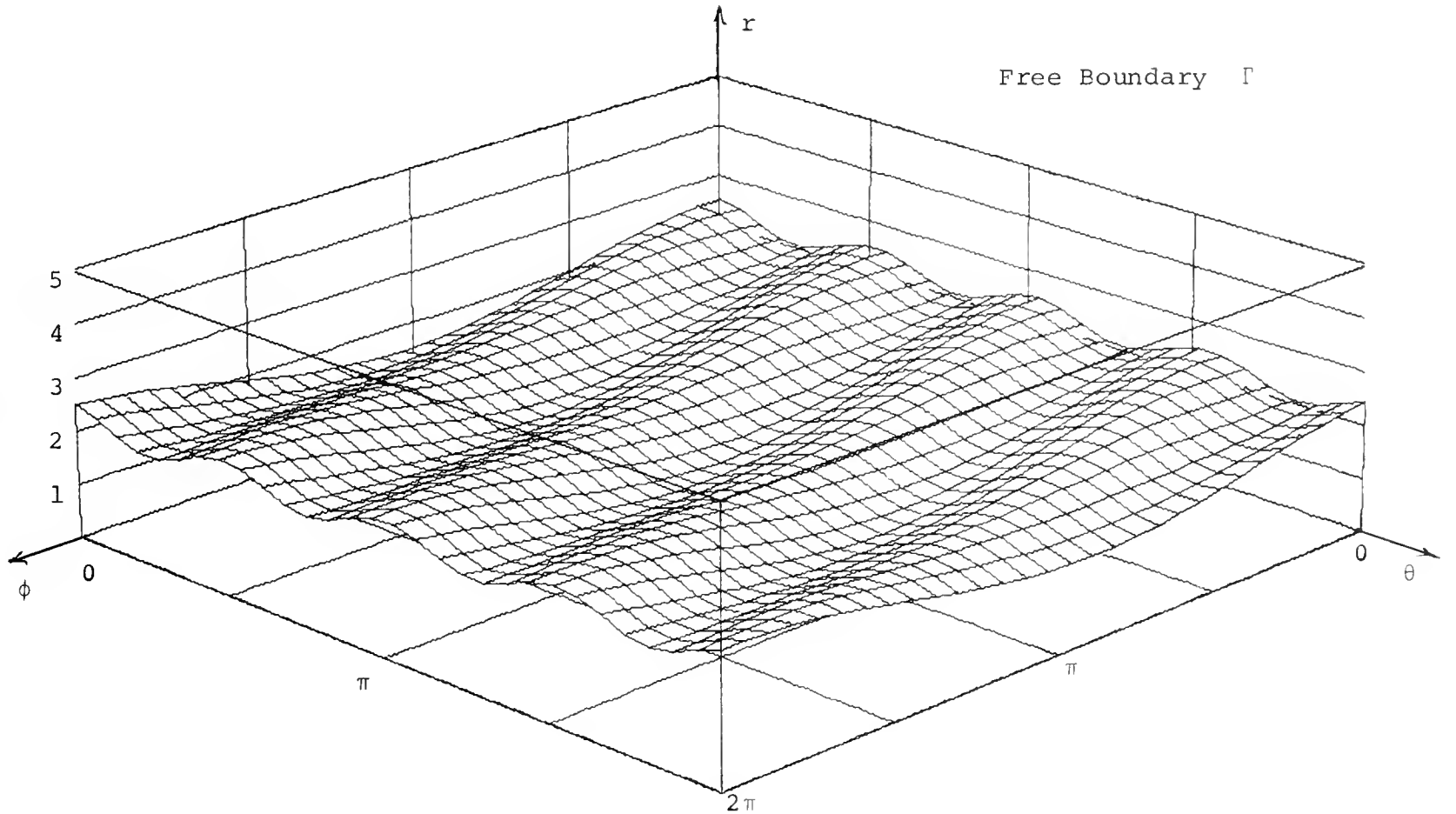

Fig. 5.6. C: $r^2(\phi,\theta) = 9[(\cos\phi + 0.15\cos 4\theta)^2 + (\sin\phi + 0.15\sin 4\theta)^2]$.

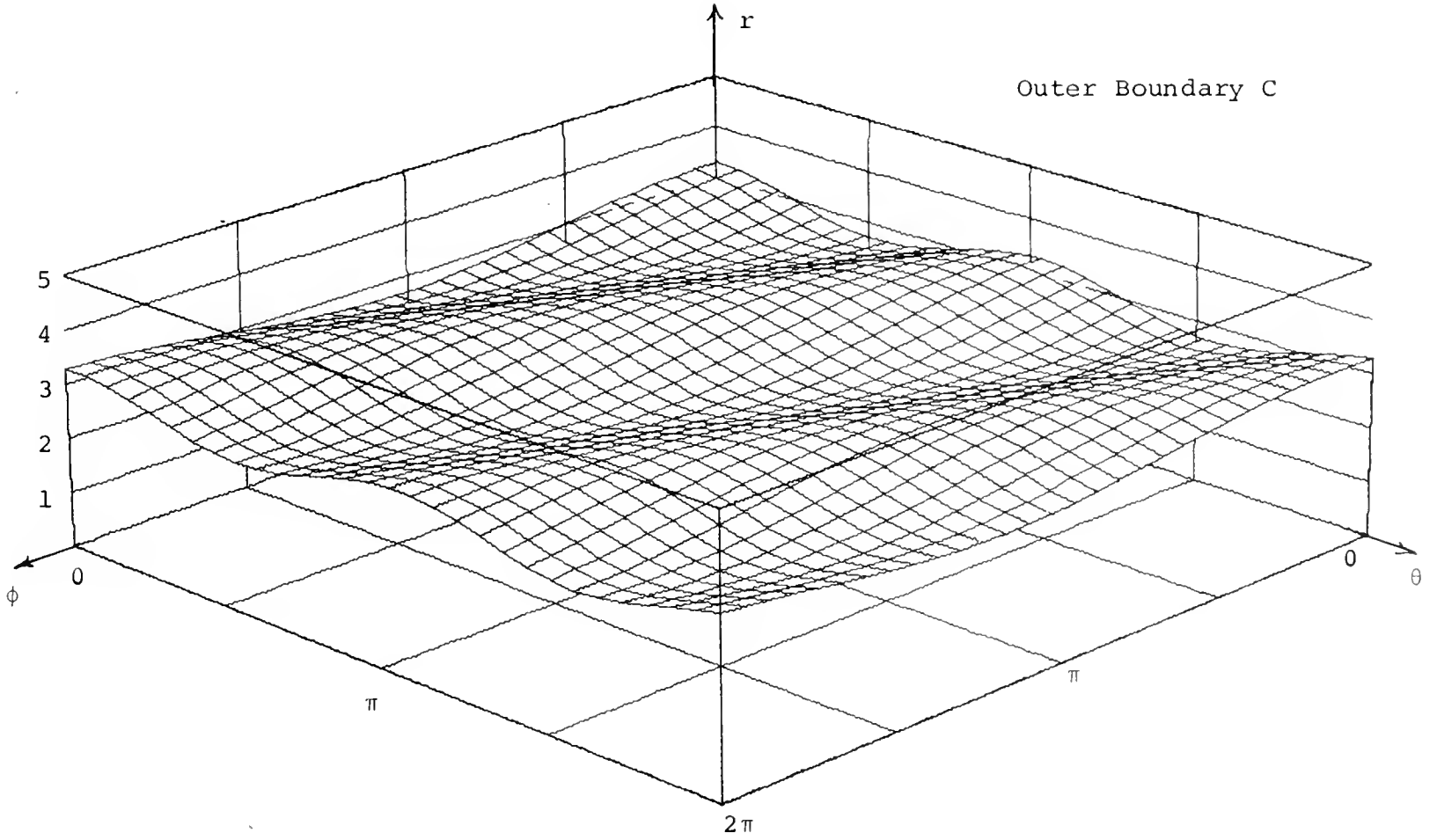

Fig. 5.7. C: $r(\phi,\theta) = 3[1.0 + 0.1 \cos(\phi+2\theta)]$.

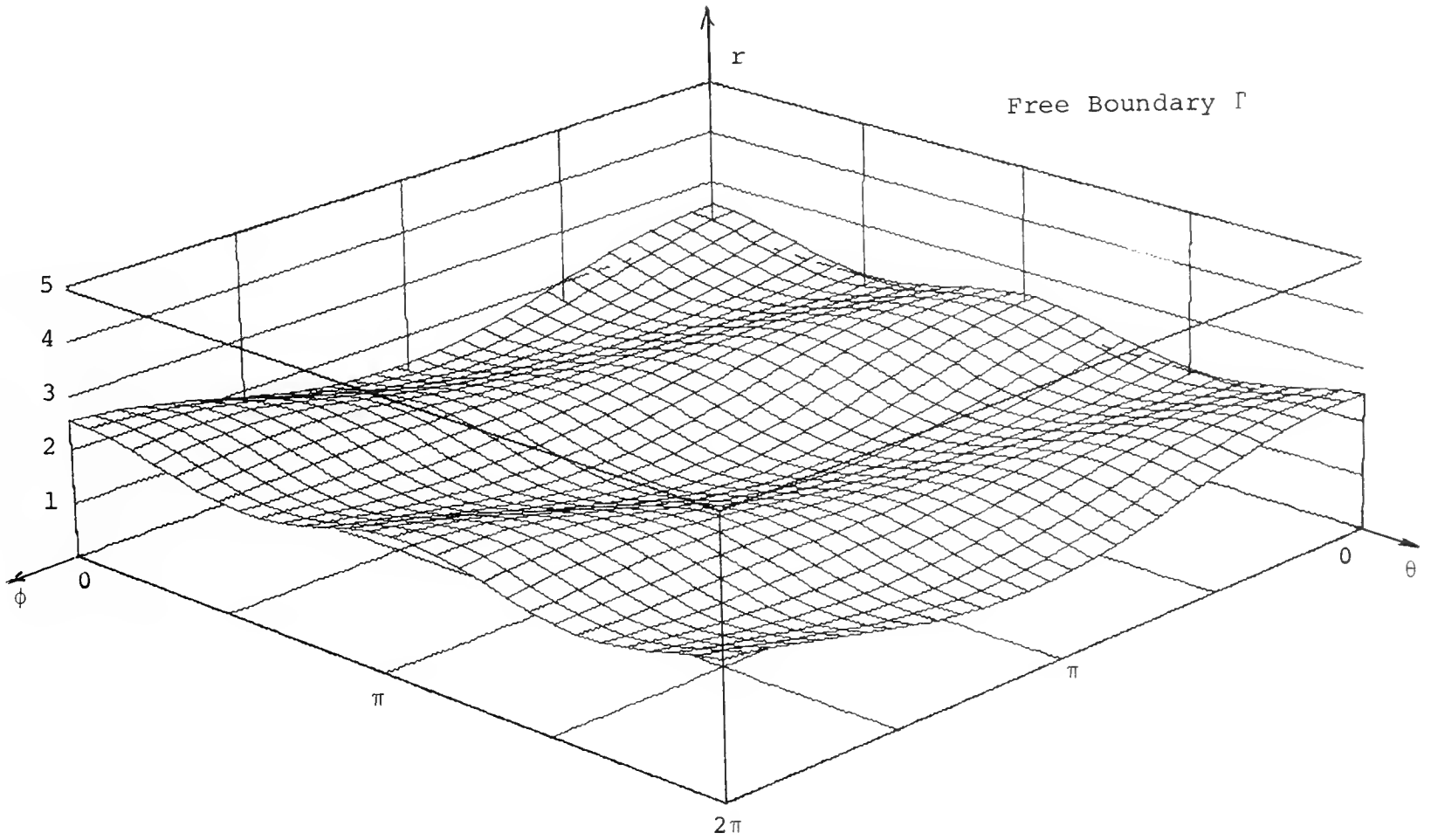

Fig. 5.8. C: $r(\phi,\theta) = 3[1.0 + 0.1 \cos(\phi+2\theta)]$.

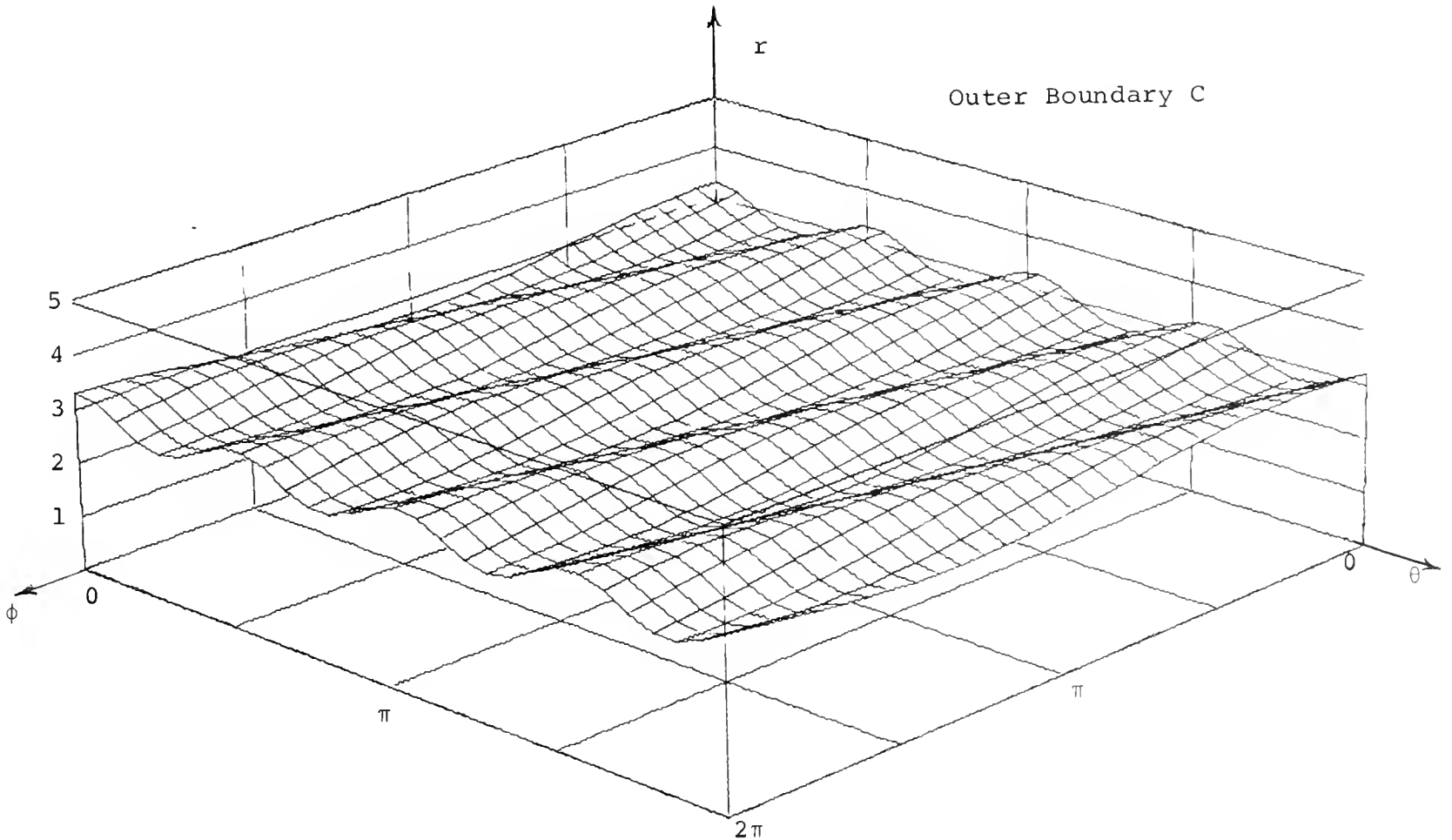

Fig. 5.9. C: $r(\phi,\theta) = 3[1.0 + 0.1 (\cos \phi + 4\theta)]$.

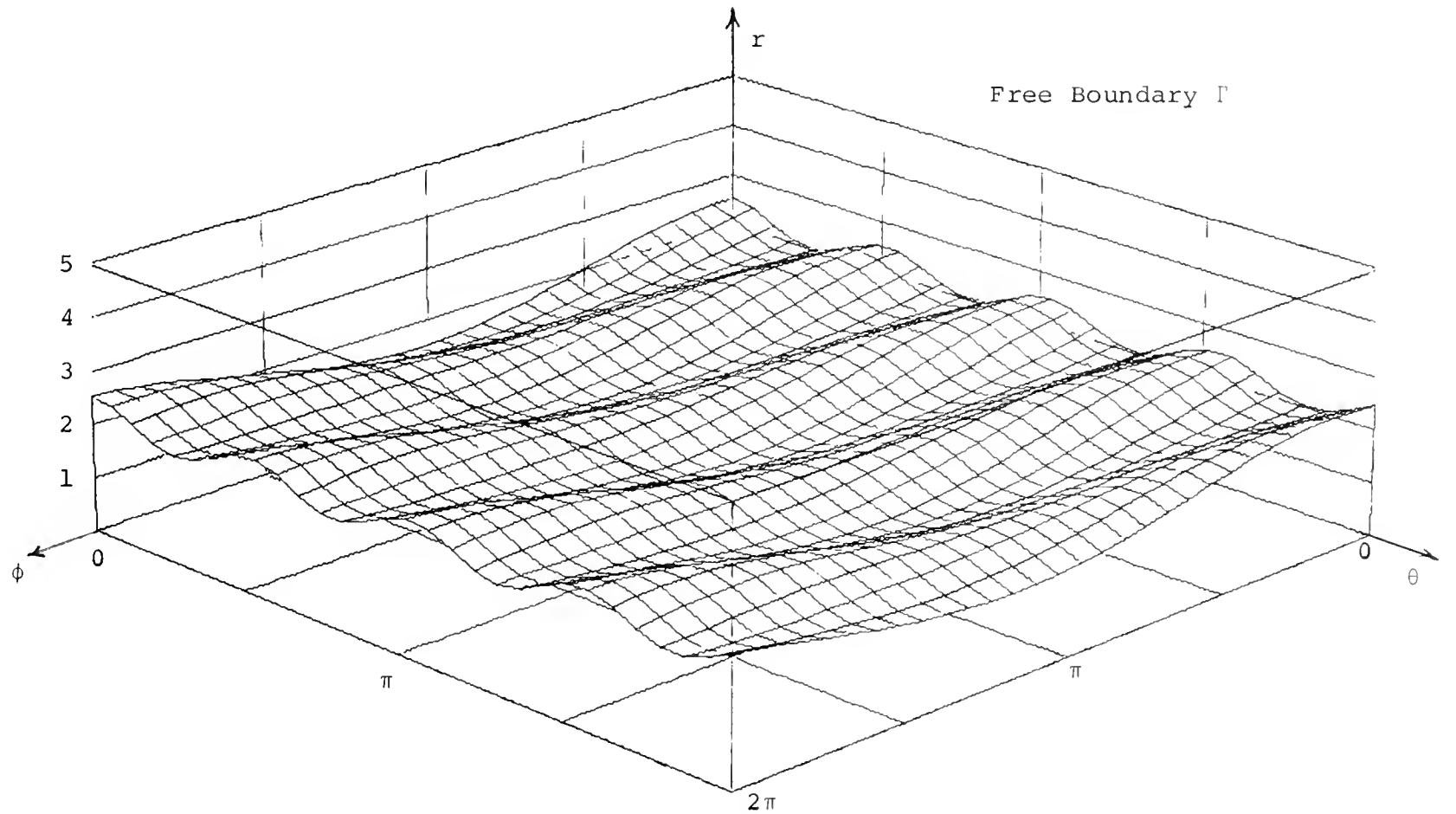

Fig. 5.10. C: $r(\phi,\theta) = 3[1.0 + 0.1 \cos(\phi+4\theta)]$.

```
      PROGRAM BETA(INPUT,OUTPUT,TAPE1,TAPE2)
      COMMON G(9,52,52),A(9,52,52),U(9,52,52),R(52,52),F(52,52),T(52,52)
     1,C1(9,52),C2(9,52),E1(9,52),E2(9,52),CF(52),B1(52),B2(52),D1(52),
     2D2(52),RA,RC,RI,NI,NJ,PETE,PEFI,BETE,GRA,H,HS,VOL,ENER,RELB
      COMMON EX(52,52),EF(52,52),ET(52,52),A11,A12,A22,A33
      IALL=LOCF(A33)-LOCF(G(1,1,1))+1
      CALL ZERO(G,IALL)
C     READ IN INITIAL PARAMETERS
      READ 1,RA,RC,RI
    1 FORMAT(3F7.2)
      READ 2,PETE,PEFI,BETE,GRA
    2 FORMAT(4F7.2)
      READ 3,NI,NJ
    3 FORMAT(2I4)
      READ 4,RELI,RULA,RELB,ERRI,ERRB
    4 FORMAT(3F6.3,2F10.7)
      PRINT 5,RA,RC,RI
    5 FORMAT(*1*,2X,*BIG RADIUS*,2X,F7.2,2X,*SMALL RADIUS*,2X,F7.2,2X,
     1*INITIAL SURFACE*,2X,F7.2)
      PRINT 6,PETE,PEFI,BETE,GRA
    6 FORMAT(* *,2X,*VACUUM THETA PERIOD*,2X,F7.2,2X,*VAGUUM FI PERIOD*,
     12X,F7.2,2X,*PLASMA THETA PERIOD*,2X,F7.2,2X,*INITIAL PRESSURE*,2X,
     2F7.2)
      PRINT 7,RELI,RULA,RELB,ERRI,ERRB
    7 FORMAT(* *,2X,*VACUUM REL*,2X,F6.3,2X,*PLASMA REL*,2X,F6.3,2X,
     1*BOUND REL*,2X,F6.3,2X,*INTERIOR ERROR*,2X,F6.3,2X,*BOUND ERROR
     2*,2X,F10.7)
      READ 1557,ASYE,FAC
 1557 FORMAT(2F7.5)
      READ 1558,FEC,ORRI,ORRB
 1558 FORMAT(F5.3,2F15.7)
      PRINT 1559,FAC,FEC,ORRI,ORRB
 1559 FORMAT(* *,3X,2F10.3,2F15.7)
      GAS=5.0/3.0
      READ 1580,IND,RCAT,TOM
 1580 FORMAT(I2,F10.7,F10.1)
C     IF IND LESS THAN 0,WE USE AS INPUT PREVIOUS SOLUTION STORED
C     IN TAPE1.
      IF(IND.LE.0) GO TO 1581
C     COMPUTE AXIALLY SYMMETRIC SOLUTION
      CALL ASYM(FLU1,FLU2,FLU3,ASYE)
      CON=0.5*GRA*(VOL**GAS)
 1581 CONTINUE
      UIN=0.0
      ARRI=ERRI
      BMAX=1.0
      PI=3.1415926536
      PP=1.0/(2.0*PI)
      H=(2.0*PI)/(NJ+0.0)
```

```
      HS=1.0/(NI-1.0)
      N1=NJ+1
      N2=NJ+2
      N3=2
      REF=1.0
      HA=0.5/HS
      HB=0.5/H
      HC=(H*H)/(HS*HS)
      HD=H/(2.0*HS)
      REO=1.0-RELI
      RAO=1.0-RULA
      NI1=NI-1
      RA2=0.5*RA
      TER=1.0/3.0
      IF(IND.LT.0) GO TO 1560
C     COMPUTE OUTER BOUNDARY AND INITIAL GUESS FOR FREE BOUNDARY
      CALL SURF
      CALL SARF
C     SET INITIAL SOLUTION EQUAL TO SOLUTION TO AXIALLY SYMMETRIC CASE
      DO 8 J=1,N2
      DO 8 K=1,N2
      DO 8 I=1,NI
      A(I,J,K)=PP*(K-2)*H
      U(I,J,K)=PP*(K-2)*H
    8 G(I,J,K)=C1(I,J)
      GO TO 1561
 1560 REWIND 1
      N3=4
C     READ INITIAL SOLUTION FROM TAPE1
      READ(1) (((A(I,J,K),J=1,N2),K=1,N2),I=1,NI)
      READ(1) (((U(I,J,K),J=1,N2),K=1,N2),I=1,NI)
      READ(1) (((G(I,J,K),J=1,N2),K=1,N2),I=1,NI)
      READ(1) ((R(J,K),J=1,N2),K=1,N2)
      READ(1) ((EX(J,K),J=1,N2),K=1,N2)
      READ(1) FLU1,FLU2,FLU3,CON
 1561 CONTINUE
 2000 CONTINUE
      DO 9 J=1,N2
    9 CF(J)=COS((J-2)*H)
C     COMPUTE DERIVATIVES OF OUTER SURFACE
      DO 710 K=2,N1
      DO 710 J=2,N1
      EF(J,K)=HB*(EX(J+1,K)-EX(J-1,K))
  710 ET(J,K)=HB*(EX(J,K+1)-EX(J,K-1))
C     PERIODICITY CONDITIONS FOR DERIVATIVES OF OUTER SURFACE
      DO 711 K=1,N2
      EF(1,K)=EF(N1,K)
      ET(1,K)=ET(N1,K)
```

```
      EF(N2,K)=EF(2,K)
  711 ET(N2,K)=ET(2,K)
      DO 712 J=1,N2
      EF(J,1)=EF(J,N1)
      ET(J,1)=ET(J,N1)
      EF(J,N2)=EF(J,2)
  712 ET(J,N2)=ET(J,2)
      ITER=0
      NTER=0
      INER=0
      PRINT 10
   10 FORMAT(≠1≠,4X,≠ITERATION NUMBER≠,5X,≠VOLUME≠,5X,≠PRESSURE≠,8X,
     1≠MAX RES≠,7X,≠MAX RES INTERIOR≠,7X,≠MAX ERROR ON BOUND≠)
C     PERIODICITY CONDITIONS FOR FREE BOUNDARY
  100 DO 603 K=1,N2
      R(1,K)=R(N1,K)
      R(N2,K)=R(2,K)
  603 CONTINUE
      DO 604 J=1,N2
      R(J,1)=R(J,N1)
      R(J,N2)=R(J,2)
  604 CONTINUE
C     COMPUTE DERIVATIVES OF FREE BOUNDARY
      DO 11 K=2,N1
      DO 11 J=2,N1
      F(J,K)=HB*(R(J+1,K)-R(J-1,K))
      T(J,K)=HB*(R(J,K+1)-R(J,K-1))
   11 CONTINUE
C     PERIODICITY CONDITIONS FOR DERIVATIVES OF FREE BOUNDARY
      DO 600 K=1,N2
      F(1,K)=F(N1,K)
      T(1,K)=T(N1,K)
      F(N2,K)=F(2,K)
      T(N2,K)=T(2,K)
  600 CONTINUE
      DO 601 J=1,N2
      F(J,1)=F(J,N1)
      T(J,1)=T(J,N1)
      F(J,N2)=F(J,2)
      T(J,N2)=T(J,2)
  601 CONTINUE
C     ITERATE SOLUTION FOR POTENTIALS G AND A IN THE VACUUM REGION
  200 UE=0.0
      DO 72 I=1,NI
      SV=(I-0.5)*HS+1.0
      DO 71 J=2,N1
      R1=0.5*(R(J,2)+R(J,N1))
      R2=0.5*(T(J,2)+T(J,N1))
```

```
      R5=0,5*(EX(J,2)+EX(J,N1))
      R4=0,5*(ET(J,2)+ET(J,N1))
      R3=(I-1,0)*HS*(R5-R1)+R1
      C1(I,J)=(R3*(R5-R1))/(RA*R3*CF(J))
      R3=(I-0,5)*HS*(R5-R1)+R1
      E1(I,J)=(HD*R3*(SV*R2-R4*((I-0,5)*HS))/(RA*R3*CF(J))
   71 CONTINUE
   72 CONTINUE
      DO 12 K=2,N1
      R4=0,5*(CF(2)+CF(N1))
      DO 70 I=1,NI
      R1=0,5*(R(2,K)+R(N1,K))
      R2=0,5*(F(2,K)+F(N1,K))
      R6=0,5*(EX(2,K)+EX(N1,K))
      R5=0,5*(EF(2,K)+EF(N1,K))
      S=(I-1)*HS
      R3=S*(R6-R1)+R1
      B1(I)=(RA*R3*R4)*(R6-R1)/R3
      R3=(S+0,5*HS)*(R6-R1)+R1
      D1(I)=(HD*(RA*R3*R4)*(R2*(S+0,5*HS*1,0)-(S+0,5*HS)*R5))/R3
   70 CONTINUE
      DO 13 J=2,N1
      R1=0,5*(R(J,K)+R(J+1,K))
      R2=0,5*(EX(J,K)+EX(J+1,K))
      F1=0,5*(F(J,K)+F(J+1,K))
      F2=0,5*(EF(J,K)+EF(J+1,K))
      R3=0,5*(R(J,K)+R(J,K+1))
      R4=0,5*(EX(J,K)+EX(J,K+1))
      T3=0,5*(T(J,K)+T(J,K+1))
      T4=0,5*(ET(J,K)+ET(J,K+1))
      CF1=0,5*(CF(J)+CF(J+1))
      SP=0,5*HS
      SV=SP-1,0
      X1=SP*(EX(J,K)-R(J,K))+R(J,K)
      X2=RA*X1*CF(J)
      F6=F(J,K)*SV-SP*EF(J,K)
      T2=T(J,K)*SV-SP*ET(J,K)
      A1=(HC*X1*X2*(1,0+(F6*F6)/(X1*X1)+(T2*T2)/(X2*X2)))/(EX(J,K)-R(J,K
     1))
      B2(1)=B1(1)
      B1(1)=(RA*R1*CF1)*(R2-R1)/R1
      C2(1,J)=C1(1,J)
      C1(1,J)=(R3*(R4-R3))/(RA*R3*CF(J))
      D2(1)=D1(1)
      X1=SP*(R2-R1)+R1
      D1(1)=(HD*(RA*X1*CF1)*(F1*SV-SP*F2))/X1
      E2(1,J)=E1(1,J)
      X1=SP*(R4-R3)+R3
```

```
 E1(1,J)=(HD*X1*(SV*T3-SP*T4))/(RA+X1*CF(J))
 GAM=A1+0.5*(B1(1)+B2(1)+C1(1,J)+C2(1,J))+D1(1)-D2(1)+E1(1,J)-E2(1,
1J)
 WP=(A1*G(2,1,K)+0.5*(B1(1)*G(1,J+1,K)+B2(1)*G(1,J-1,K)+C1(1,J)*
1G(1,J,K+1)+C2(1,J)*G(1,J,K-1))+D1(1)*G(2,J+1,K)-D2(1)*G(2,J-1,K)+
2E1(1,J)*G(2,J,K+1)-E2(1,J)*G(2,J,K-1))/GAM
 UP=REO*G(1,1,K)+RELI*WP
 UA=UP-G(1,J,K)
 UD=ABS(UA)
 UE=AMAX1(UE,UD)
 G(1,J,K)=UP
 WP=(A1*A(2,1,K)+0.5*(B1(1)*A(1,J+1,K)+B2(1)*A(1,J-1,K)+C1(1,J)*
1A(1,J,K+1)+C2(1,J)*A(1,J,K-1))+D1(1)*A(2,J+1,K)-D2(1)*A(2,J-1,K)+
2E1(1,J)*A(2,J,K+1)-E2(1,J)*A(2,J,K-1))/GAM
 UP=REO*A(1,1,K)+RELI*WP
 UA=UP-A(1,J,K)
 UD=ABS(UA)
 UE=AMAX1(UE,UD)
 A(1,J,K)=UP
 DO 14 I=2,NI1
 S=(I-1)*HS
 SP=S+0.5*HS
 SS=S-1.0
 ST=SP-1.0
 A2=A1
 X1=SP*(EX(J,K)-R(J,K))+R(J,K)
 X2=RA+X1*CF(J)
 F6=F(J,K)*ST-SP*EF(J,K)
 T2=T(J,K)*ST-SP*ET(J,K)
 A1=(HC*X1*X2*(1.0+(F6*F6)/(X1*X1)+(T2*T2)/(X2*X2)))/(EX(J,K)-
1R(J,K))
 B2(I)=B1(I)
 X1=S*(R2-R1)+R1
 B1(I)=(RA+X1*CF1   )*(R2-R1)/X1
 C2(I,J)=C1(I,J)
 X1=S*(R4-R3)+R3
 C1(I,J)=X1*(R4-R3)/(RA+X1*CF(J))
 D2(I)=D1(I)
 X1=SP*(R2-R1)+R1
 D1(I)=(HD*(RA+X1*CF1)*(F1*ST-SP*F2))/X1
 E2(I,J)=E1(I,J)
 X1=SP*(R4-R3)+R3
 E1(I,J)=(HD*X1*(T3*ST-SP*T4))/(RA+X1*CF(J))
 GAM=A1+A2+B1(I)+B2(I)+C1(I,J)+C2(I,J)+D1(I)-D2(I)-B1(I-1)+D2(I-1)+
1E1(I,J)-E2(I,J)-E1(I-1,J)+E2(I-1,J)
 WP=(A1*G(I+1,J,K)+A2*G(I-1,J,K)+B1(I)*G(I,J+1,K)+B2(I)*G(I,J-1,K)+
1C1(I,J)*G(I,J,K+1)+C2(I,J)*G(I,J,K-1)+D1(I)*G(I+1,J+1,K)-D1(I-1)*
2G(I-1,J+1,K)-D2(I)*G(I+1,J-1,K)+D2(I-1)*G(I-1,J-1,K)+E1(I,J)*
```

```
     3G(I+1,J,K+1)-E2(I,J)*G(I+1,J,K-1)-E1(I-1,J)*G(I-1,J,K+1)+E2(I-1,J)
     4*G(I-1,J,K-1))/GAM
      UP=RE0*G(I,J,K)+RELI*WP
      UA=UP-G(I,J,K)
      UD=ABS(UA)
      UE=AMAX1(UE,UD)
      G(I,J,K)=UP
      WP=(A1*A(I+1,J,K)+A2*A(I-1,J,K)+B1(I)*A(I,J+1,K)+B2(I)*A(I,J-1,K)+
     1C1(I,J)*A(I,J,K+1)+C2(I,J)*A(I,J,K-1)+D1(I)*A(I+1,J+1,K)-D1(I-1)*
     2A(I-1,J+1,K)-D2(I)*A(I+1,J-1,K)+D2(I-1)*A(I-1,J-1,K)+E1(I,J)*
     3A(I+1,J,K+1)-E2(I,J)*A(I+1,J,K-1)-E1(I-1,J)*A(I-1,J,K+1)+E2(I-1,J)
     4*A(I-1,J,K-1))/GAM
      UP=RE0*A(I,J,K)+RELI*WP
      UA=UP-A(I,J,K)
      UD=ABS(UA)
      UE=AMAX1(UE,UD)
      A(I,J,K)=UP
   14 CONTINUE
      B2(NI)=B1(NI)
      B1(NI)=(RA+R2*CF1)*(R2-R1)/R2
      C2(NI,J)=C1(NI,J)
      C1(NI,J)=R4*(R4-R3)/(RA+R4*CF(J))
      GAM=A1+0.5*(B1(NI)+B2(NI)+C1(NI,J)+C2(NI,J))+D2(NI1)-D1(NI1)+
     1E2(NI1,J)-E1(NI1,J)
      WP=(A1*G(NI1,J,K)+0.5*(B1(NI)*G(NI,J+1,K)+B2(NI)*G(NI,J-1,K)+
     1C1(NI,J)*G(NI,J,K+1)+C2(NI,J)*G(NI,J,K-1))+D2(NI1)*G(NI1,J+1,K)-
     2D1(NI1)*G(NI1,J+1,K)+E2(NI1,J)*G(NI1,J,K-1)-E1(NI1,J)*G(NI1,J,K+1)
     3)/GAM
      UP=RE0*G(NI,J,K)+RELI*WP
      UA=UP-G(NI,J,K)
      UD=ABS(UA)
      UE=AMAX1(UE,UD)
      G(NI,J,K)=UP
      WP=(A1*A(NI1,J,K)+0.5*(B1(NI)*A(NI,J+1,K)+B2(NI)*A(NI,J-1,K)+
     1C1(NI,J)*A(NI,J,K+1)+C2(NI,J)*A(NI,J,K-1))+D2(NI1)*A(NI1,J-1,K)-
     2D1(NI1)*A(NI1,J+1,K)+E2(NI1,J)*A(NI1,J,K-1)-E1(NI1,J)*A(NI1,J,K+1)
     3)/GAM
      UP=RE0*A(NI,J,K)+RELI*WP
      UD=ABS(UA)
      UE=AMAX1(UE,UD)
      A(NI,J,K)=UP
   13 CONTINUE
   12 CONTINUE
C     PERIODICITY CONDITIONS FOR POTENTIALS IN VACUUM REGION
      DO 17 I=1,NI
      DO 18 K=1,N2
      A(I,1,K)=A(I,N1,K)
      A(I,N2,K)=A(I,2,K)
```

```
      G(I,1,K)=G(I,N1,K)-1.0
      G(I,N2,K)=G(I,2,K)+1.0
   18 CONTINUE
      DO 19 J=1,N2
      A(I,J,1)=A(I,J,N1)-1.0
      A(I,J,N2)=A(I,J,2)+1.0
      G(I,J,1)=G(I,J,N1)
      G(I,J,N2)=G(I,J,2)
   19 CONTINUE
   17 CONTINUE
      NTER=NTER+1
      ITER=ITER+1
C     CHECK ERROR IN THE SOLUTION
      IF(UE.GE.ERR)GO TO 200
  320 UIN=0.0
      SV=0.5*HS
      DO 400 J=2,N1
      R1=0.5*(R(J,2)+R(J,N1))
      R2=0.5*(T(J,2)+T(J,N1))
      E1(1,J)=-(SV*SV*R1*R2*HD)/(RA*SV*R1*CF(J))
  400 CONTINUE
C     ITERATE SOLUTION AT SINGULAR POINTS
      DO 401 K=2,N1
      SUM1=0.0
      SUM2=0.0
      R1=0.5*(R(2,K)+R(N1,K))
      R2=0.5*(F(2,K)+F(N1,K))
      R3=0.5*(CF(2)+CF(N1))
      D1(1)=-(HD*R2*(RA+SV*R1*R3))/R1
      DO 402 J=2,N1
      X1=RA+SV*R(J,K)*CF(J)
      A1=HC*SV*X1*(1.0+(F(J,K)*F(J,K))/(R(J,K)*R(J,K))+(SV*SV*T(J,K)*
     1T(J,K))/(X1*X1))
      D2(1)=D1(1)
      R1=0.5*(R(J,K)+R(J+1,K))
      D1(1)=-(HD*0.5*(F(J,K)+F(J+1,K))*(RA+SV*R1*0.5*(CF(J)+CF(J+1))))/
     1R1
      E2(1,J)=E1(1,J)
      R3=0.5*(R(J,K)+R(J,K+1))
      E1(1,J)=-(HD*SV*SV*0.5*(T(J,K)+T(J,K+1))*R3)/(RA*SV*R3*CF(J))
      SUM1=SUM1+A1*U(2,J,K)+D1(1)*U(2,J+1,K)+D2(1)*U(2,J-1,K)+E1(1,J)*
     1U(2,J,K+1)+E2(1,J)*U(2,J,K-1)
      SUM2=SUM2+A1+D1(1)+D2(1)+E1(1,J)+E2(1,J)
  402 CONTINUE
      AA=SUM1/SUM2
      UA=AA*U(1,2,K)
      UD=ABS(UA)
      UIN=AMAX1(UD,UIN)
```

```
      DO 403 J=2,N1
  403 U(1,J,K)=AA
  401 CONTINUE
C     ITERATE SOLUTION FOR POTENTIAL U IN PLASMA REGION
      DO 302 I=1,NI
      SV=(I-0.5)*HS
      DO 301 J=2,N1
      R1=0.5*(R(J,2)+R(J,N1))
      R2=0.5*(T(J,2)+T(J,N1))
      S=(I-1)*HS
      C1(I,J)=(S*R1*R1)/(RA+S*R1*CF(J))
      E1(I,J)=-(SV*SV*R1*R2*HD)/(RA+SV*R1*CF(J))
  301 CONTINUE
  302  CONTINUE
      DO 312 K=2,N1
      R3=0.5*(CF(2)+CF(N1))
      R1=0.5*(R(2,K)+R(N1,K))
      R2=0.5*(F(2,K)+F(N1,K))
       R4=R1*R3
      R5=HD*R2
      DO 520 I=1,NI
      S=(I-1)*HS
      B1(I)=(RA+S*R4)/S
  520 CONTINUE
      DO 521 I=1,NI
      S=(I-1)*HS
      SP=S+0.5*HS
      D1(I)=-(R5*(RA+SP*R4))/R1
  521 CONTINUE
      DO 313 J=2,N1
      R1=0.5*(R(J,K)+R(J+1,K))
      F1=0.5*(F(J,K)+F(J+1,K))
      R3=0.5*(R(J,K)+R(J,K+1))
      T3=0.5*(T(J,K)+T(J,K+1))
      CF1=0.5*(CF(J)+CF(J+1))
      SP=0.5*HS
      F2=F(J,K)*F(J,K)
      T2=T(J,K)*T(J,K)
      RR2=R(J,K)*R(J,K)
      X1=RA+SP*R(J,K)*CF(J)
      A1=HC*SP*X1*(1.0+F2/RR2+(SP*SP*T2)/(X1*X1))
      D2(1)=D1(1)
      D1(1)=-(HD*F1*(RA+SP*R1*CF1))/R1
      E2(1,J)=E1(1,J)
      E1(1,J)=-(HD*SP*SP*T3*R3)/(RA+SP*R3*CF(J))
      DO 314 I=2,NI1
      S=(I-1)*HS
      SP=S+0.5*HS
```

```
      SS=SP*SP
      A2=A1
      X1=RA*SP*R(J,K)*CF(J)
      A1=HC*SP*X1*(1.0*F2/RR2+(SS*T2)/(X1*X1))
      B2(I)=B1(I)
      B1(I)=(RA+S*R1*CF1)/S
      C2(I,J)=C1(I,J)
      C1(I,J)=(S*R3*R3)/(RA+S*R3*CF(J))
      D2(I)=D1(I)
      D1(I)=-(HD*F1*(RA+SP*R1*CF1))/R1
      E2(I,J)=E1(I,J)
      E1(I,J)=-(HD*SS*T3*R3)/(RA+SP*R3*CF(J))
      GAM=A1+A2+B1(I)+B2(I)+C1(I,J)+C2(I,J)+D1(I)-D2(I)-B1(I-1)+D2(I-1)+
     1E1(I,J)-E2(I,J)-E1(I-1,J)+E2(I-1,J)
      WP=(A1*U(I+1,J,K)+A2*U(I-1,J,K)+B1(I)*U(I,J+1,K)+B2(I)*U(I,J-1,K)+
     1C1(I,J)*U(I,J,K+1)+C2(I,J)*U(I,J,K-1)+D1(I)*U(I+1,J+1,K)-D1(I-1)*
     2U(I-1,J+1,K)-D2(I)*U(I+1,J-1,K)+D2(I-1)*U(I-1,J-1,K)+E1(I,J)*
     3U(I+1,J,K+1)-E2(I,J)*U(I+1,J,K-1)-E1(I-1,J)*U(I-1,J,K+1)+E2(I-1,J)
     4*U(I-1,J,K-1))/GAM
      UP=RAO*U(I,J,K)+RULA*WP
      UA=UP-U(I,J,K)
      UD=ABS(UA)
      UIN=AMAX1(UD,UIN)
      U(I,J,K)=UP
  314 CONTINUE
      B2(NI)=B1(NI)
      B1(NI)=RA+R1*CF1
      C2(NI,J)=C1(NI,J)
      C1(NI,J)=(R3*R3)/(RA+R3*CF(J))
      GAM=A1+0.5*(B1(NI)+B2(NI)+C1(NI,J)+C2(NI,J))+D2(NI1)-D1(NI1)+
     1E2(NI1,J)-E1(NI1,J)
      WP=(A1*U(NI1,J,K)+0.5*(B1(NI)*U(NI,J+1,K)+B2(NI)*U(NI,J-1,K)+
     1C1(NI,J)*U(NI,J,K+1)+C2(NI,J)*U(NI,J,K-1))+D2(NI1)*U(NI1,J-1,K)-
     2D1(NI1)*U(NI1,J+1,K)+E2(NI1,J)*U(NI1,J,K-1)-E1(NI1,J)*U(NI1,J,K+1)
     3)/GAM
      UP=RAO*U(NI,J,K)+RULA*WP
      UA=UP-U(NI,J,K)
      UD=ABS(UA)
      UIN=AMAX1(UIN,UD)
      U(NI,J,K)=UP
  313 CONTINUE
  312 CONTINUE
C     PERIODICITY CONDITIONS FOR POTENTIAL IN THE PLASMA REGION
      DO 317 I=1,NI
      DO 318 K=1,N2
      U(I,1,K)=U(I,N1,K)
      U(I,N2,K)=U(I,2,K)
  318 CONTINUE
```

```
      DO 319 J=1,N2
      U(I,J,1)=U(I,J,N1)+1.0
      U(I,J,N2)=U(I,J,2)+1.0
  319 CONTINUE
  317 CONTINUE
      INER=INER+1
C     CHECK ERROR IN THE SOLUTION
      IF(UIN.GE.UE)GO TO 320
      BMAX=0.0
      SUM=0.0
C     COMPUTE VOLUME OF PLASMA REGION
      DO 51 J=2,N1
      FI3=CF(J)*TER
      DO 50 K=2,N1
      AUX=R(J,K)*R(J,K)*(RA2+R(J,K)*FI3)
      SUM=SUM+AUX
   50 CONTINUE
   51 CONTINUE
      VOL=H*H*SUM
C     COMPUTE PRESSURE IN THE PLASMA
      GRA=(2.0*CON)/(VOL**GAS)
C     COMPUTE CURRENTS Q1,Q2,Q3
      CALL FLAX(FLU1,FLU2,FLU3,Q1,Q2,Q3)
C     COMPUTE ERROR IN THE BOUNDARY AND USE STEEPEST DESCENT METHOD TO
C     UPDATE BOUNDARY POSITION
      CALL GRAD(BMAX,PRO1,Q1,Q2,Q3)
      PRO1=PRO1/(NJ*NJ)
      BET=GRA/PRO1
      PRINT 21,ITER,VOL,GRA,UE,UIN,BMAX,Q1,Q2,Q3,BET,ENER
   21 FORMAT(* *,2X,I4,6X,F8.3,4X,F6.3,3X,E10.4,6X,E10.4,6X,F10.4,3X,
     1F5.1,3X,F5.1,3X,F5.1,3X,F5.3,3X,E11.6)
      IF(NTER.GE.100)GO TO 23
C     COMPUTE ERROR TO BE ALLOWED IN SOLUTION IN THE INTERIOR,AS A
C     FUNCTION OF THE ERROR IN THE BOUNDARY
      BMN=FAC*BMAX/Q1
      ERRI=AMIN1(ARRI,BMN)
      CALL SECOND(TIM)
C     CHECK TIME ELLAPSED,AND IF GREATER THAN TOM,TERMINATE THE
C     COMPUTATION
      IF(TIM.GE.TOM) GO TO 1570
C     CHECK BOUNDARY ERROR
      IF(BMAX.GE.ERRB)GO TO 100
      PRINT 22,((R(J,K),J=2,N1,N3),K=2,N1,N3)
   22 FORMAT(* *,13F7.3)
      IF(IND.LE.0) STOP
      IF(REF.LE.0.0)STOP
      GO TO 25
   23 CONTINUE
```

```
      PRINT 32
   32 FORMAT(≠1≠,≠FREE SURFACE≠)
      PRINT 22,((R(J,K),K=2,N1,N3),J=2,N1)
      PRINT 35,A11,A12,A22,A33
   35 FORMAT(≠ ≠,3X,4E15.4)
      NTER=0
      GO TO 100
   25 CONTINUE
C     REFINE THE MESH,AND COMPUTE INITIAL SOLUTION BY EXTRAPOLATION
C     OF SOLUTION FOR THE PREVIOUS MESH
      H=0.5*H
      HS=0.5*HS
      HA=0.5/HS
      HB=0.5/H
      HC=(H*H)/(HS*HS)
      HD=H/(2.0*HS)
      DO 800 II=1,NI
      I=NI-II+1
      DO 800 J=2,N1
      DO 800 K=2,N1
      A(2*I-1,J,K)=A(I,J,K)
      U(2*I-1,J,K)=U(I,J,K)
  800 G(2*I-1,J,K)=G(I,J,K)
      DO 801 I=1,NI1
      DO 801 J=2,N1
      DO 801 K=2,N1
      A(2*I,J,K)=0.5*(A(2*I-1,J,K)+A(2*I+1,J,K))
      G(2*I,J,K)=0.5*(G(2*I-1,J,K)+G(2*I+1,J,K))
  801 U(2*I,J,K)=0.5*(U(2*I-1,J,K)+U(2*I+1,J,K))
      NI=2*NI-1
      NI1=NI-1
      DO 802 JJ=2,N1
      J=N1*2-JJ
      DO 802 K=2,N1
      R(2*J-2,K)=R(J,K)
      DO 802 I=1,NI
      A(I,2*J-2,K)=A(I,J,K)
      G(I,2*J-2,K)=G(I,J,K)
  802 U(I,2*J-2,K)=U(I,J,K)
      DO 803 J=2,NJ
      DO 803 K=2,N1
      R(2*J-1,K)=0.5*(R(2*J,K)+R(2*J-2,K))
      DO 803 I=1,NI
      A(I,2*J-1,K)=0.5*(A(I,2*J,K)+A(I,2*J-2,K))
      G(I,2*J-1,K)=0.5*(G(I,2*J,K)+G(I,2*J-2,K))
  803 U(I,2*J-1,K)=0.5*(U(I,2*J,K)+U(I,2*J-2,K))
      DO 810 K=2,N1
      R(2*N1-1,K)=0.5*(R(2,K)+R(2*N1-2,K))
```

```
      DO 810 I=1,NI
      A(I,2*N1-1,K)=0.5*(A(I,2,K)+A(I,2*N1-2,K))
      G(I,2*N1-1,K)=0.5*(G(I,2,K)+G(I,2*N1-2,K)+1.0)
  810 U(I,2*N1-1,K)=0.5*(U(I,2,K)+U(I,2*N1-2,K))
      NN=2*NJ
      NN1=NN+1
      DO 804 KK=2,N1
      K=N1*2-KK
      DO 804 J=2,NN1
      R(J,2*K-2)=R(J,K)
      DO 804 I=1,NI
      A(I,J,2*K-2)=A(I,J,K)
      G(I,J,2*K-2)=G(I,J,K)
  804 U(I,J,2*K-2)=U(I,J,K)
      DO 805 K=2,NJ
      DO 805 J=2,NN1
      R(J,2*K-1)=0.5*(R(J,2*K)+R(J,2*K-2))
      DO 805 I=1,NI
      A(I,J,2*K-1)=0.5*(A(I,J,2*K)+A(I,J,2*K-2))
      G(I,J,2*K-1)=0.5*(G(I,J,2*K)+G(I,J,2*K-2))
  805 U(I,J,2*K-1)=0.5*(U(I,J,2*K)+U(I,J,2*K-2))
      DO 811 J=2,NN1
      R(J,2*N1-1)=0.5*(R(J,2)+R(J,2*N1-2))
      DO 811 I=1,NI
      A(I,J,2*N1-1)=0.5*(A(I,J,2)+A(I,J,2*N1-2)+1.0)
      G(I,J,2*N1-1)=0.5*(G(I,J,2)+G(I,J,2*N1-2))
  811 U(I,J,2*N1-1)=0.5*(U(I,J,2)+U(I,J,2*N1-2)+1.0)
      NJ=2*NJ
      N1=NJ+1
      N2=NJ+2
      CALL SARF
      DO 807 I=1,NI
      DO 808 K=1,N2
      A(I,1,K)=A(I,N1,K)
      U(I,1,K)=U(I,N1,K)
      G(I,1,K)=G(I,N1,K)-1.0
      A(I,N2,K)=A(I,2,K)
      U(I,N2,K)=U(I,2,K)
  808 G(I,N2,K)=G(I,2,K)+1.0
      DO 809 J=1,N2
      A(I,J,1)=A(I,J,N1)-1.0
      U(I,J,1)=U(I,J,N1)-1.0
      G(I,J,1)=G(I,J,N1)
      A(I,J,N2)=A(I,J,2)+1.0
      U(I,J,N2)=U(I,J,2)+1.0
  809 G(I,J,N2)=G(I,J,2)
  807 CONTINUE
      REF=-1.0
```

```
      N3=4
      ERRB=ORRB
      ERRI=ORRI
      FAC=FEC
      RELI=RELI+0,5*(2,0-RELI)
      RULA=RULA+0,5*(2,0-RULA)
      REO=1,0-RELI
      RAO=1,0-RULA
      GO TO 2000
 1570 CONTINUE
      REWIND 2
C     WRITE RESULTS IN TAPE1
      WRITE(2) (((A(I,J,K),J=1,N2),K=1,N2),I=1,NI)
      WRITE(2) (((U(I,J,K),J=1,N2),K=1,N2),I=1,NI)
      WRITE(2) (((G(I,J,K),J=1,N2),K=1,N2),I=1,NI)
      WRITE(2) ((R(J,K),J=1,N2),K=1,N2)
      WRITE(2) ((EX(J,K),J=1,N2),K=1,N2)
      WRITE(2) FLU1,FLU2,FLU3,CON
      STOP
      END



      SUBROUTINE ASYM(FLU3,FLU2,FLU1,ASYE)
C     COMPUTES THE VALUES OF THE FIXED FLUXES FLU1,FLU2,FLU3,IN TERMS
C     OF THE VALUES OF THE INITIAL CURRENTS,COMPUTES AXIALLY SYMMETRIC
C     SOLUTION WHICH WILL BE USED AS INITIAL GUESS FOR GENERAL SOLUTION
      COMMON GG(9,52,52),GX(9,52,52),GY(9,52,52),G1(52,52),G2(52,52),
     1G3(52,52),G(9,52),A(9,52),B(9,52),D(9,52),CF(52),F(52),R(52),
     2EX(52),EF(52),RA,RO,RI,NI,NJ,PETE,FAFI,BETE,GRA,H,HS,VOL,ENER,
     3RELB
      DIMENSION CP(52),CV(52)
      PEF=1,0
  305 FORMAT(* *,3X,3F15,3)
      ERRI=0,00001
      RELI=1,9
      ICO=1
      ACO=1,0
      ERRB=ASYE
      ARRI=ERRI
      BMAX=1,0
      PI=3,1415926535898
      FIT=PETE/(2,0*PI)
      FTP=BETE/(2,0*PI)
      FTV=PETE/(2,0*PI)
      PP=1,0/(2,0*PI)
      H=(2,0*PI)/(NJ-0,0)
```

```
      HS=1.0/(NI-1.0)
      N1=NJ+1
      N2=NJ+2
      HA=0.5/HS
      HB=0.5/H
      HC=(H*H)/(HS*HS)
      HD=H/(2.0*HS)
      REO=1.0-RELI
      NI1=NI-1
      VOL=2.0*PI*PI*RI*RI*RA
      GAS=5.0/3.0
      CON=0.5*GRA*(VOL**GAS)
      RA2=0.5*RA
      CALL ELI
      DO 300 J=2,N1
300   EF(J)=HB*(EX(J+1)-EX(J-1))
      DO 1 J=1,N2
      DO 1 I=1,NI
 1    G(I,J)=PP*PEFI*(J-2)*H
      DO 2 J=1,N2
 2    CF(J)=COS((J-2)*H)
      SUM1=0.0
      SUM2=0.0
       DO 501 J=2,N1
      SEM1=0.0
      SEM2=0.0
      DO 502 I=1,NI1
      S=(I-1)*HS+0.5*HS
      R1=S*R(J)
      R2=(EX(J)-R(J))*S+R(J)
      SEM1=SEM1+R1/(RA+R1*CF(J))
      SEM2=SEM2+R2/(RA+R2*CF(J))
502   CONTINUE
      SUM1=SEM1*R(J)+SUM1
      SUM2=SEM2*(EX(J)-R(J))+SUM2
501   CONTINUE
      SUM1=SUM1*H*HS
      SUM2=SUM2*H*HS
      FLU2=FTV*SUM2
      FLU1=FTP*SUM1
      ITER=0
      NTER=0
 100  R(1)=R(N1)
      R(N2)=R(2)
      EF(1)=EF(N1)
      EF(N2)=EF(2)
      DO 3 J=2,N1
 3    F(J)=HB*(R(J+1)-R(J-1))
```

```
      F(1)=F(N1)
      F(N2)=F(2)
      DO 4 J=2,N1
      R1=0,5*(R(J)+R(J+1))
      F1=0,5*(F(J)+F(J+1))
      R2=0,5*(EX(J)+EX(J+1))
      F2=0,5*(EF(J)+EF(J+1))
      CF1=0,5*(CF(J)+CF(J+1))
      CV(J)=(R(J)*(EX(J)-R(J)))/(RA+R(J)*CF(J))
      CP(J)=(R(J)*R(J))/(RA+R(J)*CF(J))
      DO 5 I=1,NI
      S=(I-1)*HS
      SP=S+0,5*HS
      X1=SP*(EX(J)-R(J))+R(J)
      X2=F(J)*(SP-1,0)-SP*EF(J)
      A(I,J)=(HC*X1*(RA+X1*CF(J))*(1,0+(X2*X2)/(X1*X1)))/(EX(J)-R(J))
      X1=S*(R2-R1)+R1
      B(I,J)=(RA+X1*CF1)*(R2-R1)/X1
      X1=SP*(R2-R1)+R1
      X2=F1*(SP-1,0)-SP*F2
      D(I,J)=(HD*X2*(RA+X1*CF1))/X1
5     CONTINUE
4     CONTINUE
      CV(1)=CV(N1)
      CV(N2)=CV(2)
      CP(1)=CP(N1)
      CP(N2)=CP(2)
      DO 6 I=1,NI
      B(I,1)=B(I,N1)
      B(I,N2)=B(I,2)
      A(I,1)=A(I,N1)
      A(I,N2)=A(I,2)
      D(I,1)=D(I,N1)
6     D(I,N2)=D(I,2)
200   UE=0,0
      DO 7 J=2,N1
      GAM=A(1,J)+0,5*(B(1,J)+B(1,J-1))+D(1,J)-D(1,J-1)
      WP=A(1,J)*G(2,J)+0,5*(B(1,J)*G(1,J+1)+B(1,J-1)*G(1,J-1))+D(1,J)*
     1G(2,J+1)-D(1,J-1)*G(2,J-1)
      WP=WP/GAM
      UP=REO*G(1,J)+RELI*WP
      UA=UP-G(1,J)
      UD=ABS(UA)
      UE=AMAX1(UE,UD)
      G(1,J)=UP
      DO 8 I=2,NI1
      GAM=A(I,J)+A(I-1,J)+B(I,J)+B(I,J-1)+D(I,J)-D(I-1,J)-D(I,J-1)+
     1D(I-1,J-1)
```

```
      WP=A(I,J)*G(I+1,J)+A(I-1,J)*G(I-1,J)+B(I,J)*G(I,J+1)+B(I,J-1)*
     1G(I,J-1)+D(I,J)*G(I+1,J+1)-D(I-1,J)*G(I-1,J+1)-D(I,J-1)*G(I+1,J-1)
     2+D(I-1,J-1)*G(I-1,J-1)
      WP=WP/GAM
      UP=REO*G(I,J)+RELI*WP
      UA=UP-G(I,J)
      UD=ABS(UA)
      UE=AMAX1(UE,UD)
      G(I,J)=UP
8     CONTINUE
      GAM=A(NI-1,J)+0.5*(B(NI,J)+B(NI,J-1))+D(NI-1,J-1)+B(NI-1,J)
      WP=A(NI-1,J)*G(NI-1,J)+0.5*(B(NI,J)*G(NI,J+1)+B(NI,J-1)*G(NI,J-1))
     1+D(NI-1,J-1)*G(NI1,J-1)-D(NI-1,J)*G(NI1,J+1)
      WP=WP/GAM
      UP=REO*G(NI,J)+RELI*WP
      UA=UP-G(NI,J)
      UD=ABS(UA)
      UE=AMAX1(UE,UD)
      G(NI,J)=UP
7     CONTINUE
      DO 9 I=1,NI
      G(I,1)=G(I,N1)-PEFI
9     G(I,N2)=G(I,2)-PEFI
      ITER=ITER+1
      IF(UE.GE.ERRI)GO TO 200
      NTER=NTER+1
      ENER=0.0
      DO 60 J=2,N1
      DO 61 I=1,NI1
      X1=G(I+1,J)-G(I,J)
      X2=G(I+1,J+1)-G(I,J)
      X3=G(I+1,J)-G(I,J+1)
61    ENER=ENER+A(I,J)*X1*X1+D(I,J)*(X2*X2-X3*X3)
      X1=G(1,J+1)-G(1,J)
      ENER=ENER+B(1,J)*X1*X1*0.5
      X1=G(NI,J+1)-G(NI,J)
      ENER=ENER+B(NI,J)*X1*X1*0.5
      DO 62 I=2,NI1
      X1=G(I,J+1)-G(I,J)
62    ENER=ENER+B(I,J)*X1*X1
60    CONTINUE
      ENER=(ENER+HS)/H
      ANER=ENER*2.0*PI
      BMAX=0.0
      SUM=0.0
      IF(ACO.LE.0.0) GO TO 500
      ACO=-1.0
      FLUJ=ANER*PAFI
```

```
500   ALA=FLU3/ANER
      ENER=0.5*ANER*ALA*ALA+0.75*GRA*VOL
      CALL FLUX(FLU1,FLU2,FTV,FTP)
      ENER=ENER+PI*(FTP*FLU1+FTV*FLU2)
      DO 10 J=2,N1
      AUX=R(J)*R(J)*(RA2+(R(J)*CF(J))/3.0)
 10   SUM=SUM+AUX
      VOL=2.0*PI*H*SUM
      GRA=(2.0*CON)/(VOL**GAS)
      DO 11 J=2,N1
      A2=1.0/(RA+R(J)*CF(J))
      X1=G(2,J-1)-G(1,J-1)
      X2=G(2,J)-G(1,J)
      X3=G(2,J)-G(2,J-1)
      X4=G(1,J)-G(1,J-1)
      X5=G(2,J)-G(1,J-1)
      X6=G(1,J)-G(2,J-1)
      X7=G(2,J)-G(1,J)
      X8=G(2,J+1)-G(1,J+1)
      X9=G(2,J+1)-G(2,J)
      X10=G(1,J+1)-G(1,J)
      X11=G(2,J+1)-G(1,J)
      X12=G(1,J+1)-G(2,J)
      SAM=0.5*(0.5*(A(1,J-1)*X1*X1+A(1,J)*X2*X2)+0.5*(B(1,J-1)*X4*X4+
     1B(1,J-1)*X4*X4)+D(1,J-1)*(X5*X5-X6*X6)+0.5*(A(1,J)*X7*X7+A(1,J+1)*
     2X8*X8)+                    B(1,J)*X10*X10 +D(1,J)*(X11*X11-X12*X12))
      R1=H*H*R(J)*(RA+R(J)*CF(J))
      SAM=SAM/(R1*(EX(J)-R(J)))
      VAM=H*H*(2.0*CV(J)+CV(J-1)+CV(J+1))*0.25
      PAM=H*H*(2.0*CP(J)+CP(J-1)+CP(J+1))*0.25
      VAM=VAM/(R1*(EX(J)-R(J)))
      PAM=PAM/(R1*R(J))
      SAM=SAM*ALA*ALA
      VAM=VAM*FTV*FTV
      PAM=PAM*FTP*FTP
      TAM=SAM+VAM
      PRA=PAM+GRA
      DIF=TAM-PRA
      DAF=DIF/TAM
      CC=ABS(DAF)
      BMAX=AMAX1(BMAX,CC)
 11   R(J)=R(J)-RELB*DIF
      PRINT 12,ITER,VOL,GRA,UE,BMAX,ENER, ALA,FTV,FTP
 12   FORMAT(' ',3X,I5,4X,F8.3,4X,F8.3,4X,E10.4,4X,E10.4,4X,F12.6,3X,
     13F9.1)
      IF(ITER.GE.40000)GO TO 23
      IF(NTER.GE.50)GO TO 27
      BMN=0.1*BMAX/ALA
```

```
      ERRI=AMIN1(ARRI,BMN)
      IF(BMAX,GE,ERRB)GO TO 100
      PRINT 22,(R(J),J=2,N1,2)
   22 FORMAT(≠ ≠,15F7.3)
      PRINT 22,(EX(J),J=2,N1,2)
      PRINT 305,FLU1,FLU2,FLU3
      GO TO 25
   27 NTER=0
      PRINT 22,(R(J),J=2,N1,2)
      PRINT 22,(EX(J),J=2,N1,2)
       PRINT 28
   28 FORMAT(≠1≠)
      GO TO 100
   23 CONTINUE
      STOP
   25 CONTINUE
      PRINT 53
   53 FORMAT(≠1≠)
      RETURN
      END



      SUBROUTINE FLUX(FLU1,FLU2,FTV,FTP)
C       COMPUTES VALUES OF THE CURRENTS FOR AXIALLY SYMMETRIC CASE
      COMMON GG(9,52,52),GX(9,52,52),GY(9,52,52),G1(52,52),G2(52,52),
     1G3(52,52),G(9,52),A(9,52),B(9,52),D(9,52),CF(52),F(52),R(52),
     2D1(52),D2(52),RA,RO,RI,NI,NJ,PETE,PAFI,BETE,GRA,H,HS,VOL
      SUM1=0.0
      SUM2=0.0
      NA=NI-1
      N1=NJ+1
      DO 1 J=2,N1
      SEM1=0.0
      SEM2=0.0
      DO 2 I=1,NA
      S=(I-1)*HS+0.5*HS
      R1=S*R(J)
      R2=(RO-R(J))*S+R(J)
      SEM1=SEM1+R1/(RA+R1*CF(J))
      SEM2=SEM2+R2/(RA+R2*CF(J))
   2  CONTINUE
      SUM1=SEM1*R(J)+SUM1
      SUM2=SEM2*(RO-R(J))+SUM2
   1  CONTINUE
      SUM1=SUM1*H*HS
      SUM2=SUM2*H*HS
```

```
      FTV=FLU2/SUM2
      FTP=FLU1/SUM1
      RETURN
      END



      SUBROUTINE FLAX(FLU1,FLU2,FLU3,Q1,Q2,Q3)
C     COMPUTES VALUES OF THE CURRENTS Q1,Q2,Q3,FOR EACH POSITION OF
C     THE FREE BOUNDARY, IN TERMS OF THE GIVEN FLUXES FLU1,FLU2,FLU3
      COMMON G(9,52,52),A(9,52,52),U(9,52,52),R(52,52),F(52,52),T(52,52)
     1,C1(9,52),C2(9,52),E1(9,52),E2(9,52),CF(52),B1(52),B2(52),D1(52),
     2D2(52),RA,RC,RI,NI,NJ,PETE,PEFI,BETE,GRA,H,HS,VOL,ENER,RELR
      COMMON EX(52,52),EF(52,52),ET(52,52),A11,A12,A22,A33
      N=NJ+1
      M=NI-1
      N1=NJ+1
      HC=(H*H)/(HS*HS)
      HD=H/(2.0*HS)
      A11=0.0
      A12=0.0
      A22=0.0
      A33=0.0
      DO 31 K=2,N1
      DO 32 J=2,N1
      R1=0.5*(R(J,K)+R(J+1,K))
      R2=0.5*(EX(J,K)+EX(J+1,K))
      F1=0.5*(F(J,K)+F(J+1,K))
      F2=0.5*(EF(J,K)+EF(J+1,K))
      R3=0.5*(R(J,K)+R(J,K+1))
      R4=0.5*(EX(J,K)+EX(J,K+1))
      T3=0.5*(T(J,K)+T(J,K+1))
      T4=0.5*(ET(J,K)+ET(J,K+1))
      CF1=0.5*(CF(J)+CF(J+1))
      G8=G(1,J,K)
      A8=A(1,J,K)
      U8=U(1,J,K)
      G1=G(2,J,K)-G8
      A1=A(2,J,K)-A8
      U1=U(2,J,K)-U8
      G2=G(1,J+1,K)-G8
      A2=A(1,J+1,K)-A8
      G3=G(1,J,K+1)-G8
      A3=A(1,J,K+1)-A8
      G4=G(2,J+1,K)-G8
      A4=A(2,J+1,K)-A8
      U4=U(2,J+1,K)-U8
```

```
      G5=G(2,J,K)-G(1,J+1,K)
      A5=A(2,J,K)-A(1,J+1,K)
      U5=U(2,J,K)-U(1,J+1,K)
      G6=G(2,J,K+1)-G8
      A6=A(2,J,K+1)-A8
      U6=U(2,J,K+1)-U8
      G7=G(2,J,K)-G(1,J,K+1)
      A7=A(2,J,K)-A(1,J,K+1)
      U7=U(2,J,K)-U(1,J,K+1)
      SP=0.5*HS
      SV=SP-1.0
      X1=SP*(EX(J,K)-R(J,K))+R(J,K)
      X2=RA+X1*CF(J)
      F6=F(J,K)*SV-SP*EF(J,K)
      T2=T(J,K)*SV-SP*ET(J,K)
      X3=(HC*X1*X2*(1.0+(F6*F6)/(X1*X1)+(T2*T2)/(X2*X2)))/(EX(J,K)-
     1R(J,K))
      X1=RA+SP*R(J,K)*CF(J)
      Y3=HC*SP*X1*(1.0+(F(J,K)*F(J,K))/(R(J,K)*R(J,K))*(SP*SP*T(J,K)*
     1T(J,K))/(X1*X1))
      X4=(RA+R1*CF1)*(R2-R1)/R1
      X5=(R3*(R4-R3))/(RA+R3*CF(J))
      X1=SP*(R2-R1)+R1
      X6=(HD*(RA+X1*CF1)*(F1*SV-SP*F2))/X1
      Y6=-(HD*F1*(RA+SP*R1*CF1))/R1
      X1=SP*(R4-R3)+R3
      X7=(HD*X1*(SV*T3-SP*T4))/(RA+X1*CF(J))
      Y7=-(HD*SP*SP*T3*R3)/(RA+SP*R3*CF(J))
      A11=A11+X3*G1*G1+0.5*(X4*G2*G2+X5*G3*G3)*X6*(G4*G4-G5*G5)+X7*
     1(G6*G6-G7*G7)
      A22=A22+X3*A1*A1+0.5*(X4*A2*A2+X5*A3*A3)*X6*(A4*A4-A5*A5)+
     1X7*(A6*A6-A7*A7)
      A12=A12+X3*A1*G1+0.5*(X4*A2*G2+X5*A3*G3)*X6*(A4*G4-A5*G5)+
     1X7*(A6*G6-A7*G7)
      A33=A33+Y3*U1*U1+Y6*(U4*U4-U5*U5)+Y7*(U6*U6-U7*U7)
      DO 33 I=2,M
      S=(I-1)*HS
      SP=S+0.5*HS
      SS=S-1.0
      SF=SP-1.0
      G8=G(I,J,K)
      A8=A(I,J,K)
      U8=U(I,J,K)
      G1=G(I+1,J,K)-G8
      A1=A(I+1,J,K)-A8
      U1=U(I+1,J,K)-U8
      G2=G(I,J+1,K)-G8
      A2=A(I,J+1,K)-A8
```

```
      U2=U(I,J+1,K)-U8
      G3=G(I,J,K+1)-G8
      A3=A(I,J,K+1)-A8
      U3=U(I,J,K+1)-U8
      G4=G(I+1,J+1,K)-G8
      A4=A(I+1,J+1,K)-A8
      U4=U(I+1,J+1,K)-U8
      G5=G(I+1,J,K)-G(I,J+1,K)
      A5=A(I+1,J,K)-A(I,J+1,K)
      U5=U(I+1,J,K)-U(I,J+1,K)
      G6=G(I+1,J,K+1)-G8
      A6=A(I+1,J,K+1)-A8
      U6=U(I+1,J,K+1)-U8
      G7=G(I+1,J,K)-G(I,J,K+1)
      A7=A(I+1,J,K)-A(I,J,K+1)
      U7=U(I+1,J,K)-U(I,J,K+1)
      X1=SP*(EX(J,K)-R(J,K))+R(J,K)
      X2=RA*X1*CF(J)
      F6=F(J,K)*ST-SP*EF(J,K)
      T2=T(J,K)*ST-SP*ET(J,K)
      X3=(HC*X1*X2*(1.0+(F6*F6)/(X1*X1)+(T2*T2)/(X2*X2)))/(EX(J,K)-
     1R(J,K))
      X1=RA+SP*R(J,K)*CF(J)
      Y3=HC*SP*X1*(1.0+(F(J,K)*F(J,K))/(R(J,K)*R(J,K))+(SP*SP*T(J,K)*
     1T(J,K))/(X1*X1))
      X1=S*(R2-R1)+R1
      X4=(RA+X1*CF1)*(R2-R1)/X1
      Y4=(RA+S*R1*CF1)/S
      X1=S*(R4-R3)+R3
      X5=X1*(R4-R3)/(RA+X1*CF(J))
      Y5=(S*R3*R3)/(RA+S*R3*CF(J))
      X1=SP*(R2-R1)+R1
      X6=(HD*(RA+X1*CF1)*(F1*ST-SP*F2))/X1
      Y6=-(HD*F1*(RA+SP*R1*CF1))/R1
      X1=SP*(R4-R3)+R3
      X7=(HD*X1*(T3*ST-SP*T4))/(RA+X1*CF(J))
      Y7=-(HD*SP*SP*T3*R3)/(RA+SP*R3*CF(J))
      A11=A11+X3*G1*G1+X4*G2*G2+X5*G3*G3+X6*(G4*G4-G5*G5)+X7*(G6*G6-
     1G7*G7)
      A22=A22+X3*A1*A1+X4*A2*A2+X5*A3*A3+X6*(A4*A4-A5*A5)+X7*
     1(A6*A6-A7*A7)
      A12=A12+X3*A1*G1+X4*A2*G2+X5*A3*G3+X6*(A4*G4-A5*G5)+X7*
     1(A6*G6-A7*G7)
      A33=A33+Y3*U1*U1+Y4*U2*U2+Y5*U3*U3+Y6*(U4*U4-U5*U5)+Y7*
     1(U6*U6-U7*U7)
33    CONTINUE
      G1=G(NI,J+1,K)-G(NI,J,K)
      A1=A(NI,J+1,K)-A(NI,J,K)
```

```
      U1=U(NI,J+1,K)-U(NI,J,K)
      G2=G(NI,J,K+1)-G(NI,J,K)
      A2=A(NI,J,K+1)-A(NI,J,K)
      U2=U(NI,J,K+1)-U(NI,J,K)
      X3=(RA+R2*CF1)*(R2-R1)/R2
      Y3=RA+R1*CF1
      X4=R4*(R4-R3)/(RA+R4*CF(J))
      Y4=(R3*R3)/(RA+R3*CF(J))
      A11=A11+0.5*(X3*G1*G1+X4*G2*G2)
      A22=A22+0.5*(X3*A1*A1+X4*A2*A2)
      A12=A12+0.5*(X3*A1*G1+X4*A2*G2)
      A33=A33+0.5*(Y3*U1*U1+Y4*U2*U2)
   32 CONTINUE
   31 CONTINUE
      A11=A11*HS
      A12=A12*HS
      A22=A22*HS
      A33=A33*HS
      A21=A12
      DEL=A11*A22-A21*A21
      Q1=(A22*FLU1-A21*FLU2)/DEL
      Q2=(-A21*FLU1+A11*FLU2)/DEL
      Q3=FLU3/A33
      ENER=0.5*(Q1*FLU1+Q2*FLU2+Q3*FLU3)*0.75*GRA*VOL
      RETURN
      END



      SUBROUTINE GRAD(BMAX,PRO1,Q1,Q2,Q3)
C     COMPUTES THE SQUARE OF THE GRADIENT ON THE FREE BOUNDARY,AND
C     USES STEEPEST DESCENT METHOD TO UPDATE THE POSITION OF THE
C     BOUNDARY
      COMMON G(9,52,52),A(9,52,52),U(9,52,52),R(52,52),F(52,52),T(52,52)
     1,X1(52),X2(52),X3(52),X4(52),Y1(52),Y2(52),Y3(52),Y4(52),B1(52),
     2B2(52),B3(52),B4(52),B5(52),B6(52),B7(52),B8(52),C1(52),C2(52),
     3C3(52),C4(52),D1(52),D2(52),D3(52),D4(52),E1(52),E2(52),E3(52),
     4E4(52),GX1(52),GX2(52),GX3(52),GX4(52),GB1(52),GB2(52),GB3(52),
     5GB4(52),CF(52),D5(52),D6(52),D7(52),D8(52),RA,RO,RY,NI,NJ,PETE,
     6PEF1,BETE,GRA,H,HS,VOL,ENER,RELB
      COMMON EX(52,52),EF(52,52),ET(52,52),A11,A12,A22,A33
      DIMENSION DIF(52,52),GD1(52),GD2(52),GD3(52),GD4(52),GF1(52),
     1GE2(52),GE3(52),GE4(52),RA1(2),RA2(2),V1(3),V2(3),V3(3),V4(3),
     2RC1(2),RC2(2),RC3(2),RC4(2),RE1(2),RE2(2),C5(3),C6(3),C7(3),C8(3),
     3E5(3),E6(3) ,E7(3),E8(3),GC1(52),GC2(52),GC3(52),GC4(52)
      N1=NJ+1
      N2=NJ+2
```

```
      HA=0,5/HS
      HB=0,5/H
      HC=(H*H)/(HS*HS)
      HD=H/(2,0*HS)
      S1=0,5*HS
      S2=HS
      S3=1,0-0,5*HS
      S4=1,0-HS
      BMAX=0,0
      PRO1=0,0
      DO 1 J=2,N1
      R1=S1*(EX(J,1)-R(J,1))*R(J,1)
      R2=RA+R1*CF(J)
      R3=F(J,1)*(S1-1,0)-S1*EF(J,1)
      R4=T(J,1)*(S1-1,0)-S1*ET(J,1)
      PA1=(HC*R1*R2*(1,0+(R3*R3)/(R1*R1)*(R4*R4)/(R2*R2)))/(EX(J,1)-
     1R(J,1))
      R1=S1*(EX(J,2)-R(J,2))*R(J,2)
      R2=RA+R1*CF(J)
      R3=F(J,2)*(S1-1,0)-S1*EF(J,2)
      R4=T(J,2)*(S1-1,0)-S1*ET(J,2)
      PA2=(HC*R1*R2*(1,0+(R3*R3)/(R1*R1)*(R4*R4)/(R2*R2)))/
     1(EX(J,2)-R(J,2))
      R1=RA+S3*F(J,1)*CF(J)
      PA3=HC*S3*R1*(1,0+(F(J,1)*F(J,1))/(R(J,1)*R(J,1))+(S3*S3*T(J,1)*
     1T(J,1))/(R1*R1))
      R1=RA+S3*F(J,2)*CF(J)
      PA4=HC*S3*R1*(1,0+(F(J,2)*F(J,2))/(R(J,2)*R(J,2))+(S3*S3*T(J,2)*
     1T(J,2))/(R1*R1))
20    CONTINUE
      CF1=0,5*(CF(J)+CF(J+1))
      R1=0,5*(R(J,1)+R(J+1,1))
      R2=0,5*(R(J,2)+R(J+1,2))
      R3=0,5*(EX(J,1)+EX(J+1,1))
      R4=0,5*(EX(J,2)+EX(J+1,2))
      PB1=(RA+R1*CF1)*(R3-R1)/R1
      PB3=(RA+R2*CF1)*(R4-R2)/R2
      PB6=RA+R1*CF1
      PB8=RA+R2*CF1
      R5=0,5*(F(J,1)+F(J+1,1))
      R6=0,5*(F(J,2)+F(J+1,2))
      R7=0,5*(EF(J,1)+EF(J+1,1))
      R8=0,5*(EF(J,2)+EF(J+1,2))
      R9=S1*(R3-R1)+R1
21    CONTINUE
      PD1=(HD*(R5*(S1-1,0)-S1*R7)*(RA+R9*CF1))/R9
      R9=S1*(R4-R2)+R2
      PD2=(HD*(R6*(S1-1,0)-S1*R8)*(RA+R9*CF1))/R9
```

```
      PD3=-(HD*R5*(RA+S3*CF1*R1))/R1
      PD4=-(HD*R6*(RA+S3*CF1*R2))/R2
      R1=0.5*(R(J,1)+R(J,2))
      R2=0.5*(EX(J,1)+EX(J,2))
      PC1=(R1*(R2-R1))/(RA+R1*CF(J))
      PC4=(R1*R1)/(RA+R1*CF(J))
      R3=0.5*(T(J,1)+T(J,2))
      R4=0.5*(ET(J,1)+ET(J,2))
      R5=S1*(R2-R1)+R1
      PE1=(HD*R5*(R3*(S1-1.0)-S1*R4))/(RA+R5*CF(J))
      PE2=-(HD*S3*S3*R1*R3)/(RA+S3*R1*CF(J))
22    CONTINUE
      R1=G(2,J,1)-G(1,J,1)
      R2=A(2,J,1)-A(1,J,1)
      X1(J)=PA1*R1*R1
      X2(J)=PA1*R2*R2
      X3(J)=PA1*R1*R2
      R1=U(NI,J,1)-U(NI-1,J,1)
      X4(J)=PA3*R1*R1
      R1=G(2,J,2)-G(1,J,2)
      R2=A(2,J,2)-A(1,J,2)
      Y1(J)=PA2*R1*R1
      Y2(J)=PA2*R2*R2
      Y3(J)=PA2*R1*R2
      R1=U(NI,J,2)-U(NI-1,J,2)
      Y4(J)=PA4*R1*R1
      R1=G(1,J+1,1)-G(1,J,1)
      R3=A(1,J+1,1)-A(1,J,1)
      B1(J)=PB1*R1*R1
      B2(J)=PB1*R3*R3
      B3(J)=PB1*R1*R3
23    CONTINUE
      R2=U(NI,J+1,1)-U(NI,J,1)
      B4(J)=            PB6*R2*R2
      R1=G(1,J+1,2)-G(1,J,2)
      R3=A(1,J+1,2)-A(1,J,2)
      B5(J)=PB3*R1*R1
      B6(J)=PB3*R3*R3
      B7(J)=PB3*R1*R3
      R2=U(NI,J+1,2)-U(NI,J,2)
      B8(J)=            PB8*R2*R2
      R1=G(1,J,2)-G(1,J,1)
      R3=A(1,J,2)-A(1,J,1)
      C1(J)=PC1*R1*R1
      C2(J)=PC1*R3*R3
      C3(J)=PC1*R1*R3
      R2=U(NI,J,2)-U(NI,J,1)
      C4(J)=            PC4*R2*R2
```

```
      R1=G(2,J+1,1)-G(1,J,1)
      R2=G(2,J,1)-G(1,J+1,1)
      R3=A(2,J+1,1)-A(1,J,1)
      R4=A(2,J,1)-A(1,J+1,1)
   24 CONTINUE
      D1(J)=PD1*(R1*R1-R2*R2)
      D2(J)=PD1*(R3*R3-R4*R4)
      D3(J)=PD1*(R1*R3-R2*R4)
      R1=U(NI,J+1,1)-U(NI-1,J,1)
      R2=U(NI,J,1)-U(NI-1,J+1,1)
      D4(J)=PD3*(R1*R1-R2*R2)
      R1=G(2,J+1,2)-G(1,J,2)
      R2=G(2,J,2)-G(1,J+1,2)
      R3=A(2,J+1,2)-A(1,J,2)
      R4=A(2,J,2)-A(1,J+1,2)
      D5(J)=PD2*(R1*R1-R2*R2)
      D6(J)=PD2*(R3*R3-R4*R4)
      D7(J)=PD2*(R1*R3-R2*R4)
      R1=U(NI,J+1,2)-U(NI-1,J,2)
      R2=U(NI,J,2)-U(NI-1,J+1,2)
      D8(J)=PD4*(R1*R1-R2*R2)
   25 CONTINUE
      R1=G(2,J,2)-G(1,J,1)
      R2=G(2,J,1)-G(1,J,2)
      R3=A(2,J,2)-A(1,J,1)
      R4=A(2,J,1)-A(1,J,2)
      E1(J)=PE1*(R1*R1-R2*R2)
      E2(J)=PE1*(R3*R3-R4*R4)
      E3(J)=PE1*(R1*R3-R2*R4)
      R1=U(NI,J,2)-U(NI-1,J,1)
      R2=U(NI,J,1)-U(NI-1,J,2)
      E4(J)=PE2*(R1*R1-R2*R2)
    1 CONTINUE
      DO 2 K=2,N1
      X1(N2)=X1(2)
      X1(1)=X1(N1)
      X2(N2)=X2(2)
      X2(1)=X2(N1)
      X3(N2)=X3(2)
      X3(1)=X3(N1)
      X4(N2)=X4(2)
      X4(1)=X4(N1)
      Y1(N2)=Y1(2)
      Y1(1)=Y1(N1)
      Y2(N2)=Y2(2)
      Y2(1)=Y2(N1)
      Y3(N2)=Y3(2)
      Y3(1)=Y3(N1)
```

```
      Y4(N2)=Y4(2)
      Y4(1)=Y4(N1)
      B1(1)=B1(N1)
      B2(1)=B2(N1)
      B3(1)=B3(N1)
      B4(1)=B4(N1)
      B5(1)=B5(N1)
      B6(1)=B6(N1)
      B7(1)=B7(N1)
      B8(1)=B8(N1)
      C1(N2)=C1(2)
      C1(1)=C1(N1)
   26 CONTINUE
      C2(N2)=C2(2)
      C2(1)=C2(N1)
      C3(N2)=C3(2)
      C3(1)=C3(N1)
      C4(N2)=C4(2)
      C4(1)=C4(N1)
      D1(1)=D1(N1)
      D2(1)=D2(N1)
      D3(1)=D3(N1)
      D4(1)=D4(N1)
      D5(1)=D5(N1)
      D6(1)=D6(N1)
      D7(1)=D7(N1)
      D8(1)=D8(N1)
      E1(N2)=E1(2)
      E1(1)=E1(N1)
      E2(N2)=E2(2)
      E2(1)=E2(N1)
      E3(N2)=E3(2)
      E3(1)=E3(N1)
      E4(N2)=E4(2)
      E4(1)=E4(N1)
   27 CONTINUE
      DO 3 J=1,2
      R1=S1*(EX(J,3)-R(J,3))*R(J,3)
      R2=RA*R1*CF(J)
      R3=F(J,3)*(S1-1.0)-S1*EF(J,3)
      R4=T(J,3)*(S1-1.0)-S1*ET(J,3)
      RA1(J)=(HC*R1*R2*(1.0+(R3*R3)/(R1*R1)+(R4*R4)/(R2*R2)))/
     1(EX(J,3)-R(J,3))
      R1=RA*S3*F(J,3)*CF(J)
      RA2(J)=HC*S3*R1*(1.0+(F(J,3)*F(J,3))/(R(J,3)*R(J,3))+
     1(S3*S3*T(J,3)*T(J,3))/(R1*R1))
      R1=G(2,J,3)-G(1,J,3)
      R2=A(2,J,3)-A(1,J,3)
```

```
      V1(J)=RA1(J)*R1*R1
      V2(J)=RA1(J)*R2*R2
      V3(J)=RA1(J)*R1*R2
      R1=U(NI,J,3)-U(NI-1,J,3)
 3    V4(J)=RA2(J)*R1*R1
      CF1=0,5*(CF(1)+CF(2))
      R1=0,5*(R(1,3)+R(2,3))
      R2=0,5*(EX(1,3)+EX(2,3))
      RB1=(RA+R1*CF1)*(R2-R1)/R1
      R4=G(1,2,3)*G(1,1,3)
      R6=A(1,2,3)*A(1,1,3)
      P1=RB1*R4*R4
      P2=RB1*R6*R6
      P3=RB1*R4*R6
      RB4=RA+R1*CF1
      R5=U(NI,2,3)-U(NI,1,3)
      P4=            RB4*R5*R5
      R3=0,5*(F(1,3)+F(2,3))
      R4=0,5*(EF(1,3)+EF(2,3))
      R5=S1*(R2-R1)*R1
      RD1=(HD*(R3*(S1-1,0)-S1*R4)*(RA+R5*CF1))/R5
 28   CONTINUE
      R5=G(2,2,3)*G(1,1,3)
      R6=G(2,1,3)*G(1,2,3)
      R7=A(2,2,3)*A(1,1,3)
      R8=A(2,1,3)*A(1,2,3)
      Z1=RD1*(R5*R5-R6*R6)
      Z2=RD1*(R7*R7-R8*R8)
      Z3=RD1*(R5*R7-R6*R8)
      RD2=-(HD*(RA+S3*R1*CF1)*R3)/R1
      R5=U(NI,2,3)-U(NI-1,1,3)
      R6=U(NI,1,3)-U(NI-1,2,3)
      Z4=RD2*(R5*R5-R6*R6)
 29   CONTINUE
      DO 4 J=1,2
      R1=0,5*(R(J,2)+R(J,3))
      R2=0,5*(EX(J,2)+EX(J,3))
      RC1(J)=(R1*(R2-R1))/(RA+R1*CF(J))
      R3=G(1,J,3)-G(1,J,2)
      R5=A(1,J,3)-A(1,J,2)
      C5(J)=RC1(J)*R3*R3
      C6(J)=RC1(J)*R5*R5
      C7(J)=RC1(J)*R3*R5
      RC4(J)=(R1*R1)/(RA+R1*CF(J))
      R4=U(NI,J,3)-U(NI,J,2)
      C8(J)=                RC4(J)*R4*R4
      R3=0,5*(T(J,2)+T(J,3))
      R4=0,5*(ET(J,2)+ET(J,3))
```

```
      R5=S1*(R2-R1)+R1
30    CONTINUE
      RE1(J)=(HD*R5*(R3*(S1-1.0)-S1*R4))/(RA+R5*CF(J))
      R5=G(2,J,3)*G(1,J,2)
      R6=G(2,J,2)*G(1,J,3)
      R7=A(2,J,3)*A(1,J,2)
      R8=A(2,J,2)*A(1,J,3)
      E5(J)=RE1(J)*(R5*R5-R6*R6)
      E6(J)=RE1(J)*(R7*R7-R8*R8)
      E7(J)=RE1(J)*(R5*R7-R6*R8)
      RE2(J)=-(HD*S3*S3*R3*R1)/(RA+S3*R1*CF(J))
      R5=U(NI,J,3)-U(NI-1,J,2)
      R6=U(NI,J,2)-U(NI-1,J,3)
4     E8(J)=RE2(J)*(R5*R5-R6*R6)
      DO 5 J=2,N1
      SUM1=0.0
      SUM2=0.0
       SUM3=0.0
      SUM4=0.0
      R1=S1*(EX(J+1,K+1)-R(J+1,K+1))+R(J+1,K+1)
      R2=RA+R1*CF(J+1)
      R3=F(J+1,K+1)*(S1-1.0)-S1*EF(J+1,K+1)
      R4=T(J+1,K+1)*(S1-1.0)-S1*ET(J+1,K+1)
      QA1=(HC*R1*R2*(1.0+(R3*R3)/(R1*R1)+(R4*R4)/(R2*R2)))/
     1(EX(J+1,K+1)-R(J+1,K+1))
      R1=G(2,J+1,K+1)-G(1,J+1,K+1)
      R2=A(2,J+1,K+1)-A(1,J+1,K+1)
      V1(3)=QA1*R1*R1
      V2(3)=QA1*R2*R2
      V3(3)=QA1*R1*R2
      R1=RA+S3*R(J+1,K+1)*CF(J+1)
31    CONTINUE
      QA2=HC*S3*R1*(1.0+(F(J+1,K+1)*F(J+1,K+1))/(R(J+1,K+1)*R(J+1,K+1))+
     1(S3*S3*T(J+1,K+1)*T(J+1,K+1))/(R1*R1))
      R1=U(NI,J+1,K+1)-U(NI-1,J+1,K+1)
      V4(3)=QA2*R1*R1
      SUM1=SUM1+Y1(J)+0.5*(Y1(J+1)+X1(J)*Y1(J-1)+V1(2))+0.25*(X1(J+1)+
     1V1(1)+X1(J-1)+V1(3))
      SUM2=SUM2+Y2(J)+0.5*(Y2(J+1)+X2(J)*Y2(J-1)+V2(2))+0.25*(X2(J+1)+
     1V2(1)+X2(J-1)+V2(3))
      SUM3=SUM3+Y3(J)+0.5*(Y3(J+1)+X3(J)*Y3(J-1)+V3(2))+0.25*(X3(J+1)+
     1V3(1)+X3(J-1)+V3(3))
      SUM4=SUM4+Y4(J)+0.5*(Y4(J+1)+X4(J)*Y4(J-1)+V4(2))+0.25*(X4(J+1)+
     1V4(1)+X4(J-1)+V4(3))
32    CONTINUE
      GX1(J)=V1(2)
      V1(1)=V1(2)
      V1(2)=V1(3)
```

```
      GX2(J)=V2(2)
      V2(1)=V2(2)
      V2(2)=V2(3)
      GX3(J)=V3(2)
      V3(1)=V3(2)
      V3(2)=V3(3)
      GX4(J)=V4(2)
      V4(1)=V4(2)
      V4(2)=V4(3)
      R1=0.5*(R(J,K+1)+R(J+1,K+1))
      R2=0.5*(EX(J,K+1)+EX(J+1,K+1))
      CF1=0.5*(CF(J)+CF(J+1))
      QB1=(RA+R1*CF1)*(R2-R1)/R1
      R3=G(1,J+1,K+1)-G(1,J,K+1)
      R5=A(1,J+1,K+1)-A(1,J,K+1)
      P5=QB1*R3*R3
      P6=QB1*R5*R5
      P7=QB1*R3*R5
      QB4=RA+R1*CF1
      R4=U(NI,J+1,K+1)-U(NI,J,K+1)
      P8=            QB4*R4*R4
33    CONTINUE
      SUM1=SUM1+      B5(J)+B5(J-1) +0.50*(B1(J)+B1(J+1)+P1+P5)
      SUM2=SUM2+      B6(J)+B6(J-1) +0.50*(B2(J)+B2(J+1)+P2+P6)
      SUM3=SUM3+      B7(J)+B7(J-1) +0.50*(B3(J)+B3(J+1)+P3+P7)
      SUM4=SUM4+      B8(J)+B8(J-1) +0.50*(B4(J)+B4(J+1)+P4+P8)
      GB1(J)=P5
      P1=P5
      GB2(J)=P6
      P2=P6
      GB3(J)=P7
      P3=P7
      GB4(J)=P8
      P4=P8
      R3=0.5*(F(J,K+1)+F(J+1,K+1))
      R4=0.5*(EF(J,K+1)+EF(J+1,K+1))
      R5=S1*(R2-R1)+R1
      QD1=(HD*(R3*(S1-1.0)-S1*R4)+(RA+R5*CF1))/R5
      R5=G(2,J+1,K+1)-G(1,J,K+1)
      R6=G(2,J,K+1)-G(1,J+1,K+1)
      R7=A(2,J+1,K+1)-A(1,J,K+1)
34    CONTINUE
      R8=A(2,J,K+1)-A(1,J+1,K+1)
      Z5=QD1*(R5*R5-R6*R6)
      Z6=QD1*(R7*R7-R8*R8)
      Z7=QD1*(R5*R7-R6*R8)
      R5=S3*(R2-R1)+R1
      QD2=(HD*R3*(RA+S3*R1*CF1))/R1
```

```
      R5=U(NI,J+1,K+1)-U(NI-1,J,K+1)
      R6=U(NI,J,K+1)-U(NI-1,J+1,K+1)
      Z8=QD2*(R5*R5-R6*R6)
      SUM1=SUM1+D5(J)+D5(J-1)+0,5*(D1(J)*D1(J-1)+Z1+Z5)
      SUM2=SUM2+D6(J)+D6(J-1)+0,5*(D2(J)*D2(J-1)+Z2+Z6)
      SUM3=SUM3+D7(J)+D7(J-1)+0,5*(D3(J)*D3(J-1)+Z3+Z7)
      SUM4=SUM4+D8(J)+D8(J-1)+0,5*(D4(J)*D4(J-1)+Z4+Z8)
35    CONTINUE
      GD1(J)=Z5
      Z1=Z5
      GD2(J)=Z6
      Z2=Z6
      GD3(J)=Z7
      Z3=Z7
      GD4(J)=Z8
      Z4=Z8
      R1=0,5*(R(J+1,K)+R(J+1,K+1))
      R2=0,5*(EX(J+1,K)+EX(J+1,K+1))
      QC1=(R1*(R2-R1))/(RA*R1*CF(J+1))
      R3=G(1,J+1,K+1)-G(1,J+1,K)
      R5=A(1,J+1,K+1)-A(1,J+1,K)
      C5(3)=QC1*R3+R3
      C6(3)=QC1*R5+R5
      C7(3)=QC1*R3+R5
      QC4=(R1*R1)/(RA+R1+CF(J+1))
      R4=U(NI,J+1,K+1)-U(NI,J+1,K)
      C8(3)=            QC4*R4+R4
      SUM1=SUM1+      C1(J)+C5(2) +0,50+(C1(J+1)+C1(J-1)+C5(1)+C5(3))
      SUM2=SUM2+      C2(J)+C6(2) +0,50+(C2(J+1)+C2(J-1)+C6(1)+C6(3))
      SUM3=SUM3+      C3(J)+C7(2) +0,50+(C3(J+1)+C3(J-1)+C7(1)+C7(3))
      SUM4=SUM4+      C4(J)+C8(2) +0,50+(C4(J+1)+C4(J-1)+C8(1)+C8(3))
36    CONTINUE
      GC1(J)=C5(2)
      C5(1)=C5(2)
      C5(2)=C5(3)
      GC2(J)=C6(2)
      C6(1)=C6(2)
      C6(2)=C6(3)
      GC3(J)=C7(2)
      C7(1)=C7(2)
      C7(2)=C7(3)
      GC4(J)=C8(2)
      C8(1)=C8(2)
      C8(2)=C8(3)
      R3=0,5*(T(J+1,K)+T(J+1,K+1))
      R4=0,5*(ET(J+1,K)+ET(J+1,K+1))
      R5=S1*(R2-R1)+R1
      QE1=(HD*R5*(R3*(S1-1,0)-S1*R4))/(RA*R5*CF(J+1))
```

```
      R5=G(2,J+1,K+1)-G(1,J+1,K)
      R6=G(2,J+1,K)-G(1,J+1,K+1)
      R7=A(2,J+1,K+1)-A(1,J+1,K)
      R8=A(2,J+1,K)-A(1,J+1,K+1)
      E5(3)=QE1*(R5*R5-R6*R6)
      E6(3)=QE1*(R7*R7-R8*R8)
      E7(3)=QE1*(R5*R7-R6*R8)
      QE2=-(HD*(S3*S3*R3*R1))/(RA+S3*R1*CF(J+1))
      R5=U(NI,J+1,K+1)-U(NI-1,J+1,K)
      R6=U(NI,J+1,K)-U(NI-1,J+1,K+1)
      E8(3)=QE2*(R5*R5-R6*R6)
37    CONTINUE
      SUM1=SUM1+E5(2)+E1(J)+0.5*(E1(J+1)+E1(J-1)+E5(1)+E5(3))
      SUM2=SUM2+E6(2)+E2(J)+0.5*(E2(J+1)+E2(J-1)+E6(1)+E6(3))
      SUM3=SUM3+E7(2)+E3(J)+0.5*(E3(J+1)+E3(J-1)+E7(1)+E7(3))
      SUM4=SUM4+E8(2)+E4(J)+0.5*(E4(J+1)+E4(J-1)+E8(1)+E8(3))
      GE1(J)=E5(2)
      E5(1)=E5(2)
      E5(2)=E5(3)
      GE2(J)=E6(2)
      E6(1)=E6(2)
      E6(2)=E6(3)
      GE3(J)=E7(2)
      E7(1)=E7(2)
      E7(2)=E7(3)
      GE4(J)=E8(2)
      E8(1)=E8(2)
      E8(2)=E8(3)
      R2=W*H*(RA+R(J,K)*CF(J))*4.0*R(J,K)
      R1=R2*(EX(J,K)-R(J,K))
      R3=R2*R(J,K)
      GRAD1=(Q1*Q1*SUM1+2.0*Q1*Q2*SUM3+Q2*Q2*SUM2)/R1
      GRAD2=(Q3*Q3*SUM4)/R3+GRA
      PRO1=PRO1+GRAD2
      DIF(J,K)=GRAD1-GRAD2
      DAF=DIF(J,K)/GRAD2
      CC=ABS(DAF)
      BMAX=AMAX1(BMAX,CC)
5     CONTINUE
      DO 6 J=2,N1
      X1(J)=Y1(J)
      Y1(J)=GX1(J)
      X2(J)=Y2(J)
      Y2(J)=GX2(J)
      X3(J)=Y3(J)
      Y3(J)=GX3(J)
      X4(J)=Y4(J)
      Y4(J)=GX4(J)
```

```
      B1(J)=B5(J)
      B5(J)=GB1(J)
      B2(J)=B6(J)
      B6(J)=GB2(J)
      B3(J)=B7(J)
      B7(J)=GB3(J)
      B4(J)=B8(J)
      B8(J)=GB4(J)
      C1(J)=GC1(J)
      C2(J)=GC2(J)
      C3(J)=GC3(J)
      C4(J)=GC4(J)
      D1(J)=D5(J)
      D5(J)=GD1(J)
      D2(J)=D6(J)
      D6(J)=GD2(J)
      D3(J)=D7(J)
      D7(J)=GD3(J)
      D4(J)=D8(J)
      D8(J)=GD4(J)
      E1(J)=GE1(J)
      E2(J)=GE2(J)
      E3(J)=GE3(J)
      E4(J)=GE4(J)
    6 CONTINUE
    2 CONTINUE
      DO 10 K=2,N1
      DO 10 J=2,N1
   10 R(J,K)=R(J,K)+RELB*DIF(J,K)
      RETURN
      END



      SUBROUTINE SURF
C     COMPUTES THE INITIAL POSITION OF THE FREE BOUNDARY
      COMMON G(9,52,52),A(9,52,52),U(9,52,52),R(52,52),F(52,52),T(52,52)
     1,C1(9,52),C2(9,52),E1(9,52),E2(9,52),CF(52),B1(52),B2(52),D1(52),
     2D2(52),RA,RC,RI,NI,NJ,PETE,PEFI,BETE,GRA,H,HS,VOL,ENER,RELB
      COMMON EX(52,52),EF(52,52),ET(52,52),A11,A12,A22,A33
      N2=NJ+2
      DO 1 J=1,N2
      DO 1 K=1,N2
      R(J,K)=B2(J)
    1 CONTINUE
      RETURN
      END
```

```
      SUBROUTINE SARF
C     COMPUTES THE POSITION OF THE OUTER BOUNDARY
      COMMON G(9,52,52),A(9,52,52),U(9,52,52),R(52,52),F(52,52),T(52,52)
     1,C1(9,52),C2(9,52),E1(9,52),E2(9,52),CF(52),B1(52),B2(52),D1(52),
     2D2(52),RA,RC,RI,NI,NJ,PETE,PEFI,BETE,GRA,H,HS,VOL,ENER,RELB
      COMMON EX(52,52),EF(52,52),ET(52,52),A11,A12,A22,A33
      N2=NJ*2
      DO 1 J=1,N2
      DO 1 K=1,N2
      EX(J,K)=RO
    1 CONTINUE
      RETURN
      END



      SUBROUTINE ELI
C     COMPUTES INITIAL POSITION OF THE FREE BOUNDARY,AND POSITION OF
C     FIXED OUTER BOUNDARY FOR AXIALLY SYMMETRIC CASE
      COMMON GG(9,52,52),GX(9,52,52),GY(9,52,52),G1(52,52),G2(52,52),
     1G3(52,52),G(9,52),A(9,52),B(9,52),D(9,52),CF(52),F(52),R(52),
     2EX(52),EF(52),RA,RO,RI,NI,NJ,PETE,PEFI,BETE,GRA,H,HS,VOL,ENER,
     3RELB
      ACOR=1.0
      ALAR=1.0
      N2=NJ*2
      DO 1 J=1,N2
      FI=(J-2)*H
      X1=COS(FI)/ACOR
      X2=SIN(FI)/ALAR
      X3=X1*X1+X2*X2
      EX(J)=RO*SQRT(1.0/X3)
    1 R(J)=RI*SQRT(1.0/X3)
      RETURN
      END
```

EOF

N.Y.U. Courant Institute of
Mathematical Sciences
251 Mercer St.
New York, N. Y. 10012